DEPARTMENT OF COMMERCE
LEWIS L. STRAUSS, Secretary

WEATHER BUREAU
F. W. REICHELDERFER, Chief

MONTHLY WEATHER REVIEW

JAMES E. CASKEY, JR., Editor

Volume 87
Number 2

FEBRUARY 1959

Closed April 15, 1959
Issued May 15, 1959

COMPARISON OF BAROTROPIC AND BAROCLINIC NUMERICAL FORECASTS AND CONTRIBUTIONS OF VARIOUS EFFECTS

MAJOR LLOYD W. VANDERMAN,[1] U.S. Air Force
WILLIAM J. DREWES, U.S. Navy
and
LEO E. HOPP, U.S. Weather Bureau
Joint Numerical Weather Prediction Unit, Suitland, Md.

[Manuscript received November 7, 1958; revised January 15, 1959]

ABSTRACT

500-mb. barotropic and 500-mb. baroclinic numerical forecasts for two cases, a developing baroclinic cyclone and a quasi-barotropic cyclone, are presented and compared. The barotropic forecasts did not indicate accurately the changes in circulation or the magnitude of the height falls ahead of the circulation maxima. 700-mb. forecasts from the same initial times as the 500-mb. barotropic and baroclinic forecasts, for each of the four terms of the frictionless vorticity equation, are presented. These 700-mb. forecasts are compared with each other and in added combinations with the 700-mb. verifications and with 700-mb. barotropic forecasts. These comparisons are then used diagnostically in an analysis of the errors in the 500-mb. barotropic forecasts. Each of the four terms of the vorticity equation is discussed. An explanation for the success of the barotropic forecasting model is suggested. Contributions of the horizontal velocity divergence, vertical advection of vorticity, and twisting terms to errors in the barotropic forecasting model are discussed in some detail. It is concluded that the major problem in developing a successful baroclinic forecasting model to substitute for the existing barotropic forecasting model is that of determining in space and time an accurate approximation of the vertical profile of vertical motion.

1. INTRODUCTION

A technique frequently applied in our efforts to improve weather prognosis is that of making a detailed case study of a weather situation which allows isolation of the problem of the moment. The problem under study is baroclinic development. The purpose of this paper is to present, first, the results of a study and comparison of barotropic and baroclinic numerical forecasts from the same initial time for a case of baroclinic development. As a check on the results of the first case, a similar study was made for a case presumed to involve little or no baroclinic development—a quasi-barotropic case; these results are presented also. The analyses and 500-mb. forecasts used in the two studies were selected from the Joint Numerical Weather Prediction (JNWP) Unit and National Weather Analysis Center (NAWAC) operational files. The 700-mb. forecasts were prepared specially in JNWPU for these two studies. 500-mb. barotropic forecasts, S_2 Model[2] [1] and 500-mb. baroclinic forecasts, Thermotropic Model[3] [2] were compared.

The figures shown speak for themselves. The conclusions arrived at are the most obvious. In general they point up some inadequacies of the barotropic model and strongly suggest the inclusion of the horizontal velocity divergence, vertical advection of vorticity, and twisting terms in numerical weather prediction models. It is recalled that in the recent past the capacity of the electronic computers available for numerical weather prediction limited greatly the forecasting model. As computers increase

[1] Published with permission of Commander, Air Weather Service.

[2] The S_2 Model employs a non-divergent wind which is approximately geostrophic.

[3] The Thermotropic Model employs the geostrophic wind.

in capacity and speed, it is anticipated that the more successful forecast models developed and subsequently employed will include most of the baroclinic terms and will produce greatly improved numerical forecasts.

2. APPROACH TO THE PROBLEM

It was decided that in comparing 500-mb. barotropic and 500-mb. baroclinic forecasts it would be necessary to know more about the detailed behavior of the atmosphere than would be immediately apparent from attempting to resolve differences in basic forecasting equations, forecast contour fields, forecast height error fields, etc. Therefore, additionally, 700-mb. 12-hour height tendency forecasts were made from data for the same initial times as the 500-mb. forecasts. The techniques employed are comparable to those employed by 'Arnason [3] and Winston [4] except computations of vertical motion were not necessary since fields of large-scale 500-mb. vertical motion for the initial times (figs. 1F and 5F) were already computed and available as products of the thermotropic forecast [2,5].

The frictionless vorticity equation—

$$\frac{\partial \zeta}{\partial t}=-\mathbf{V}\cdot\nabla\eta+\eta\frac{\partial \omega}{\partial p}-\omega\frac{\partial \eta}{\partial p}-\left(\nabla\omega\times\frac{\partial \mathbf{V}}{\partial p}\right)\cdot\mathbf{k}, \tag{1}$$

in which t is time; ζ is relative vorticity; p is pressure; $\mathbf{V}$ is the horizontal wind vector; η is absolute vorticity; ω is the individual change of pressure with time, $\frac{dp}{dt}$, [6, 7]; and $\mathbf{k}$ is the unit vertical vector—was separated into four finite difference equations from which each right-hand-side term could be evaluated for 700 mb. and its field of values relaxed to obtain a 12-hour, one-time-step height tendency forecast for 700 mb. The terms on the right-hand side of equation (1) are, reading from left to right, horizontal advection of absolute vorticity, horizontal velocity divergence, vertical advection of vorticity, and twisting of the vortex tubes; these will be referred to as the horizontal advection term, the divergence term, the vertical advection term, and the twisting term, respectively.

First let

$$\frac{\partial \zeta}{\partial t}=\left(\frac{\partial \zeta}{\partial t}\right)_1+\left(\frac{\partial \zeta}{\partial t}\right)_2+\left(\frac{\partial \zeta}{\partial t}\right)_3+\left(\frac{\partial \zeta}{\partial t}\right)_4 \tag{2}$$

in which each right-hand-side term to be evaluated at 700 mb. represents the corresponding term in equation (1). Then an equation, in which $\Delta t=12$ hours (and therefore $s=43{,}200$, the number of seconds in 12 hours), for the horizontal advection term can be written,

$$\left(\frac{\partial \zeta}{\partial t}\right)_1=-s(\mathbf{V}\cdot\nabla\eta) \tag{3}$$

in which

$$\left(\frac{\partial \zeta}{\partial t}\right)_1=\frac{g}{f}\left(\nabla^2\frac{\partial z}{\partial t}\right)_1=\frac{gm^2}{fd^2}\left[\left(\frac{\Delta z}{\Delta t}\right)_n+\left(\frac{\Delta z}{\Delta t}\right)_e+\left(\frac{\Delta z}{\Delta t}\right)_s+\left(\frac{\Delta z}{\Delta t}\right)_w-4\left(\frac{\Delta z}{\Delta t}\right)_o\right]_1$$

and

$$-s(\mathbf{V}\cdot\nabla\eta)=\frac{gs}{f}\mathbf{J}(\eta,z)=\frac{gsm^2}{4fd^2}[(\eta_e-\eta_w)(z_n-z_s)-(\eta_n-\eta_s)(z_e-z_w)].$$

For evaluation at 700 mb. this reduces to

$$\left[\left(\frac{\Delta z}{\Delta t}\right)_n+\left(\frac{\Delta z}{\Delta t}\right)_e+\left(\frac{\Delta z}{\Delta t}\right)_s+\left(\frac{\Delta z}{\Delta t}\right)_w-4\left(\frac{\Delta z}{\Delta t}\right)_o\right]_1$$
$$-10.8[(\eta_e-\eta_w)(z_n-z_s)-(\eta_n-\eta_s)(z_e-z_w)]_{700}=R_1\approx 0.$$

Likewise an equation for the divergence term can be written,

$$\left(\frac{\partial \zeta}{\partial t}\right)_2=s\eta\frac{\partial \omega}{\partial p} \tag{4}$$

and reduced to

$$\left[\left(\frac{\Delta z}{\Delta t}\right)_n+\left(\frac{\Delta z}{\Delta t}\right)_e+\left(\frac{\Delta z}{\Delta t}\right)_s+\left(\frac{\Delta z}{\Delta t}\right)_w-4\left(\frac{\Delta z}{\Delta t}\right)_o\right]_2$$
$$-1.204\sin\psi(1+\sin\psi)^2\eta_{700}W_{500}=R_2\approx 0.$$

An equation for the vertical transport term can be written

$$\left(\frac{\partial \zeta}{\partial t}\right)_3=-s\omega\frac{\partial \eta}{\partial p} \tag{5}$$

and reduced to

$$\left[\left(\frac{\Delta z}{\Delta t}\right)_n+\left(\frac{\Delta z}{\Delta t}\right)_e+\left(\frac{\Delta z}{\Delta t}\right)_s+\left(\frac{\Delta z}{\Delta t}\right)_w-4\left(\frac{\Delta z}{\Delta t}\right)_o\right]_3$$
$$-1.084\sin\psi(1+\sin\psi)^2W_{500}(\eta_{1000}-\eta_{500})=R_3\approx 0.$$

An equation for the twisting term can be written,

$$\left(\frac{\partial \zeta}{\partial t}\right)_4=-s\left(\nabla\omega\times\frac{\partial \mathbf{V}}{\partial p}\right)\cdot\mathbf{k} \tag{6}$$

and reduced to,

$$\left[\left(\frac{\Delta z}{\Delta t}\right)_n+\left(\frac{\Delta z}{\Delta t}\right)_e+\left(\frac{\Delta z}{\Delta t}\right)_s+\left(\frac{\Delta z}{\Delta t}\right)_w-4\left(\frac{\Delta z}{\Delta t}\right)_o\right]_4$$
$$-.0133\{[W_e-W_w]_{500}\cdot[(z_e-z_w)_{1000}-(z_e-z_w)_{500}]+[W_n-W_s]_{500}\cdot[(z_n-z_s)_{1000}-(z_n-z_s)_{500}]\}=R_4\approx 0.$$

In these equations $\Delta t=12$ hours; $g=9.8$ m.sec.$^{-2}$; f is the Coriolis parameter; ψ is latitude: $m=\frac{1+\sin 60^\circ}{1+\sin\psi}$, the map magnification factor on a polar stereographic projection true at 60° latitude; $d=381$ km., the mesh size; W is vertical velocity in millimeters per second; η is absolute vorticity in units of sec.$^{-1}\times 10^{-4}$; z is feet, except dekafeet in

the terms z_n, z_e, z_s, and z_w; and R is the residual. Subscripts 1000, 700, and 500 designate the pressure surface at which the value is determined. Subscripts n, e, s, and w designate, in clockwise rotational order on a square mesh grid, values at the four grid points immediately surrounding a central grid point value designated with subscript o. Assumed in these equations are: (1) geostrophic velocity and vorticity at 1000 mb., 700 mb., and 500 mb.; (2) a parabolic profile of vertical velocity, $\frac{dz}{dt}$, between 1000 mb. and 500 mb. with $W=0$ at 1000 mb. and $W_{700}=0.7\ W_{500}$; (3) constant density values at 700 mb. of $\rho=9\cdot10^{-4}$ tons m.$^{-3}$ and at 500 mb. of $\rho=7\cdot10^{-4}$ tons m.$^{-3}$; and $\omega=-\rho g W$.

Over a 14×17 point grid field the boundary of which for each case is the edge of the geographical area shown in figures 1–8, grid point values from the 1000-mb., 700-mb., and 500-mb. pressure surfaces for height, latitude, and vertical velocity were determined from initial analyses and data. The absolute vorticity for each grid point of the three pressure surfaces was computed by entering a graph, specially prepared for the projection and $1:20\cdot10^6$ scale chart used, with the value of the computed finite difference height Laplacian and latitude. Values of the horizontal advection term were not computed on the outside boundary or relaxed on the adjacent inner boundary; grid point values for all four terms for 700 mb. were computed only for the inner 10×13 point grid. The field of grid point values of each individual term was then relaxed by hand using Southwell's method to obtain four 12-hour one-time-step height tendency forecasts for 700 mb. These forecasts were then added graphically in several combinations. Additionally, to obtain an independent estimate of the contribution of the horizontal advection term to a 12-hour height change at 700 mb., 700-mb. baratropic forecasts, S_2 Model [1], were made on the electronic computer.

3. A BAROCLINIC CASE

The considerations in selecting a baroclinic case for study were: (1) a measurable increase in circulation to occur in a young cyclone within a 12-hour period at both the surface (figs. 1A and 1B) and 500 mb. (figs. 1C and 1D); (2) the cyclone to be situated over the relatively flat Plains region of the United States and southern Canada, to insure minimum terrain effects on vertical motion and dense data coverage for accurate analyses; and (3) the cyclone to be associated with a baroclinic atmosphere as evidenced by the out-of-phase relation of 1000-mb. to 500-mb. thickness lines and 500-mb. contours (compare figs. 1C and 1E in the region immediately north of Montana).

The 500-mb. barotropic 12-hour forecast (fig. 2A) did not indicate accurately the increase in circulation that occurred in the developing trough over north central United States (fig. 1D) or the magnitude of height fall just ahead of the circulation maximum (fig. 2 B, C, and D). The 500-mb. thermotropic 12-hour forecast (fig. 2E) indicated errors of the same sign but was definitely superior to the barotropic forecast in the immediate region of the circulation maximum (figs. 2D and 2F). The barotropic model forecasted the heights to be too high over most of the map area shown. Since both 500-mb. forecasts were computed over a 31×34 point grid area (a number of grid lengths larger than the map area shown), boundary effects are considered to be unimportant.

The major difference in the forecasting equations employed by the two models is a baroclinic term of the Thermotropic Model, $-K(\mathbf{V}_T\cdot\nabla\zeta_T)$, comparable to a right-hand term of equation (1) in which K is an empirically determined positive constant and $\mathbf{V}_T$ and ζ_T are thermal velocity and thermal relative vorticity, respectively, for the 1000-mb. to 500-mb. layer. This term appears to be related to the process whereby potential energy is converted to kinetic energy and it can be credited for the difference between the 500-mb. thermotropic forecast and the 500-mb. baratropic forecast. From studying subjectively numerous 500-mb. thermotropic forecasts it appears that this term forecasts continuous baroclinic development. Its cumulative contribution can result in serious contamination, especially in the longer-period forecasts.[4]

The 700-mb. initial analysis (fig. 3A) is similar in appearance to the 500-mb. initial analysis (fig. 1C). The major difference is that the trough and ridge line positions at 700 mb. were east of the 500-mb. positions as is normal for moving systems in westerly flow. The same was true of the trough and ridge lines 12 hours later (figs. 3C and 1D) and also of the observed centers of 12-hour height change (figs. 3D and 2D). But the magnitudes of the observed 12-hour height change centers were considerably less at 700 mb. than at 500 mb. The 700-mb. 12-hour forecast height change (fig. 3B), obtained by graphically adding the forecasts for all four terms (figs. 4C–F), compared favorably with the observed height change (fig. 3D). However, the height fall center associated with the developing cyclone was underforecast in speed of movement and magnitude (−240 feet forecasted as compared to −310 feet observed). These differences can be explained to some degree by the fact that in the atmosphere changes operated to cause additional changes continuously throughout the 12-hour period whereas only the initial conditions were considered in making the 12-hour one-time-step forecast. The 700-mb. barotropic forecast (figs. 3E and 3F) can be compared with the 12-hour tendency forecast for the horizontal advection term (fig. 4C). The major difference between these two forecasts is in the speed of movement of the height fall center. Neither even closely

[4] In the process of converting to a new computer and a larger grid area the Joint Numerical Weather Prediction Unit discontinued routine forecasting with the Thermotropic Model in June 1957.

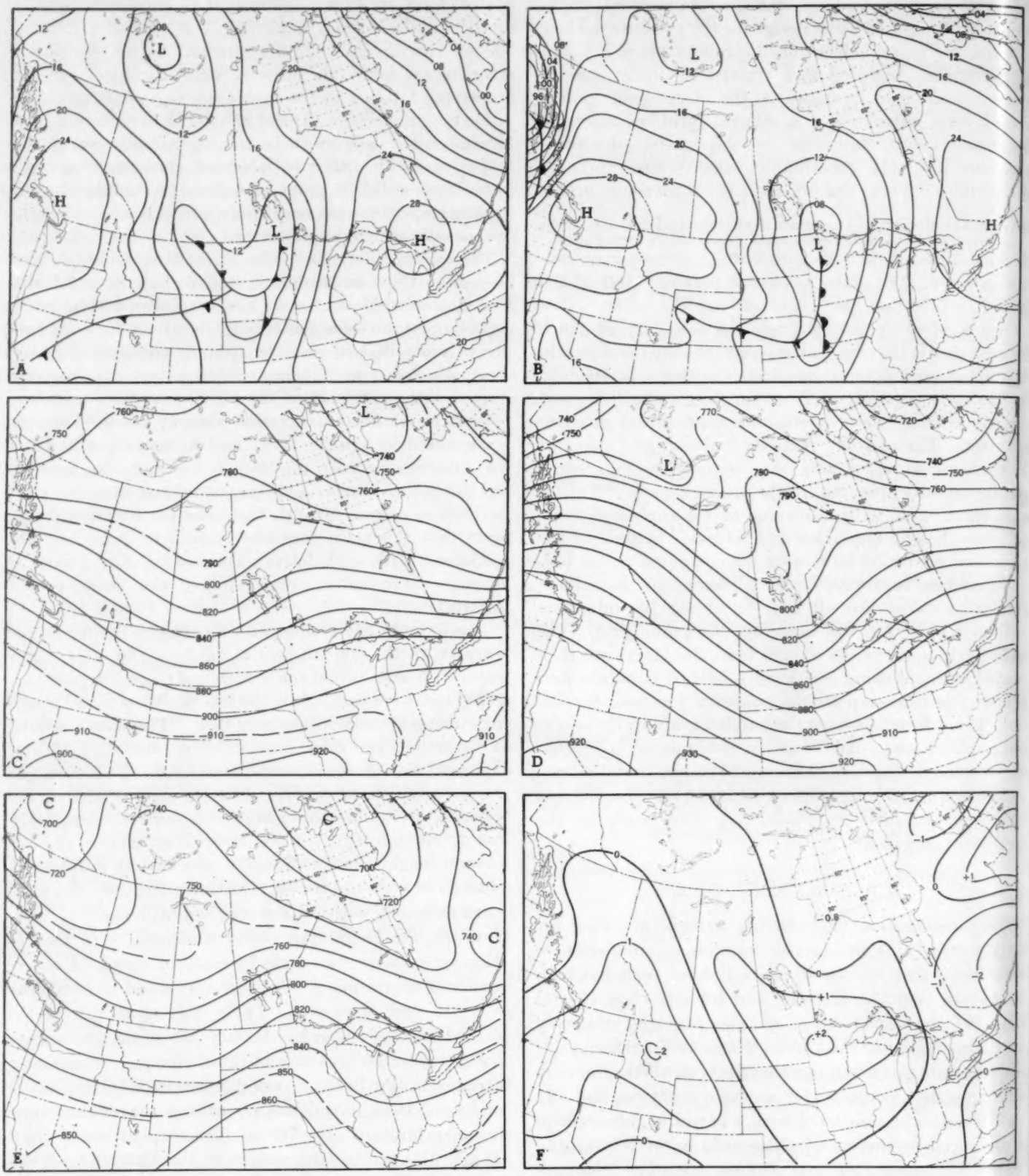

FIGURE 1.—(A) Surface analysis, 1230 GMT, Oct. 5 and (B) 0030 GMT, Oct. 6, 1956. (C) 500-mb. analysis, 1500 GMT, Oct. 5, and (D) 0300 GMT, Oct. 6, 1956. (E) 1000 to 500-mb. thickness, 1500 GMT, Oct. 5, 1956. (F) 500-mb. vertical velocity in cm.sec.$^{-1}$, 1500 GMT, Oct. 5, 1956.

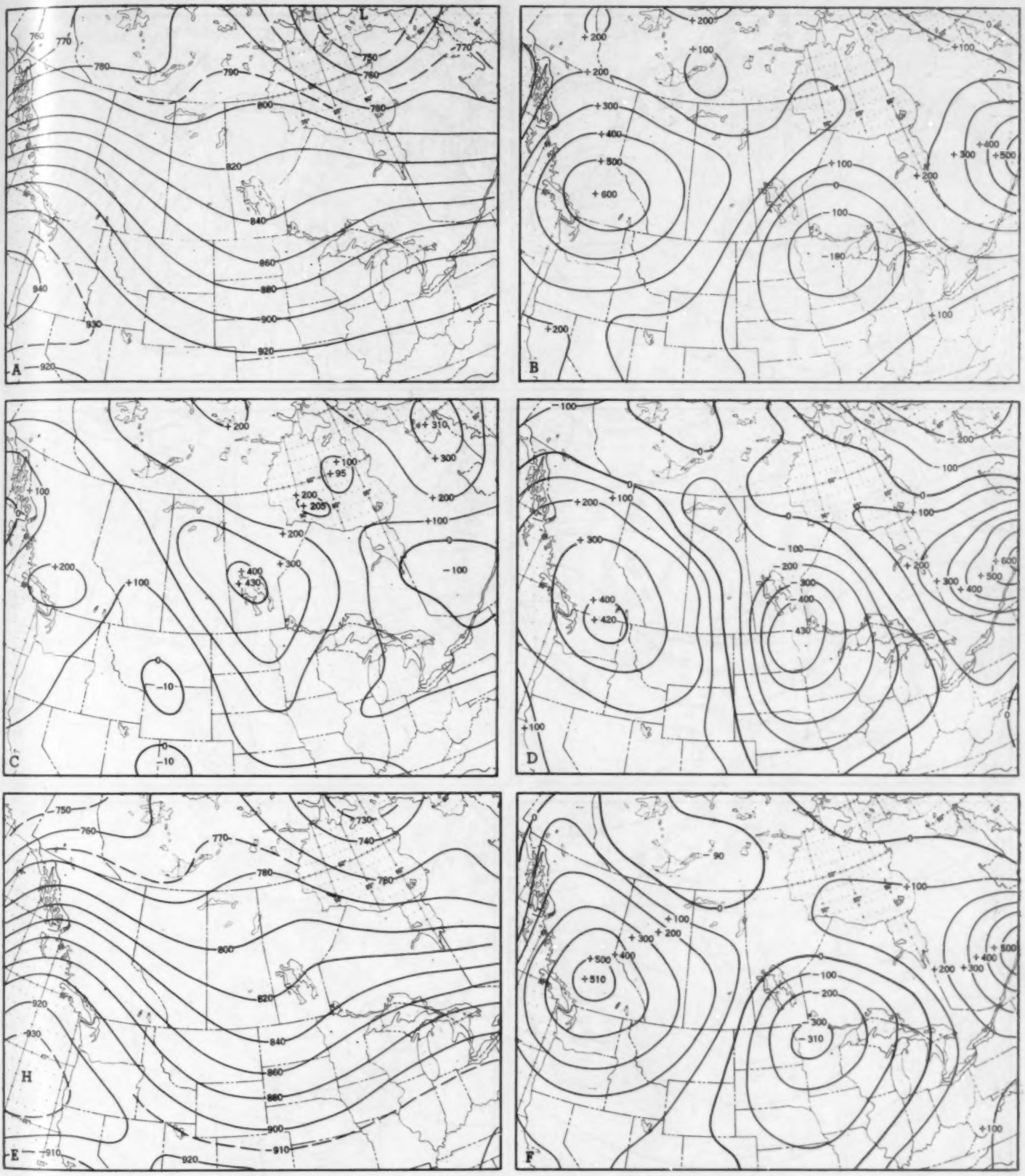

FIGURE 2.—(A) 500-mb. barotropic 12-hour forecast from 1500 GMT, Oct. 5, 1956 and (B) the height change (in feet) it represents. (C) Error of forecast height change. (D) Observed 12-hour height change from 1500 GMT. (E) 500-mb. thermotropic 12-hour forecast from 1500 GMT and (F) the height change it represents.

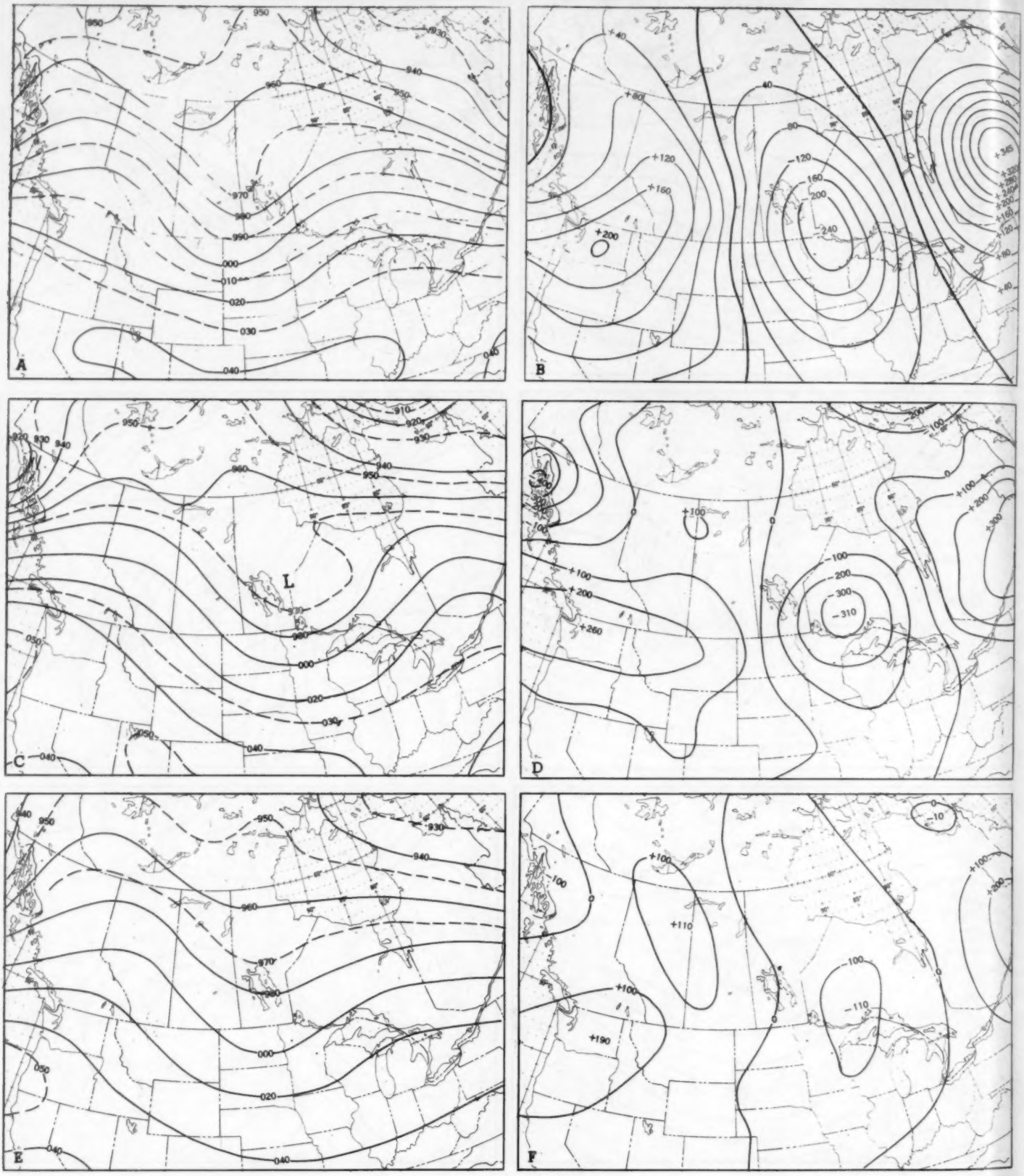

FIGURE 3.—(A) 700-mb. analysis for 1500 GMT, Oct. 5, 1956 and (B) 12-hour forecast height change (in feet) made from it using all four terms in eq. (1). (C) 700-mb. analysis for 0300 GMT, Oct. 6, 1956 and (D) 12-hour observed height change from 1500 GMT, Oct. 5, 1956. (E) 700-mb. barotropic 12-hour forecast from 1500 GMT, Oct. 5, 1956 and (F) the height change it represents.

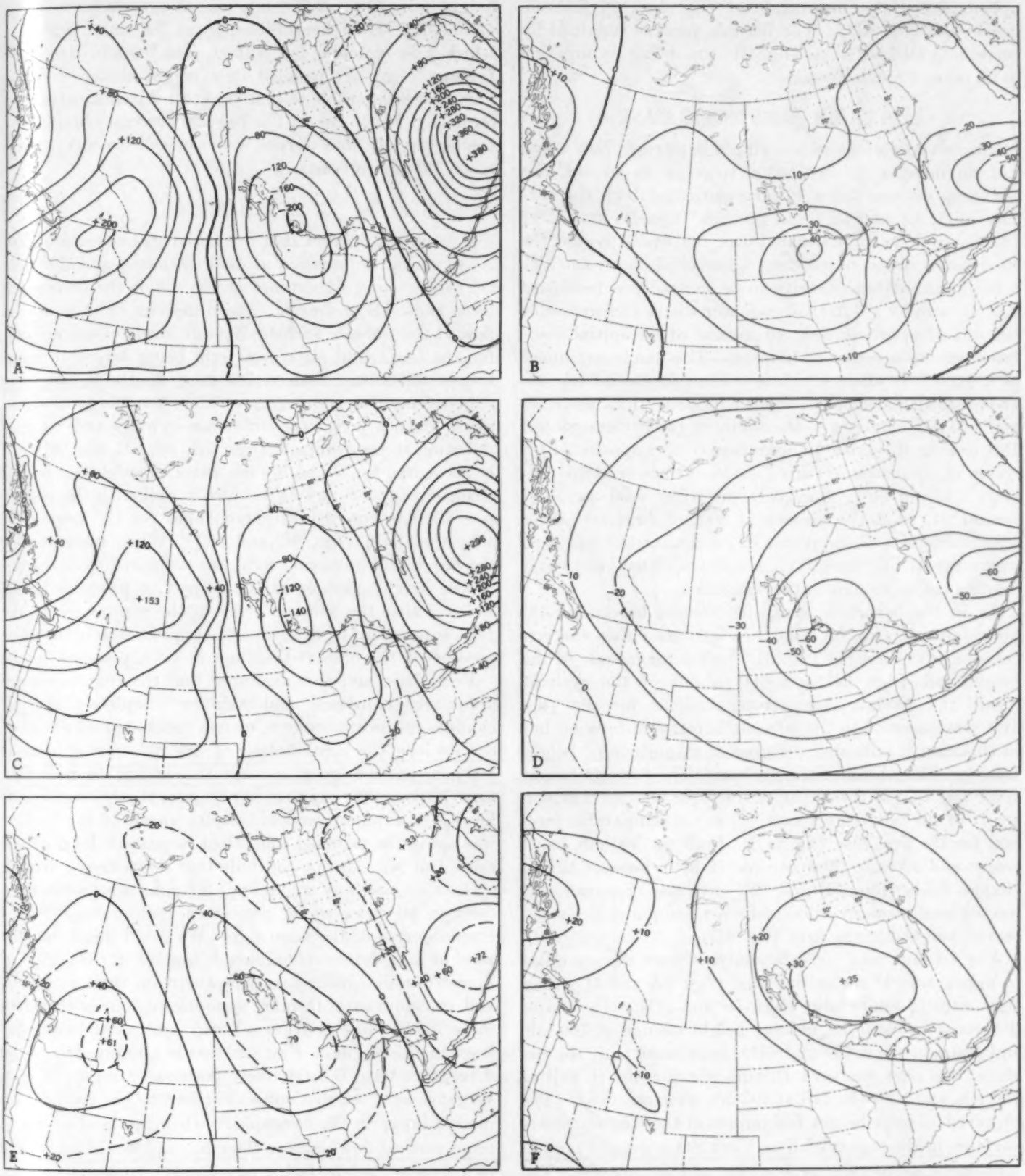

FIGURE 4.—700-mb. 12-hour forecast height change (in feet) from 1500 GMT, Oct. 5, 1956 made from (A) horizontal advection and divergence terms, $-\mathbf{V}\cdot\nabla\eta+\eta(\partial\omega/\partial p)$; (B) vertical advection and twisting terms, $-\omega(\partial\eta/\partial p)-[\nabla\omega\times(\partial\mathbf{V}/\partial p)]\cdot\mathbf{k}$; (C) horizontal advection term, $-\mathbf{V}\cdot\nabla\eta$; (D) vertical advection term, $-\omega(\partial\eta/\partial p)$; (E) divergence term, $\eta(\partial\omega/\partial p)$; (F) twisting term, $-[\nabla\omega\times(\partial\mathbf{V}/\partial p)]\cdot\mathbf{k}$.

approximated the magnitude of the observed 700-mb. height fall (fig. 3D). The 700-mb. forecast obtained by combining all four terms (fig. 3B) was definitely superior to all other 700-mb. forecasts.

4. A QUASI-BAROTROPIC CASE

The considerations in selecting a barotropic case were: (1) no increase in circulation to occur in an old, unchanging cyclone for a 12-hour period at both the surface (figs. 5A and 5B) and 500 mb. (figs. 5C and 5D); (2) the cyclone to be situated over the Plains region for the reasons stated in selecting a baroclinic case; and (3) a minimum of baroclinicity to be in evidence (compare figs. 5C and 5E). Actually an increase in circulation at 500 mb. of approximately 40 percent of the initial absolute vorticity occurred in 12 hours. This can be explained as a baroclinic effect which is evident in the initial out-of-phase orientation of 1000-mb. to 500-mb. thickness lines and 500-mb. contours to the south of the cyclone center. But during the same 12-hour period no appreciable increase in circulation occurred at the surface or at 700 mb. (hgs 7A and 7C). Twelve hours after 1500 GMT, December 24, 1956, the cyclone at 500 mb. was no longer identifiable as a closed center of circulation but had been instrumental in intensifying its associated eastward-moving major trough in the westerlies.

As in the baroclinic case, the 500-mb. barotropic 12-hour forecast (fig. 6A) did not indicate either the circulation that occurred (fig. 5D) or the magnitude of the height fall (figs. 6B and 6D) ahead of the cyclone. Again the 500-mb. thermotropic 12-hour forecast (fig. 6E) was superior to the 500-mb. barotropic forecast but in this case it indicated too great a magnitude of height fall (fig. 6F) ahead of the cyclone. The forecast height error (fig. 6C) of the 500-mb. barotropic forecast was generally of the same sign (positive) as the comparable forecast for the first case (fig. 2C). Both the 500-mb. barotropic and 500-mb. thermotropic 12-hour forecast height change fields (figs. 6B and 6F) give the appearance of having been strongly smoothed when compared to the observed height change field (fig. 6D).

The 700-mb. and 500-mb. analyses were more similar in appearance at the initial time (figs. 7A and 5C) than they were 12 hours later (figs. 7C and 5D). The major difference in observed 12-hour height change at 700 mb. and 500 mb. (figs. 7D and 6D), associated with the cyclone, was over southern Illinois where a 100-ft. fall at 700 mb. and a 330-ft. fall at 500 mb. were observed. The observed 12-hour height fall centers at these two pressure surfaces in the region of New York State were in normal agreement as to relative position and magnitude. The 700-mb. 12-hour forecast height change (fig. 7B) including all four terms (figs. 8C–F) verified well in the region of the more northerly height fall center (fig. 7D). An additional height fall center was forecast over Tennessee but did not verify. However, this latter forecast height fall center at 700 mb. was in agreement with the observed 12-hour height change at 500 mb. (fig. 6D) which shows a double fall center. The 700-mb. barotropic forecast (fig. 7E) resulted in a height change forecast (fig. 7F) comparable to that for the horizontal advection term (fig. 8C). Again the 700-mb. forecast obtained by combining all four terms was superior to any of the other 700-mb. forecasts.

5. CONCLUSIONS

It is quite apparent that the horizontal advection term is of major importance at both 500 mb. and 700 mb. Of nearly equal importance at 700 mb. is the divergence term (figs. 4E and 8E). The difference in intensity of flow at the 500-mb. and the 700-mb. levels would account for the horizontal advection term being larger in magnitude at 500 mb. than at 700 mb. And also, since the fields of positive and negative values for this term are in phase at both levels, the difference in magnitude of contribution to the forecasts (figs. 2B, 4C, 6B, and 8C) can be accounted for. The 700-mb. barotropic forecast height changes (figs. 3F and 7F) compare well with the respective 700-mb. forecast height changes for the horizontal advection term (figs. 4C and 8C). When forecasts for the horizontal advection term are compared with the observed height changes at the respective pressure levels, we note that the forecast error in the magnitude of the fall center ahead of the cyclone is approximately the same percent of the observed change at both pressure levels.

From this, and also assuming that the four terms are accurately expressed and account completely for all changes in the atmosphere, we can conclude that ahead of the cyclone the contribution of the divergence term at 500 mb. can be as great in magniture and of the same sign as at 700 mb. We can then say that for these two cases the level of maximum vertical velocity ahead of the cyclone was above the assumed equivalent barotropic level of 500 mb. But we can not conclude that downstream from a cyclone or vorticity maximum, 500-mb. barotropic forecasts in all cases would produce a comparable error or even an error of the same sign. We could guess that the level of maximum vertical flow is highest in the region of upward motion immediately downstream from a cyclone, and in comparison to other synoptic regions is therefore more likely to be above a selected equivalent barotropic level in this region. Further, this is a region where the divergence term is most likely positive—a region of convergence at a selected equivalent barotropic level of 500 mb. or lower in the atmosphere when the level of maximum vertical flow is above 500 mb.—and would contribute to a forecast height fall if considered. In the region immediately upstream from a trough or cyclone where vertical motion in the troposphere is in general downward, the divergence term in equation (1) is negative in value below the level of minimum vertical velocity and positive above it.

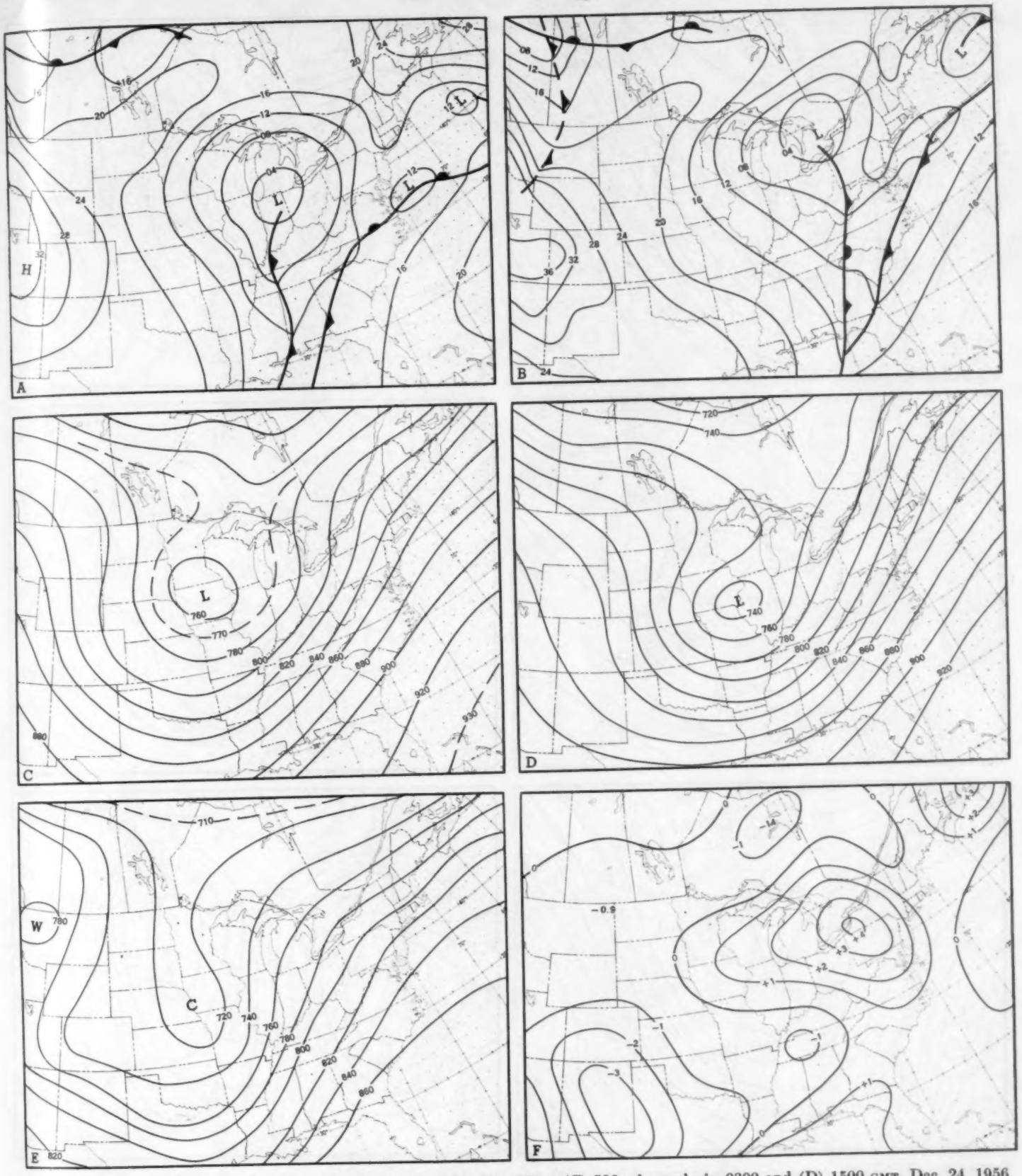

FIGURE 5.—(A) Surface analysis, 0030 and (B) 1230 GMT, Dec. 24, 1956. (C) 500-mb. analysis, 0300 and (D) 1500 GMT, Dec. 24, 1956. (E) 1000 to 500-mb. thickness analysis, 0300 GMT, Dec. 24, 1956. (F) 500-mb. vertical velocity in cm. sec.$^{-1}$, 0300 GMT, Dec. 24, 1956.

500931—59——2

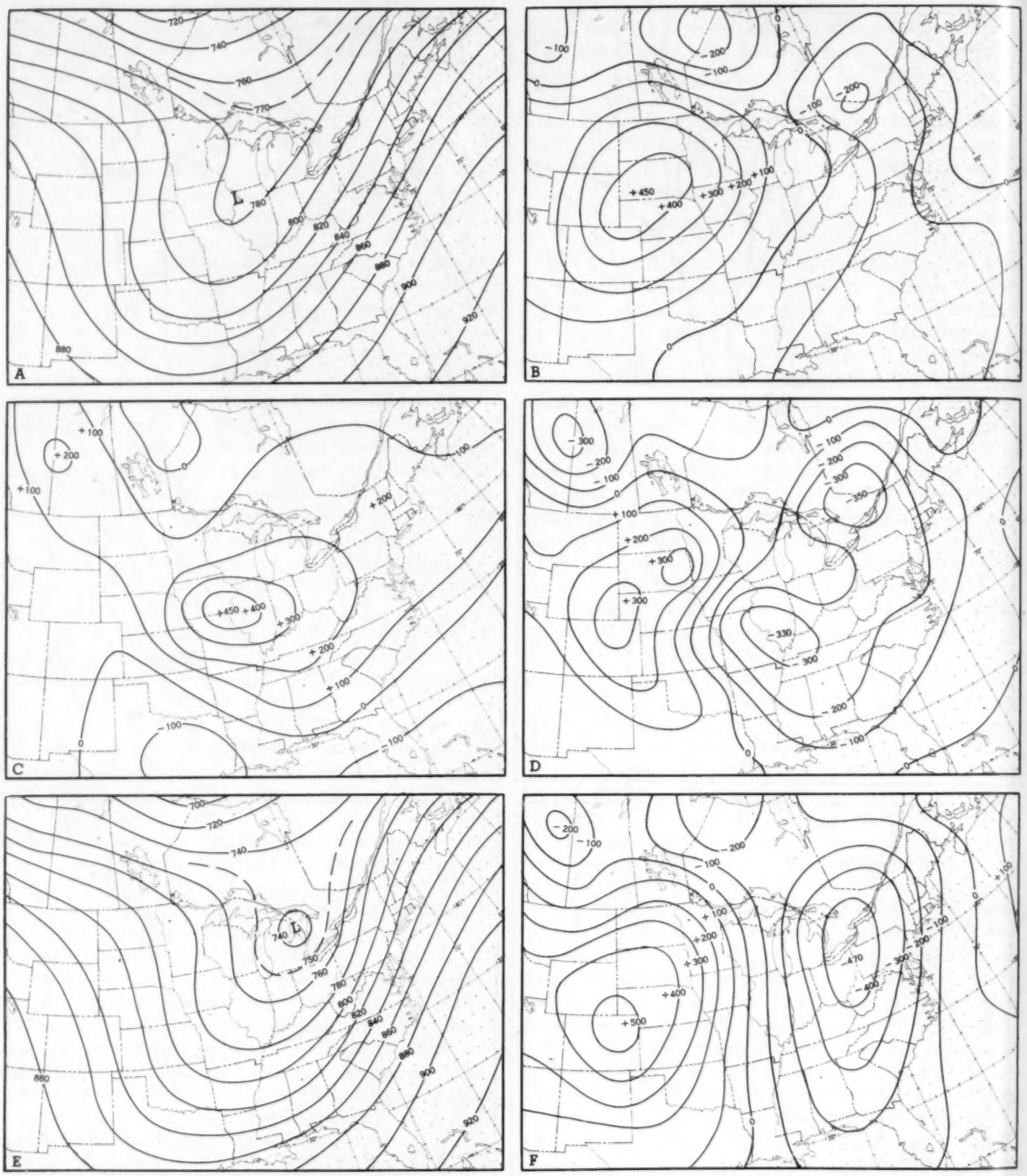

FIGURE 6.—(A) 500-mb. barotropic 12-hour forecast from 0300 GMT, Dec. 24, 1956 and (B) the height change (in feet) it represents. (C) Error of forecast height change. (D) Observed 12-hour height change from 0300 GMT. (E) 500-mb. thermotropic 12-hour forecast from 0300 GMT, and (F) the height change it represents.

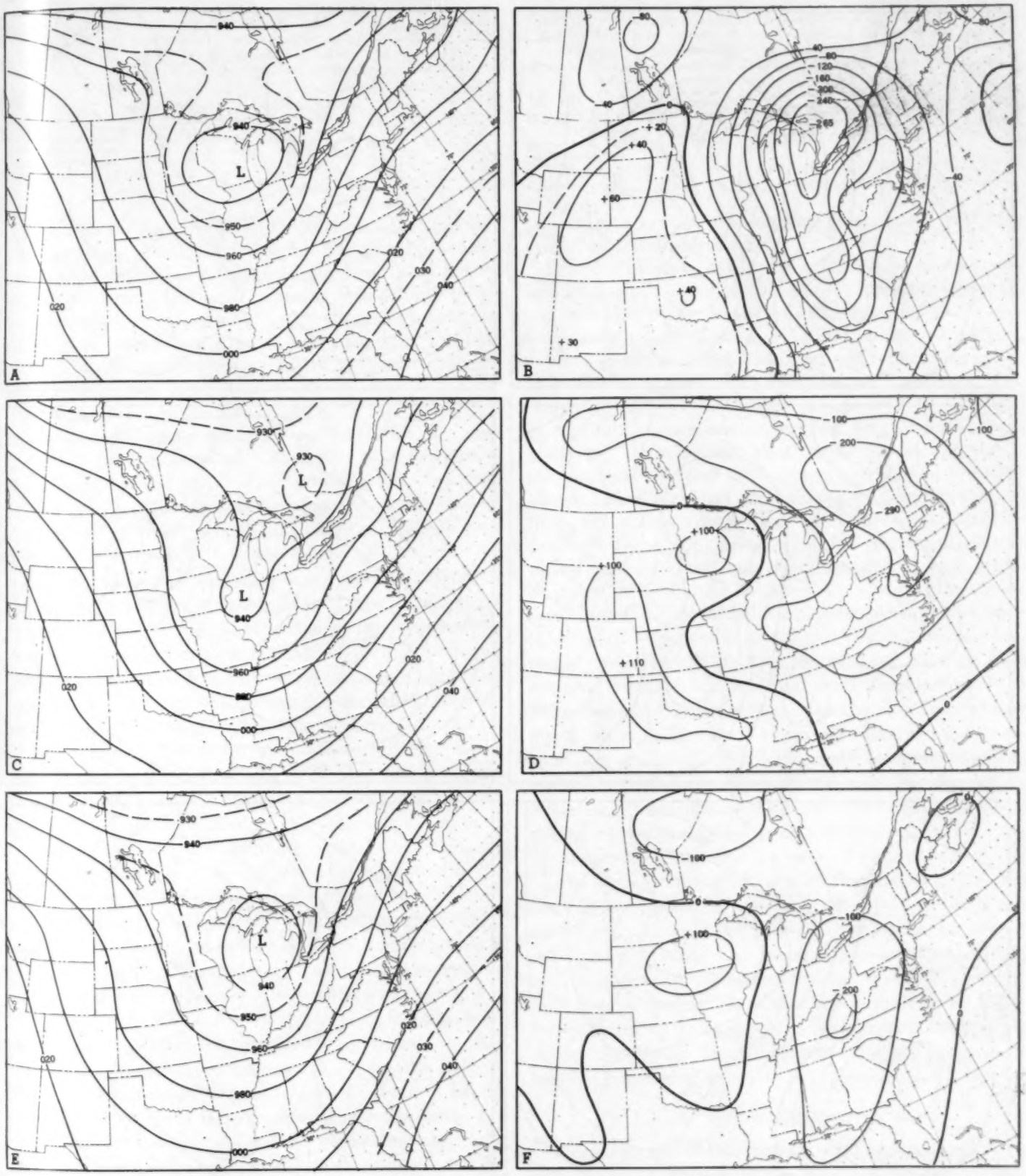

FIGURE 7.—(A) 700-mb. analysis for 0300 GMT, Dec. 24, 1956 and (B) 12-hour forecast height change made from it using all four terms of eq. (1). (C) 700-mb. analysis for 1500 GMT, Dec. 24, 1956 and (D) 12-hour observed height change from 0300 GMT. (E) 700-mb barotropic 12-hour forecast from 0300 GMT, Dec. 24, 1956 and (F) the height change it represents.

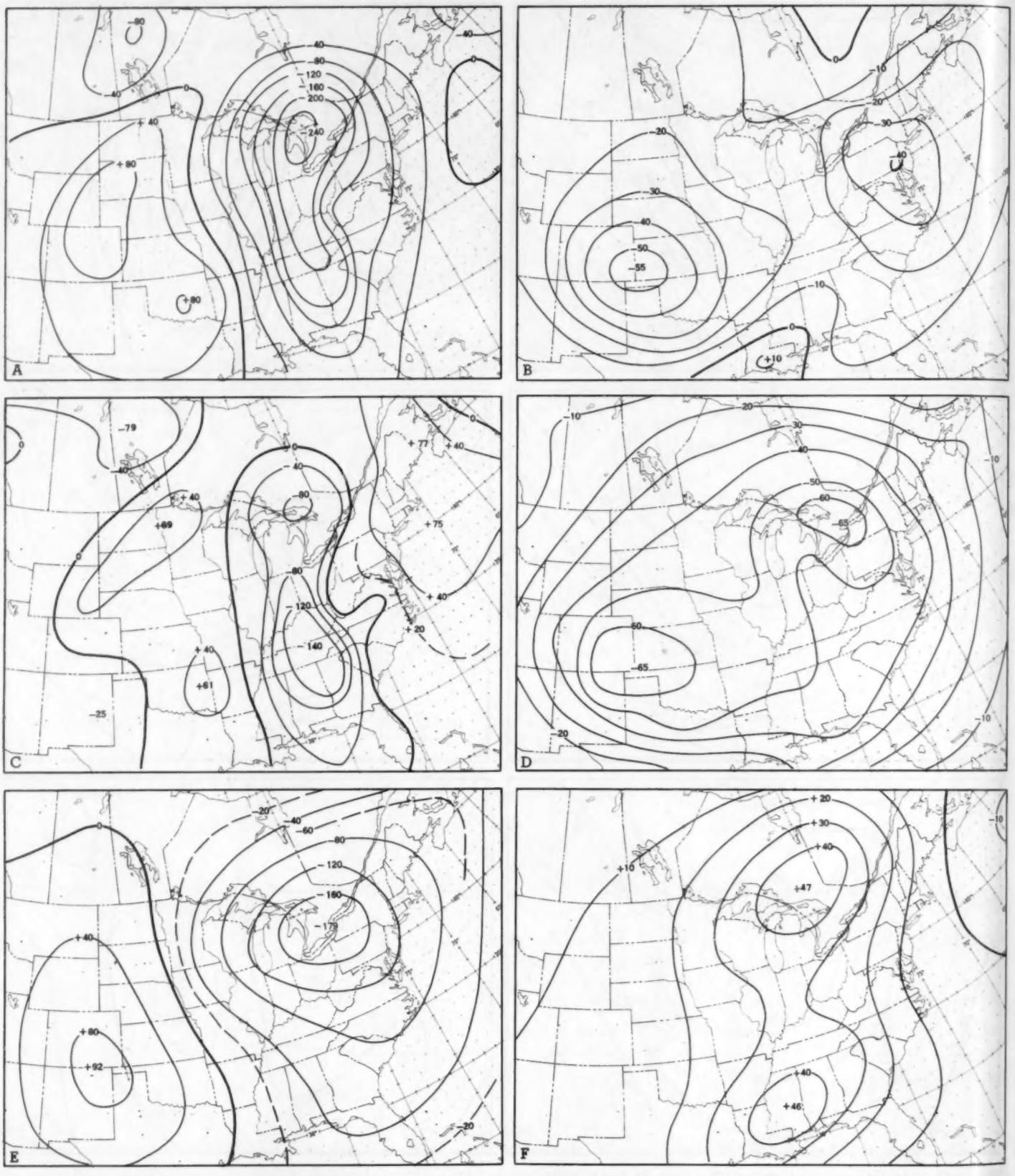

FIGURE 8.—700-mb. 12-hour forecast height change (in feet) from 0300 GMT, Dec. 24, 1956 made from (A) horizontal advection and divergence terms, $-\mathbf{V}\cdot\nabla\eta+\eta(\partial\omega/\partial p)$; (B) vertical advection and twisting terms, $-\omega(\partial\eta/\partial p)-[\nabla\omega\times(\partial\mathbf{V}/\partial p)]\cdot\mathbf{k}$; (C) horizontal advection term, $-\mathbf{V}\cdot\nabla\eta$; (D) vertical advection term, $-\omega(\partial\eta/\partial p)$; (E) divergence term, $\eta(\partial\omega/\partial p)$; (F) twisting term, $-[\nabla\omega\times(\partial\mathbf{V}/\partial p)]\cdot\mathbf{k}$.

TABLE 1.—*Mean absolute and mean algebraic values in ft./12 hours for 10×13 grid points of the individual terms of the vorticity equation at 700 mb. for 1500 GMT, October 5, 1956.*

Term	Mean absolute value	Mean algebraic value
Horizontal advection	54.5	−10.3
Divergence	21.1	−3.3
Vertical advection	6.1	3.0
Twisting	4.9	−2.5

TABLE 2.—*Mean absolute and mean algebraic values in ft./12 hours for 10×13 grid points of the individual terms of the vorticity equation at 700 mb. for 0300 GMT, December 24, 1956.*

Term	Mean absolute value	Mean algebraic value
Horizontal advection	58.4	−0.3
Divergence	18.3	1.8
Vertical advection	7.1	4.0
Twisting	7.0	−2.5

Although the magnitudes of the vertical advection and twisting terms calculated at 700 mb. for a grid point are small when compared to those of the horizontal advection or divergence terms, the values of each of these terms in equation (1) are predominantly of one sign over the entire grid, the twisting term being negative and the vertical advection term being positive and also the larger of the two terms in absolute value[5] (tables 1 and 2). Their individual contributions (figs. 4D, F and 8D, F) to a height change forecast can be a large fraction of the contributions of the horizontal advection and divergence terms (figs. 4A and 8A). To take this and the fact that they tend to counterbalance each other into consideration, a successful forecasting model would either exclude both or never include one without the other.

Although these two terms may exactly counterbalance in the mean over a large area, their fields of positive and negative contributions to the height tendency are not necessarily exactly superimposed (figs. 4B and 8B), which probably warrants their consideration in any serious attempts in extended period numerical forecasting for which the vorticity equation is employed. The twisting term should have a minimum value (greatest absolute value) at the level in the atmosphere where vertical wind shear and the horizontal gradient of vertical velocity are greatest and most nearly perpendicular [9]. This should be at or just above the level of maximum vertical flow where its magnitude should be 50 to 100 percent greater than at 700 mb. The vertical advection term, equation (1), which is a function of vertical velocity and vertical gradient of vorticity, is positive at levels in the lower troposphere where systems slope upstream with altitude; it is negative in the narrow bands between the positions of the troughs and ridges of the level for which the term is being computed and the vertically projected positions of the zero line of the 500-mb. vertical motion. When the field of the vertical advection term is relaxed to obtain a height change forecast, these narrow bands of negative values are more than counterbalanced by the predominance of surrounding positive values; however their effect can be noticeable in dividing the forecast height change field (fig. 8D) into two separate centers. The vertical advection term should have a maximum value approximately 50 percent greater than the 700-mb. value at some level near that of maximum vertical flow.

Ignoring friction, radiation, surface heating and cooling, release of heat of condensation, truncation error, error introduced by boundary assumptions, and other supposedly minor effects and considerations, we can both explain and understand the barotropic forecasting model to a certain degree. As stated, not all barotropic forecasts will verify as did the two cases presented. The level of maximum and minimum vertical flow varies in space and time. It is conceivable that the pre-selected equivalent barotropic level of the barotropic model be either above or below the level of maximum or minimum vertical flow over a large area for a period of time, which means that were the divergence term considered its contribution to the forecast at the equivalent barotropic level would be great. The relative accuracy of individual barotropic forecasts can be accounted for then by either or by a combination of two possibilities. (1) The equivalent barotropic level coincides in the mean in space and time with the level of maximum and minimum vertical flow. (2) The effects of divergence, vertical advection, and twisting terms cancel each other. If we make the reasonable assumption of no limitation in electronic computer capacity, the major problem in developing a baroclinic forecasting model as a substitute for the barotropic forecasting model is that of computing in space and time an accurate approximation of the vertical profile of vertical motion. It can be stated that the 500-mb. vertical velocity used and the vertical profile of vertical motion between 1000 mb. and 500 mb. assumed for these two case studies are subject to criticism. On the other hand independent studies [3, 5] tend to support these assumptions as do the 700-mb. 12-hour height tendency forecasts herein presented. When the problem of computing accurate vertical motion is solved finally an important milestone of progress in weather forecasting will have been passed.

ACKNOWLEDGMENTS

The authors wish to express special appreciation to Lt. Col. Philip D. Thompson for his many informative discussions and valuable suggestions and for reading the manuscript. We are also indebted to Mr. Geirmundur 'Arnason, Dr. George P. Cressman, and Mr. Edwin B. Fawcett for their encouragement, guidance, and suggestions.

[5] 'Arnason and Carstensen [8] have since determined that inconsistent truncation in computing values of these two terms would allow the twisting term to be relatively somewhat larger in magnitude.

REFERENCES

1. F. G. Shuman, "Predictive Consequences of Certain Physical Inconsistencies in the Geostrophic Barotropic Model," *Monthly Weather Review*, vol. 85, No. 7, July 1957, pp. 229–234.
2. P. D. Thompson and W. L. Gates, "A Test of Numerical Prediction Methods Based on the Barotropic and Two-Parameter Baroclinic Models," *Journal of Meteorology*, vol. 13, No. 2, April 1956, pp. 127–141.
3. G. 'Arnason, "A Case Study of the Fields of Large Scale Vertical Velocity and Horizontal Divergence," Massachusetts Institute of Technology, Technical Report No. 16 on Contract N5 ori–07804, May 15, 1955.
4. J. S. Winston, "Physical Aspects of Rapid Cyclogenesis in the Gulf of Alaska," *Tellus*, vol. 7, No. 4, November 1955, pp. 481–500.
5. H. A. Panofsky et al., "Vertical Motion and Weather," Pennsylvania State University, Scientific Report No. 2, on Contract No. AF19(604)–1025, January 1, 1957.
6. A. Eliassen, "The Quasi-Static Equations of Motion With Pressure as Independent Variable," *Geofysiske Publikasjoner*, vol. XVII, No. 3, 1949, 44 pp.
7. R. C. Sutcliffe, "A Contribution to the Problem of Development," *Quarterly Journal of the Royal Meteorological Society*, vol. 73, Nos. 317–318, July–Oct. 1947, pp. 370–383.
8. G. 'Arnason and L. P. Carstensen, "The Effects of Vertical Vorticity Advection and Turning of the Vortex Tubes in Hemispheric Forecasts with a Two-Level Model," *Monthly Weather Review*, (to be published).
9. R. J. Reed and F. Sanders, "An Investigation of the Development of a Mid-Tropospheric Frontal Zone and Its Associated Vorticity Field," *Journal of Meteorology*, vol. 10, No. 5, Oct. 1953, pp. 338–349.

ZONAL WIND ERRORS IN THE BAROTROPIC MODEL

C. L. BRISTOR

Joint Numerical Weather Prediction Unit, U.S. Weather Bureau, Suitland, Md.*

[Manuscript received September 11, 1958; revised January 20, 1959]

ABSTRACT

Zonal wind errors in a series of numerical barotropic forecasts are discussed. A characteristic error is the growth of west winds in middle latitudes and their decay to the south. Momentum transport in the absence of momentum sources and sinks in the barotropic model is suggested as the principal contributor to this type of error. Evidence of nonlinear growth of the zonal wind error suggests that use of past errors as a simple linear correction of forecast zonal profiles is not a promising solution of the problem particularly when no provision is made for stabilization of the longest waves. In an attempt to throw some light on the remaining question of what can be done to improve the barotropic model with respect to zonal wind errors, a series of experimental forecasts is made using a form of the barotropic vorticity equation with a persistent frictional term that provides crudely for momentum sources and sinks. Although the results are, to a considerable degree, inconclusive, they suggest that future efforts should be directed toward the inclusion of friction in a more realistic atmospheric model.

1. INTRODUCTION

Since October 1957, barotropic forecasts have been produced by the Joint Numerical Weather Prediction (JNWP) Unit on an octagonal grid covering most of the Northern Hemisphere and extending south of the 500-mb. zone of maximum westerlies in all regions. Prior to this time forecasts were produced on a grid having an extreme boundary problem which tended to compromise the analysis of other types of systematic errors [1]. Since boundary problems have been appreciably reduced with the octagonal grid, the resolution of the remaining types of systematic errors has become a more rewarding task. A persistent retrogression of the longest wave components, particularly in the subtropics, was brought into sharper focus as the largest systematic error. An empirical remedy for this type of error was discussed by Wolff [2] and a less restrictive remedy by Cressman [3].

Another systematic error is immediately apparent when forecasts are verified from the standpoint of the zonal wind. One observes a decrease of west winds to the south in the subtropics and an increase in temperate latitudes.

The purpose of this paper is to present a detailed discussion of the zonal wind errors of a series of 24-, 48-, and 72-hour barotropic forecasts made on a daily basis from October 4, 1957 to May 31, 1958. Also, some interpretation of the errors is attempted and some experiments aimed at providing the best empirical correction are discussed.

2. ZONAL ERRORS

Several diagnostic programs available in the JNWP Unit have made possible the accumulation of an appreciable amount of data describing the behavior of routinely produced barotropic forecasts. One such program produces mean monthly algebraic height error information over the entire grid from 24-, 48-, and 72-hr. forecasts. Further processing yields the resulting zonal wind error patterns. Figure 1 presents this information for the individual months. Here one sees the marked tendency for the forecasts to shift the maximum westerlies to the north. The same general type of error is repeated month after month suggesting a highly systematic error-producing mechanism. Figure 2 presents a day-to-day latitudinal distribution of 48-hr. forecast errors. On occasion the error pattern is interrupted but by and large the same characteristic error pattern appears day after day.

Phillips[1] has suggested momentum transport as the principal contributor to this type of error. In the isobaric system of coordinates (c.f. [4]), combination of the equations of continuity and x-component of motion gives

$$\frac{\partial u}{\partial t}+\frac{\partial (uu)}{\partial x}+\frac{\partial (uv)}{\partial y}+\frac{\partial (u\omega)}{\partial p}-fv+g\frac{\partial z}{\partial x}=0 \qquad (1)$$

where the symbols have their conventional meanings. If equation (1) is integrated around a latitude circle and throughout the depth of the atmosphere the second and sixth terms drop out. The resulting equation in integral form can be regarded as the equation for zonal momentum per unit mass:

$$\frac{\partial}{\partial t}\int_0^{2\pi}\int_0^{p_0} u\,d\lambda\,dp+\frac{\partial}{\partial y}\int_0^{2\pi}\int_0^{p_0} uv\,d\lambda\,dp+\int_0^{2\pi}(u\omega)_{p_0}\,d\lambda=0 \qquad (2)$$

where λ is longitude. The last term enters only at the

*Present affiliation: Meteorological Satellite Section, U.S. Weather Bureau.

[1] Personal communication by Prof. N. A. Phillips during his visit as consultant to JNWP Unit, November 1957. Some aspects of the forecast investigations stemmed from discussions with him during this visit.

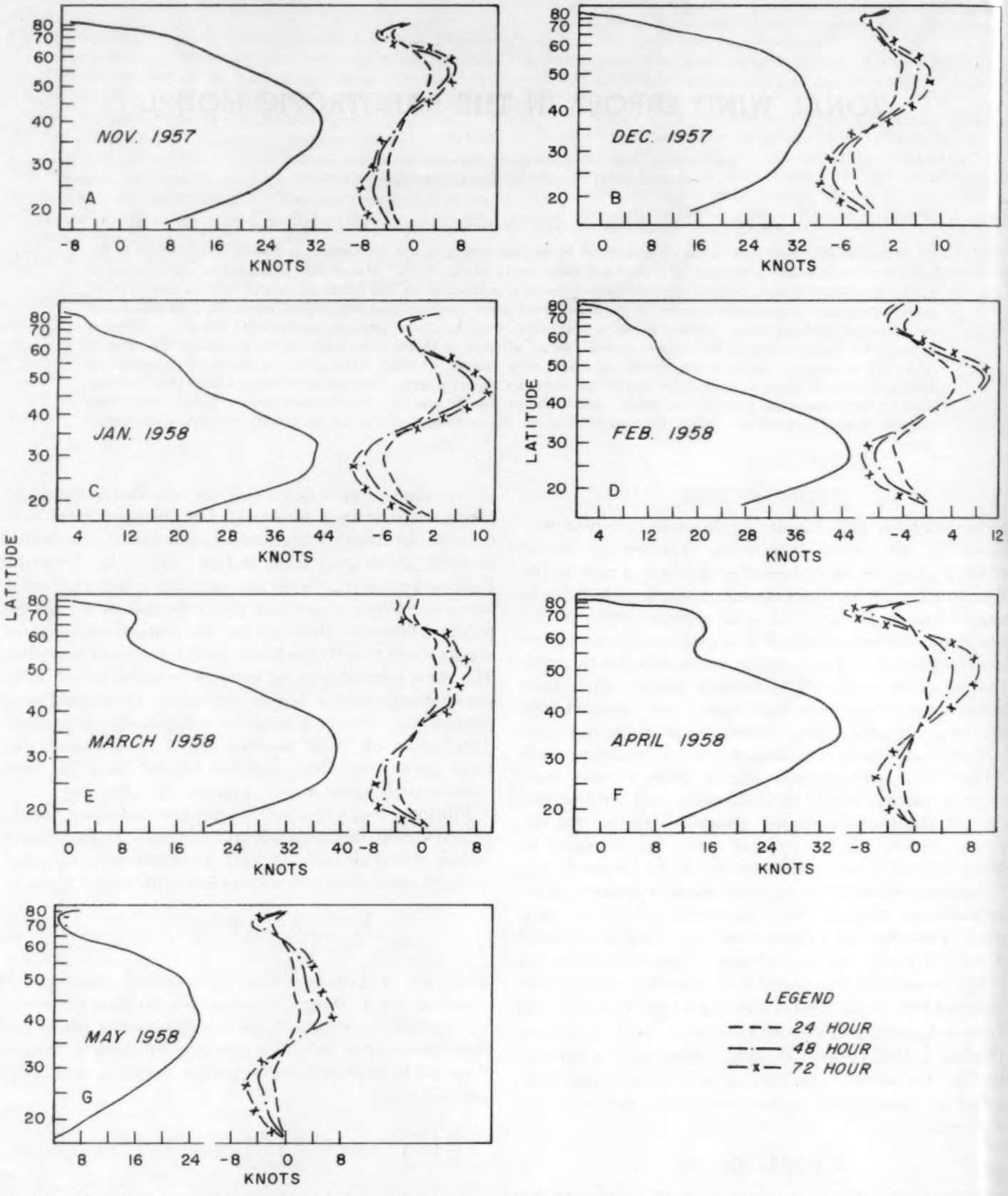

Figure 1.—Monthly average 500-mb. zonal wind profiles and average errors of barotropic forecasts. Beginning on April 10 all forecasts were altered by stabilizing the long waves.

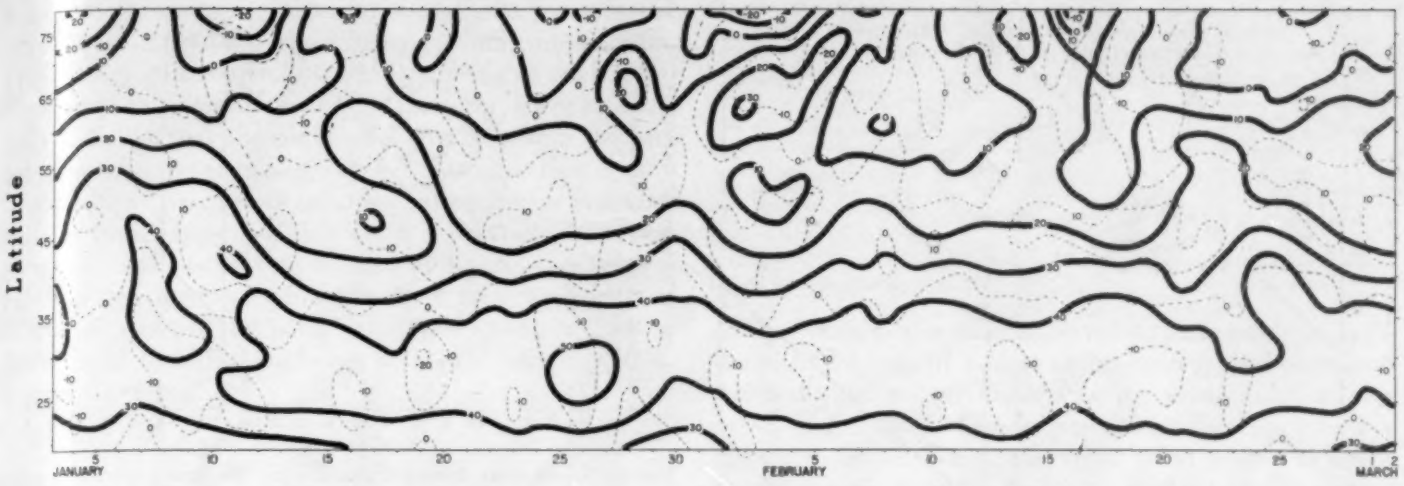

Figure 2.—Daily 500-mb. zonal wind profiles (kt.) for January and February 1958 (heavy lines) and corresponding errors of 48-hour barotropic forecasts (dashed lines).

pressure level near the surface (1000 mb.) since ω is assumed to vanish at the top of the atmosphere. There is thus an implied balance between the horizontal transport and vertical transport (source and sink) terms. From actual winds Buch [5] showed that the maximum northward transport of momentum at 500 mb. occurs near the latitude midway between the low level easterlies (momentum source) in the subtropics and the temperate latitude westerlies (momentum sink). It seems likely that the behavior of the barotropic model with regard to zonal wind errors reflects this same process, the momentum transport being a function of the orientation (tilt) of troughs and ridges, as noted earlier by Starr [6], and the observed errors thereby arising from the lack of momentum sources and sinks in the model.

It is interesting to examine some of the day-to-day fluctuations from this standpoint. A search through the 500-mb. maps for October 1957 indicated that the orientation of troughs south of 35° N. on October 22 was least favorable for the northward transport of momentum, but on the 26th was particularly favorable. These maps are presented in figure 3. The zonal wind errors (in knots) in the 48-hr. forecasts from these days are inserted in figure 3 over Mexico and the western States. It is noteworthy that the zonal wind errors south of 35° N. are strikingly different in the two cases, the depletion of west winds

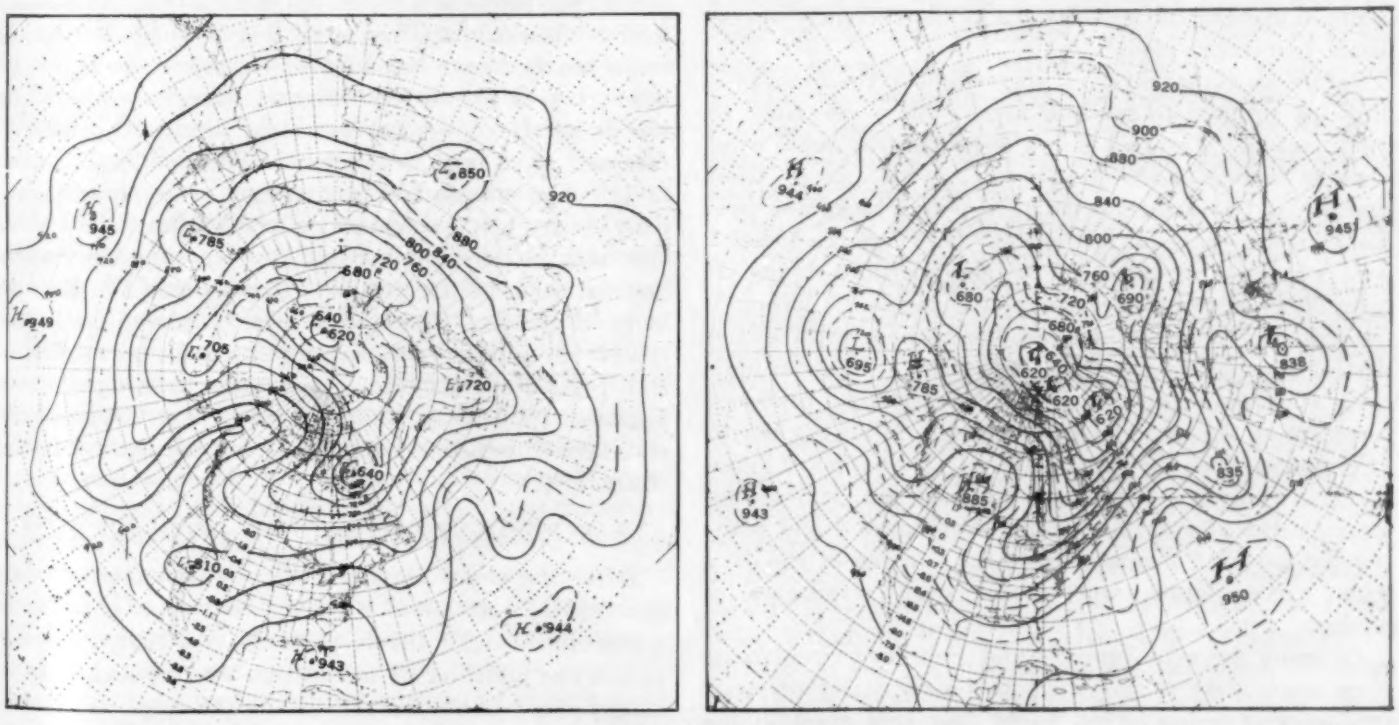

Figure 3.—Initial 500-mb. patterns and zonal wind error (listed near 105° W.) of the resulting 48-hour barotropic forecasts. (A) 0000 GMT, October 22, 1957, an example of a major northwest-southeast trough; (B) 0000 GMT, October 26, 1957, an example of a major northeast-southwest trough.

500931—59——3

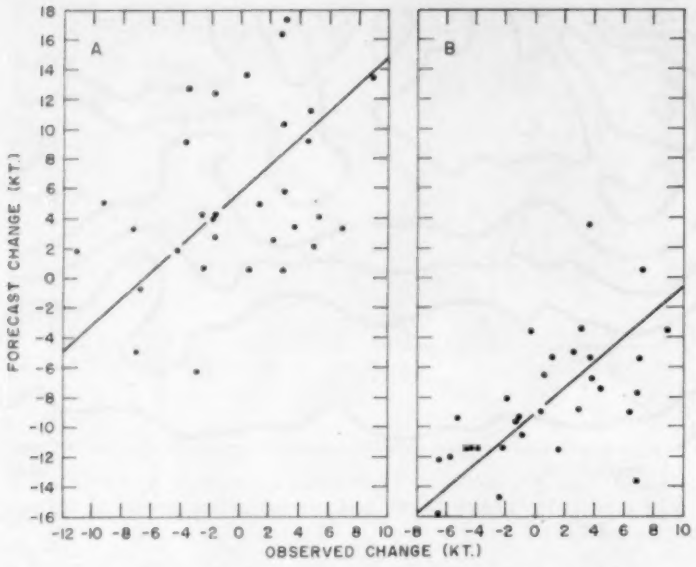

Figure 4.—48-hour forecast zonal wind changes plotted against observed zonal wind changes, January 1958. (A) 42° N., (B) 30° N.

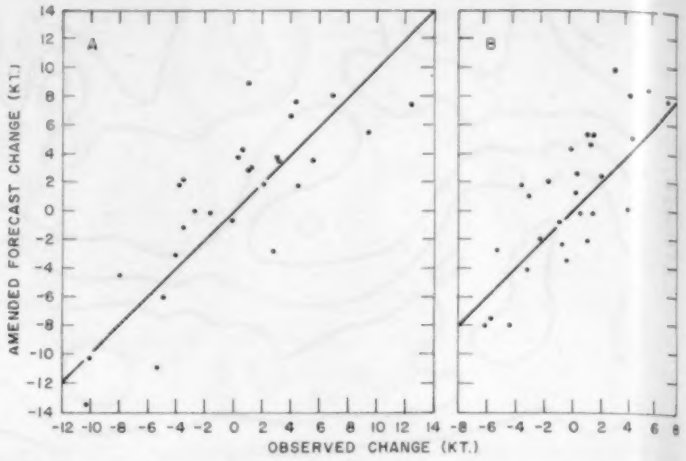

Figure 5.—48-hour forecast zonal wind changes (amended using fig. 4) plotted against the observed change, February 1958. (A) 42° N., (B) 30° N.

in the subtropics being almost negligible in the October 22 case and more than twice the monthly average in the October 26 case.

From the above discussion it is obvious that, even in the short-range forecast problem, fundamental questions of the general circulation are important. Clearly, any highly realistic atmospheric model must contain a momentum budget mechanism even for forecasts of a day or two. Short of models with such a physical mechanism there is a question of what might be done semi-empirically to improve less elegant models such as the currently operational barotropic model.

Before we make empirical corrections to the zonal profile, it is prudent to ask how much skill is contained in the forecasts. Figure 4 shows 48-hr forecast zonal wind changes versus corresponding observed zonal wind changes at two arbitrary latitude points along the profile. Figure 4A is for latitude 42° N. where the forecast west wind was in excess of the observed and figure 4B is for 30° N. where the reverse relation existed. Although the scatter of points is appreciable, definite skill beyond that of a persistence forecast is evident. Figure 5 indicates appreciable success of the operationally produced forecasts at the same latitudes for the following month (February) when they are modified by the curves of figure 4. The February forecasts were modified by entering them on the appropriate ordinate of figure 4 and reading the modified forecasts from the abscissa of the January curve. Here improvement over persistence is obvious.

In many respects January and February circulations were much alike as indicated in the similarity of zonal profiles and errors. One might therefore question the utility of such relationships for other months. However, the zonal error patterns do not show abrupt changes from month to month as do the zonal profiles themselves. For example, the crest of maximum west wind in the zonal profile changed abruptly from a weaker than normal and north of normal pattern in December to a stronger than normal and south of normal picture in January. During this same period the mean 24-hr. zonal wind error profile did not undergo any shift in phase and changed only slightly in amplitude and general shape.

Evidence of nonlinear growth of zonal wind error is also apparent, particularly in figure 1A through E. Such a situation would tend to hamper any attempt to use evidence of past errors as a simple linear persistence type correction. The retrograde long waves, an improper feature of the prediction model [2], may interact to enhance such nonlinearity. This possibility is suggested by the more nearly linear behavior of the errors in figure 1F where two-thirds of the forecasts have been altered by stabilizing the long waves and in figure 1G where all forecasts have been thus altered. Without stabilization of the long waves, forecast troughs were characteristically skewed by moving too slowly at low latitudes and too fast at high latitudes. Such skewing suggests possible augmentation of the northward transport of momentum in the forecasts. The stabilization technique (to be discussed in section 3) effectively forecasts persistence of that portion of the motion contained in the longest waves. Unfortunately no extended record of stabilized and unstabilized forecasts was available for comparison in this study.

3. EXPERIMENTAL FORECASTS WITH FRICTION

After the above diagnosis of zonal wind errors there remains the question of what can be done to improve the barotropic model in this respect. N. A. Phillips [2] has suggested the addition of momentum sources and sinks by means of a friction term involving the zonal wind in the layer of turbulent mixing. In practice, if such a model

[2] See footnote 1 on p. 57.

is to remain a single parameter model, the wind in the lower layer must be derived from 500-mb. information. Preliminary calculations by Phillips revealed such a derived wind to be unsatisfactory. However, there remains the possibility that the zonal wind profile within the turbulent mixing layer changes rather slowly so that it may provide beneficial, persistent, momentum source and sink regions throughout the forecast computation. The assumption that momentum sources and sinks can be provided in the equations of motion by a term proportional to the negative of the wind velocity near the surface in the layer of turbulent exchange yields the vorticity equation in the form

$$\frac{\partial \zeta}{\partial t} = -\mathbf{V} \cdot \nabla \zeta - \beta v - K\zeta_0 \tag{3}$$

where ζ is relative vorticity, $\mathbf{V}$ is the wind vector, β is the Rossby parameter, K is a coefficient involving the turbulent exchange of momentum between the earth's surface and the free air through convective eddies, and all quantities refer to the level of nondivergence (assumed to be 500 mb.) except where subscript o designates a surface value.

A barotropic forecast code was modified to include a full field of the third term on the right of equation (3). This field suitably scaled, was created using the relation

$$\zeta_0 = -\frac{\partial \overline{U}_0}{\partial y}, \tag{4}$$

where $\overline{U}_0$ is the zonal profile of the initial wind near the surface. This term was added as a persistent correction at each hourly time step. Such a zonally symmetric correction must obviously be harmful over some areas on occasion even though the over-all effect is beneficial because, in general, the zonal wind profile does not change a like amount in all longitudinal sectors.

Six comparative forecasts have been made with this procedure in order to judge its effect in several different synoptic situations. Other comparisons were also made by testing a corrective profile based on a time average during the forecast rather than on persistence and using 850-mb. rather than lower-level winds. As a whole these comparisons were inconclusive. Generally the modified forecasts improved the zonal profile in the subtropics but caused further deterioration about as often as improvement at middle and higher latitudes. The assumption of persistence and the choice of wind level in the corrective term seemed to be of only secondary importance. At this stage there seemed to be little point in more tests along this line. The implied balance between momentum source and sink regions and horizontal transport from the standpoint of a simple continuity argument does not appear to be a particularly useful concept when applied on a daily basis. In other words, the compensation for momentum transport at 500 mb. does not seem to be particularly direct.

TABLE 1.—*Root mean square height errors in feet for four forecast techniques. See text for explanation of models*

Initial Date	Forecast Model			
	a	b	c	d
Jan. 12, 1958	212		229	411
Jan. 14, 1958	256	313	252	414
Apr. 14, 1958	246	245	269	(*)
Apr. 16, 1958	186	178	176	
May 18, 1958	165	160	170	

*Not available after April 10, 1958.

The concept of a simple correction thus seems to be reduced to the idea of a more or less stereotyped correction which would remove the systematic error from a large group of forecasts. One way to accomplish this would be merely to impose the initial zonal wind profile as a persistent component in the forecast. Such a technique would preclude realization of inherent skill in predicting the zonal profile as suggested in the scatter diagrams of figures 4 and 5 and as suggested by the slowly changing monthly error profiles. The alternate method would involve the use of equation (3) but with the last term simulated by a mean corrective profile (ideally a concurrent one) as discussed above. The difficulty, of course, still involves the forecast of the mean error profile. Between the drawback of the persistence zonal forecast and the drawback of having to project the mean profile error ahead for several weeks, no choice can be made short of an extended series of tests. Five additional test cases of this type were carried out. Results of two of the five cases are displayed in figures 6 and 7 and are discussed later from the standpoint of zonal errors. Although such a sample is very limited, it is interesting to compare forecasts having zonal corrections with forecasts from the simple non-divergent barotropic model. Apart from zonal wind verification there remains a question of repercussions in other types of verification statistics. Table 1 indicates the root mean square height errors for several competing forecasts in each case.

Column (a) gives the scores of a model somewhat similar to that described in connection with equation (3) except that the long wave components have been stabilized by the inclusion of a fourth Jacobian term. This technique, devised by L. P. Carstensen,[3] uses an additional constant Jacobian field at each time step to stabilize the longest wave components. This Jacobian field, applied in the reversed sense, is merely the advection of relative vorticity of a space-smoothed initial field. The zonal profile term is added as described above except that it is now produced in each case from the vorticity of the 500-mb. mean zonal wind error profile from the preceding month. Column (b) presents results from a modified barotropic code, devised by Wolff [2], which imposes a persistence forecast of the zonal profile as well as waves one, two, and three. The technique which produced the results in column (c) is similar to that of (b) in that long waves

[3] Unpublished.

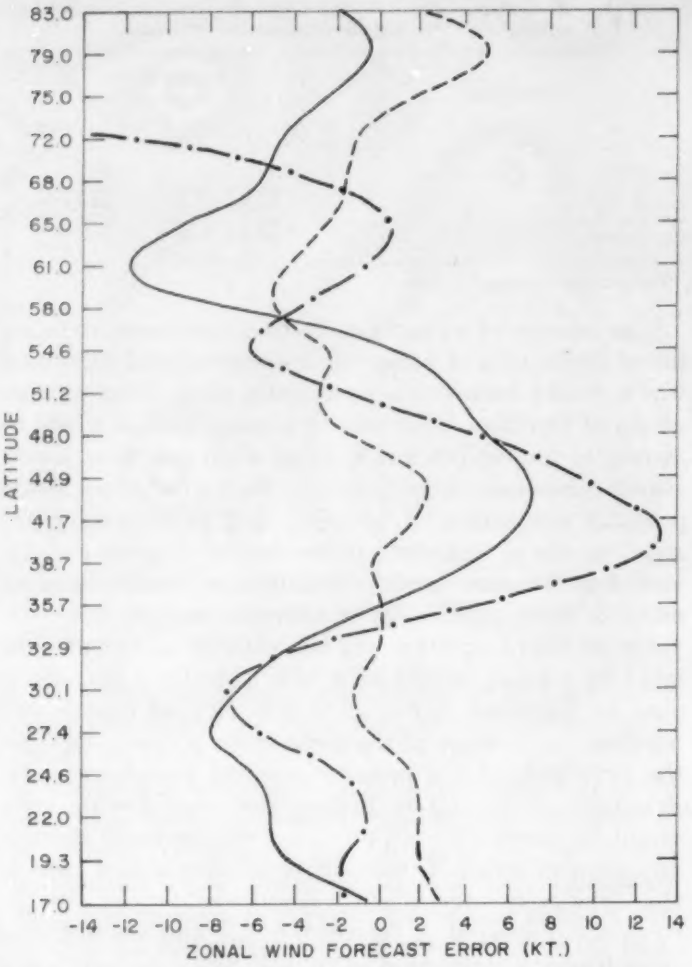

Figure 6.—Comparison of zonal wind errors for 48-hour forecasts from 0000 GMT, January 12, 1958 and produced by the non-divergent operational barotropic model (solid line), a modified model with long waves stabilized and a zonally symmetric correction (dashed line), and by persistence (dash-dot line).

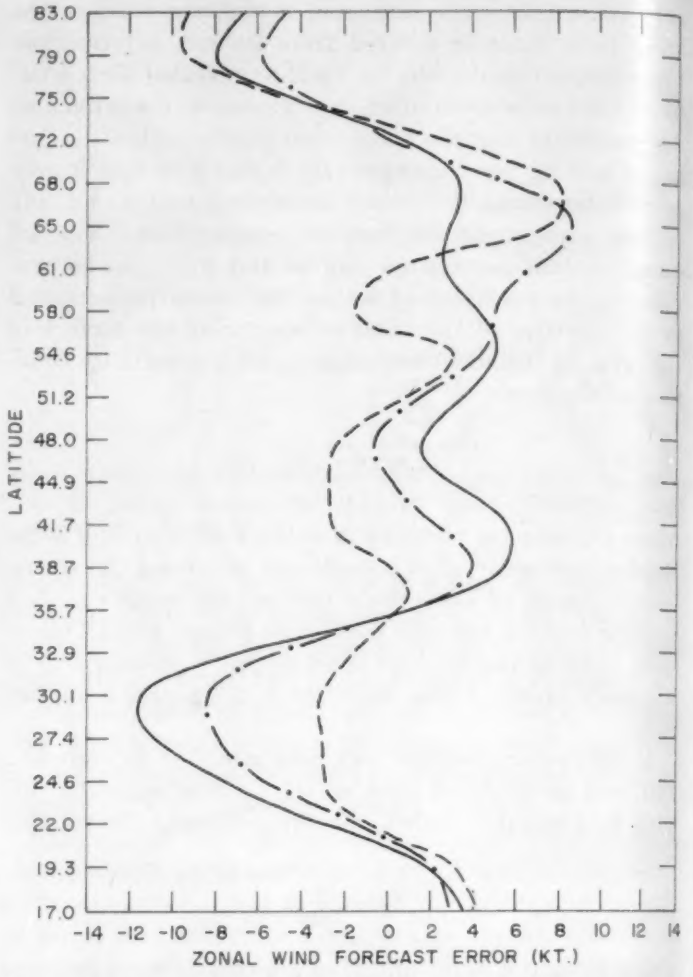

Figure 7.—Comparison of zonal wind errors for 48-hour forecasts produced by the same methods as in figure 6 from 0000 GMT, May 18, 1958.

are stabilized, but the zonal profile is not altered. Column (d) presents simple non-divergent barotropic forecast scores.

In view of the small sample size and the difference in long wave treatment there appears to be little difference between the root mean square height errors of the first three methods when considering 48-hr. forecasts. There is perhaps a slight indication that both methods for correcting the zonal errors would provide an average improvement in root mean square height error. (Two cases extended to 72 hours by P. M. Wolff indicate substantial improvement of method (b) over method (c).) From the standpoint of verification of zonal values, method (b) would obviously be less successful for cases with rapidly changing profiles. As shown in figure 2, forecasts from 0000 GMT January 12, 1958 involve this problem. The zonal errors of methods (a), (b), and (c) for this case are presented in figure 6. Here a persistence forecast has a damaging effect whereas method (a) seems to behave satisfactorily. Figure 7 presents the case from 0000 GMT May 18, 1958 which displayed a rather cut-up pattern of zonal wind changes (the negative of the persistence curve). Here persistence proved to be the better forecast although method (a) was, in general, an improvement over method (c).

4. CONCLUSIONS

Barotropic forecasts on a hemispheric scale contain an error in the zonal wind which is highly systematic in the sense that the belt of maximum westerlies is moved too far to the north. The local 48-hr. zonal wind error on either side of the maximum westerlies amounts to about 20 percent of the maximum zonal wind. Inspection of individual cases where troughs have extreme tilt lends considerable support to the suggestion that these errors are

related to momentum budget deficiencies of the model. Experiments with modified barotropic forecast codes indicate the possibility of improving the forecasts from the standpoint of zonal winds through the application of a zonally symmetric correction based upon an average of past errors.

Less improvement is obtained in similar experiments which utilize a zonal friction term obtained from the initial surface map.

In either case any improvement from the zonal standpoint is usually obtained at the expense of harmful results in some local areas—the advantage thereby being a question of usage of the prognostic chart. In view of this impasse it would seem that future efforts should be directed toward the inclusion of friction in a more realistic model.

REFERENCES

1. G. P. Cressman and W. E. Hubert, "A Study of Numerical Forecasting Errors," *Monthly Weather Review*, vol. 85, No. 7, July 1957, pp. 235–242.
2. P. M. Wolff, "The Error in Numerical Forecasts Due to Retrogression of Ultra-Long Waves," *Monthly Weather Review*, vol. 86, No. 7, July 1958, pp. 245–250.
3. G. P. Cressman, "Barotropic Divergence and Very Long Atmospheric Waves," *Monthly Weather Review*, vol. 86, No. 8, Aug. 1958, pp. 293–297.
4. R. C. Sutcliffe, "A Contribution to the Problem of Development," *Quarterly Journal of the Royal Meteorological Society*, vol. LXXIII, No. 317–318, July/Oct. 1947, pp. 370–383.
5. H. S. Buch, "Hemispheric Wind Conditions During the Year 1950," Massachusetts Institute of Technology, General Circulation Project, Final Report Part 2, contract AF 19(122)–153, May 31, 1954, 126 pp.
6. V. P. Starr, "An Essay on the General Circulation of the Earth's Atmosphere," *Journal of Meteorology*, vol. 5, No. 2, 1948, pp. 39–43.

Weather Note

LUMINOSITY ACCOMPANYING ST. LOUIS TORNADO—FEBRUARY 10, 1959

BERNARD VONNEGUT

Arthur D. Little, Inc., Cambridge, Mass.
March 20, 1959

Newspaper accounts of the 1959 St. Louis tornado which occurred at about 2:20 a.m. have described various luminous phenomena that accompanied this tornado. For example, one observer was quoted as saying, "I saw a blue flash of light and I heard a terrible roar." Another observer stated, "There was a terrific glow of light as if a cloud was illuminated, and there was a sound like the roar of a tremendous automobile racing its engine."

These accounts appear similar to Montgomery's[1] description of the Blackwell, Okla. tornado of May 25, 1955. He stated, "The fire up near the top of the funnel looked like a child's Fourth of July Pinwheel."

In an effort to learn more about the details of this luminosity, we wrote a letter to the editor of the *St. Louis Post Dispatch* requesting information from readers who might have witnessed such phenomena. Over a dozen people responded to this request and sent in letters describing their observations. The following accounts were taken verbatim from some of the letters that were sent in describing the February 10 tornado:

1. "The approach of the St. Louis 2:20 a.m. tornado was a continuous illumination not *streaks* or *strokes* as in an electric storm.

"The continuous sort of flat lightning is always an indication of wind and hail.

"I have observed such performances for a number of years, not to say that just when and where it would strike, but one can tell about that there is something coming. Continuous illuminated cloud is what I saw again from 1:30 a.m. till 2:20 a.m. when soon I heard what had happened, passing overhead, but 1½ miles to the south of where I am located, I heard the roar, a sound as if a 100-car freight train was passing by." (Martin Maurer)

2. "The lightning was not close nor did it occur often. But there were two freak shows which I had never seen before. The first in the southeast as a brilliant pink which lasted a few seconds, followed by a pale green which also lingered. It was not a streak but more like a sunset effect and clouds were outlined against it.

"The second was in the northeast and entirely different being a flame-like flare right up from the horizon just as though it were from a burning building. It was followed by a second one just like it and in the same general direction." (Miss Genevieve Plummer)

3. "The night of the storm I awoke at 2 o'clock. I thought it seemed to me it was raining hard so I arose and looked out. At once I saw a big ball of fire in the sky to the east. It looked different kind of bright yellow and then there was a long flash not like usual but very bright and to me it looked like the shape of a broad sword not slim like the flashes I have seen before." (Mrs. M. Hatch)

4. "On the night of the storm I woke as the result of heavy thunder (apparently about 2 a.m. or shortly after). The thunder stopped and a *very* heavy rain came against the west windows at about the strength of a strong fire hose. The windows did not break. After only a minute or two the rain stopped suddenly and a peculiar very rapid lightning flashing began flashing through the west window. My windows were covered by a transparent mesh-type curtain (glass fiber) so that I could see the light but their translucency did not allow me to see more and I did not realize there was more to be seen than an ordinary bad thunderstorm.

"This lightning flashing was very rapid—perhaps two or three flashes per second and not as brilliant as the usual big flash preceding a thunderclap. This flashing passed the west windows moving rapidly north and in a few moments was passing the north window going northeasterly (presumably—at least it passed by each window in about the same way. Total time of passage past both windows perhaps 3–4 min.). I don't recall hearing any sound as this rapid flashing was going on, but my windows were closed, and I was probably in a half-sleep condition." (L. B. Spiess)

[1] Floyd C. Montgomery, *Monthly Weather Review*, May 1955, vol. 83, No. 5, p. 109.

A THEORETICAL ESTIMATE OF DRAFT VELOCITIES IN A SEVERE THUNDERSTORM

DANSY T. WILLIAMS

District Meteorological Office, U.S. Weather Bureau, Kansas City, Mo.

[Manuscript received October 2, 1957; revised January 19, 1959]

ABSTRACT

Small scale surface divergence in the vicinity of a severe thunderstorm and an assumed distribution of divergence with height are used with the mass-continuity relationship to yield vertical velocity. In the case studied a maximum updraft of 218 ft. sec.$^{-1}$ and a maximum downdraft of 143 ft. sec.$^{-1}$ are computed.

1. INTRODUCTION

The Thunderstorm Project [1] has measured the magnitude of vertical motions in thunderstorms by growth of radar echoes and by displacement of aircraft in flight. Updraft velocities as great as 85 ft. sec.$^{-1}$ and downdraft velocities as great as 79 ft. sec.$^{-1}$ were evaluated. However, the storms sampled by the Thunderstorm Project were generally not severe,[1] and the magnitude of draft velocities in severe thunderstorms must be estimated indirectly.

Vertical motion, including draft velocities, can be computed by the mass-continuity relationship, using suitable values of horizontal velocity divergence integrated through a column. In order to obtain realistic values of the vertical motions in thunderstorms, however, the divergence must be computed for an area whose size is similar to that covered by the thunderstorm itself. Surface divergence on this scale can be computed from micronetworks of stations, such as used by the U.S. Weather Bureau's Thunderstorm Project and Cloud Physics Project. However, the lack of micro-scale wind observations aloft prohibits any computation of small-scale divergence above the surface, and some assumed distribution of divergence with height is required in order to estimate the draft velocities.

The case to be presented occurred over the surface micro-network of the U. S. Weather Bureau's Cloud Physics Project, Wilmington, Ohio, on March 19, 1948. The squall-line thunderstorms were locally severe with surface wind speeds in excess of 78 m.p.h. (limit of the wind speed recorders), and damage occurred to a number of farmsteads in the path of the storms. A description of some of the features of this case has been reported in a previous paper [2]. A micro-scale synoptic chart, showing the position of the squall line and a micro-Low at 1400 EST, is shown in figure 1. It is felt that this storm was of considerably greater severity than any sampled by the Thunderstorm Project aircraft. Estimates of the draft velocities should, therefore, be of interest.

[1] The U.S. Weather Bureau defines a severe thunderstorm as one in which surface wind gusts of 75 m.p.h. or greater, surface hail ¾ inch in diameter or greater, extreme turbulence, and/or tornadoes occur.

2. ASSUMPTIONS

The theoretical estimates made in this study are based on the assumptions that:

(1) Divergence at the surface is compensated by divergence of the opposite sign aloft. Compensation due to surface pressure changes is assumed to be negligibly small.

(2) Mass divergence at the 12-km. level is of equal magnitude and opposite sign to that at the surface. The choice of the 12-km. level is somewhat arbitrary. It was chosen since 12 km. is a level at which the top of the thunderstorm might be found.

(3) The distribution of mass divergence from the surface to the 12-km. level conforms to a cosine curve in the interval 0 to π, i.e.:

$$(\mathrm{Div}_2 \rho \mathbf{V})_z = (\mathrm{Div}_2 \rho \mathbf{V})_0 \cos\left(\frac{\pi z}{12}\right) \tag{1}$$

where Div_2 is the horizontal divergence operator, ρ is density, z is height, $\mathbf{V}$ is wind velocity, subscript z designates a value at any height z ($0 \leq z \leq 12$ km.), and subscript 0 at the surface. The choice of this distribution is somewhat arbitrary, too. A similar assumption was made by Beebe and Bates [3], although a lower height was used, and velocity divergence rather than mass divergence was considered.

(4) The vertical motion field depends completely upon the divergence field, regardless of the conditions that cause the vertical motion.

(5) In the mass-continuity equation, the local change in density with respect to time is negligibly small. The mass-continuity equation then is:

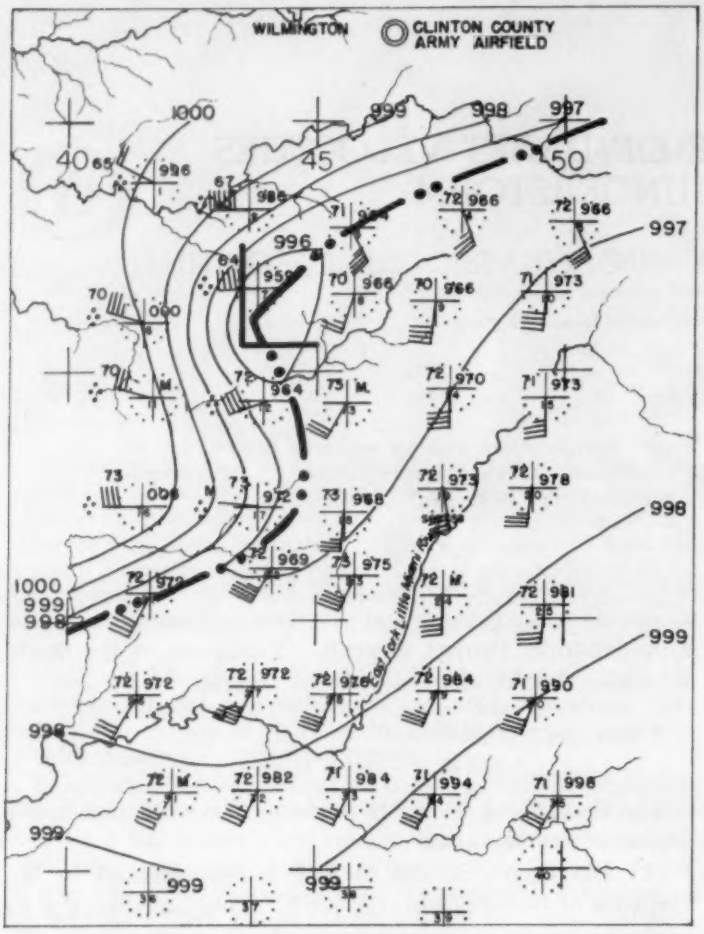

FIGURE 1.—Micro-synoptic surface chart for 1400 EST, March 19, 1948. Note the position of the squall line and micro-Low.

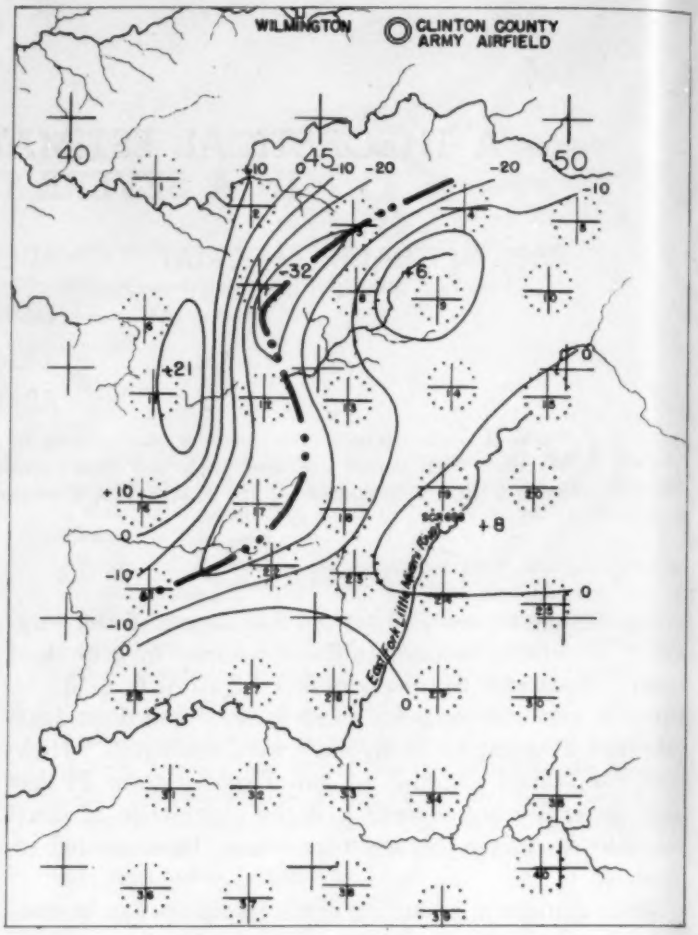

FIGURE 2.—Divergence computed from the wind field for 1400 EST, March 19, 1948. The position of the squall line is shown as a heavy solid line. Isolines of divergence are labeled in units of hr.$^{-1}$ Note the intense center of convergence along the micro-wave of the squall line and the intense center of divergence west of the squall line.

$$-\frac{\partial(\rho w)}{\partial z_i} \cong \mathrm{Div}_2\, \rho \mathbf{V} \tag{2}$$

where w is the vertical component of motion.

Substituting from (1) yields:

$$\frac{\partial(\rho w)}{\partial z} \cong -(\mathrm{Div}_2\, \rho \mathbf{V})_0 \cos\left(\frac{\pi z}{12}\right) \tag{3}$$

(6) The advection of density at the surface and the vertical motion at the surface are negligibly small. The integration of equation (3) between the limits 0 and z then yields

$$w_z \cong -\frac{12\rho_0}{\pi\rho_z}(\mathrm{Div}_2 \mathbf{V})_0 \sin\left(\frac{\pi z}{12}\right) \tag{4}$$

3. COMPUTATIONS

Equation (4) was used to compute the draft velocities w_z in the severe thunderstorm of March 19, 1948. Computations were made at 1-km. vertical intervals; i.e., $z=0, 1, 2, \ldots, 12$. Values of ρ_z were taken from tables of the standard atmosphere. Values of the surface velocity divergence were computed for selected grid position directly from the components u and v of the wind field according to the relationship:

$$(\mathrm{Div}_2 \mathbf{V})_0 = \left(\frac{\partial u}{\partial x}+\frac{\partial v}{\partial y}\right)_0 \cong \left(\frac{\Delta u}{\Delta x}+\frac{\Delta v}{\Delta y}\right)_0 \tag{5}$$

where the finite intervals Δx and Δy were taken as 2 miles. This is the approximate spacing of stations on the micro-network.

Values of the surface velocity divergence for 1400 EST are shown in figure 2. A minimum value of divergence (maximum value of convergence) of -32.0 hr.$^{-1}$ was computed just ahead of the squall line between stations 2, 3, 7, and 8; and a maximum value of divergence of 21.0 hr.$^{-1}$ was computed behind the squall line between stations 6,

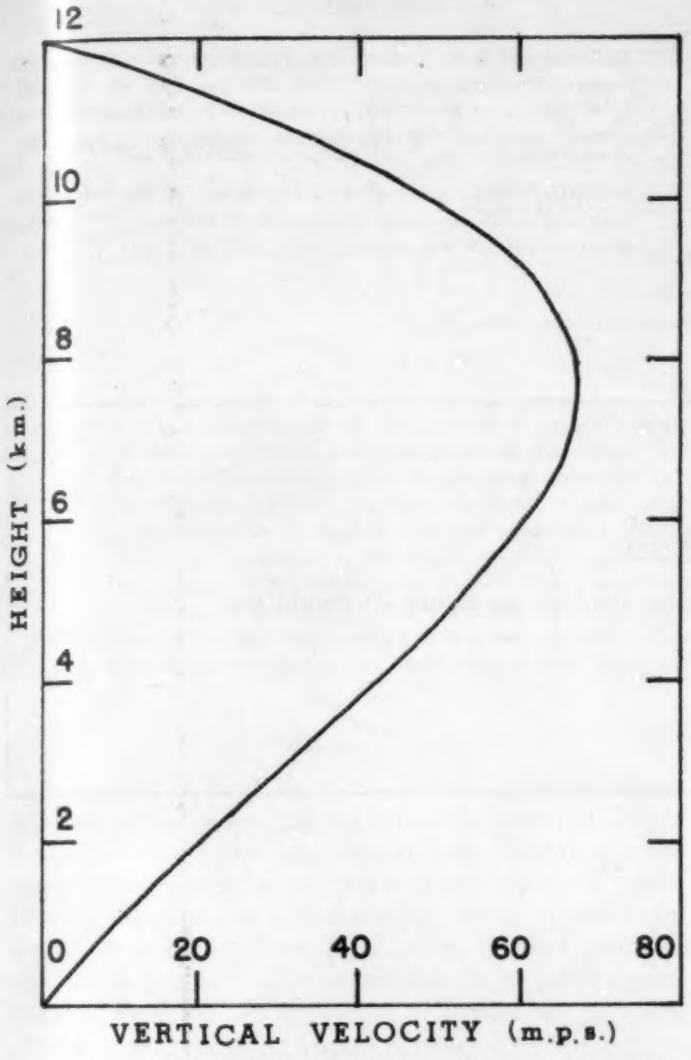

FIGURE 3.—Vertical profile of updraft velocities over a point located between stations 2, 3, 7, and 8 at 1400 EST, March 19, 1948.

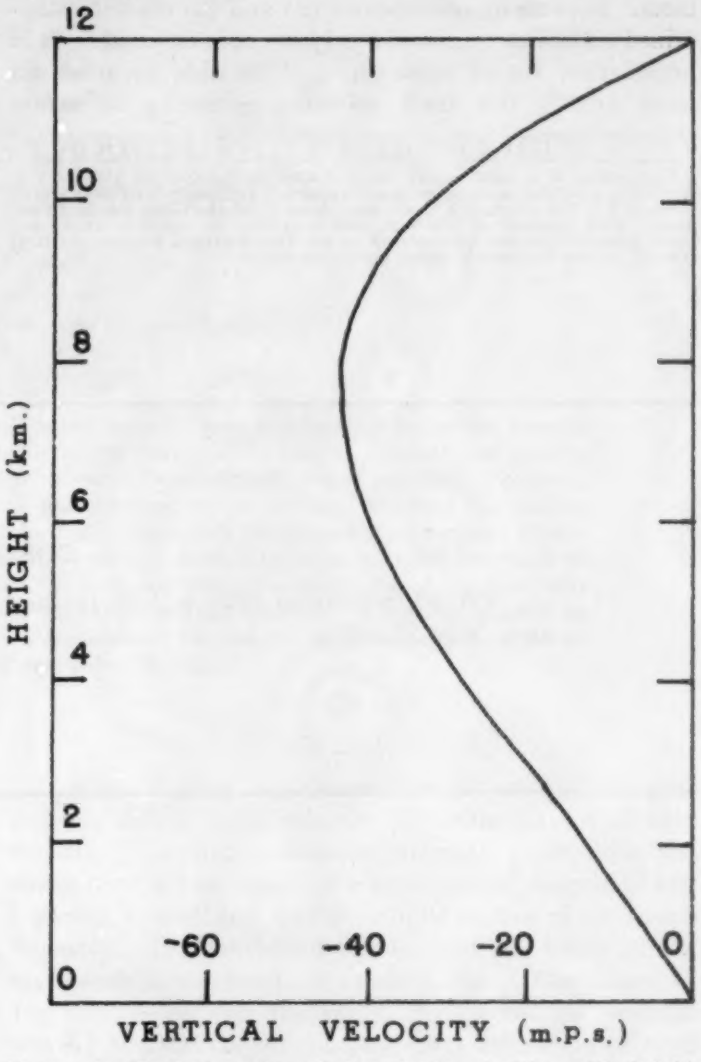

FIGURE 4.—Vertical profile of downdraft velocities with height over a point located between stations 6, 7, 11, and 12 at 1400 EST, March 19, 1948.

7, 11, and 12. These two values were used in the vertical velocity computations.

4. DRAFT VELOCITIES

Substituting the minimum value of divergence, -32.0 hr.$^{-1}$, in equation (4) yields values of upward vertical motion that are shown graphically in figure 3. Substituting the maximum value of divergence, 21.0 hr.$^{-1}$, yields values of downward vertical motion that are shown graphically in figure 4. Maximum draft velocities occurred at the 8-km. level. Maximum updraft was 66.5 m.p.s. (149 m.p.h. or 218 ft. sec.$^{-1}$). Maximum downdraft was 43.7 m.p.s. (98 m.p.h. or 143 ft. sec.$^{-1}$).

Computed drafts for this case are up to 2½ times greater than the maximum updraft of 84 ft. sec.$^{-1}$ and maximum downdraft of 79 ft. sec.$^{-1}$ evaluated by the Thunderstorm Project [1]. The difference may be accounted for, at least in part, by the fact that thunderstorms of lesser severity were sampled by the Thunderstorm Project (e.g., maximum convergence computed by the Thunderstorm Project was -20.0 hr.$^{-1}$, as compared to -32.0 hr.$^{-1}$ computed for the March 19, 1948 case) and the probability that the severest of these may not have been sampled during their brief periods of greatest severity (e.g., in the March 19, 1948 case, the convergence of -32.0 hr.$^{-1}$ existed for only a few minutes; values 5 minutes before and after this maximum were -20.0 hr.$^{-1}$ or less). Because of the limitations in sampling by the Thunderstorm Project, the computations above may be fairly representative of values in severe thunderstorms.

Aside from this, some errors undoubtedly exist in the computations just presented. Most serious, probably, is the assumed distribution of divergence with height. It may be noted that a lowering of the height of the upper divergence level would decrease draft velocities, while a raising of this height would increase them. A departure of the distribution from a cosine curve would greatly affect the velocities, and could either increase or decrease

them. Because of assumptions (2) and (3) the values obtained should be considered only as crude estimates. It is hoped that future research may be able to ascertain more exactly the draft velocities occurring in severe thunderstorms.[2]

[2] According to a pilot report at 1910 GMT on October 10, 1958, a U.S. Air Force pilot encountered extreme turbulence and heavy hail over Watertown, N.Y. The aircraft, a C–47, went from 6,000 to 10,000 feet in 30 seconds. This updraft of 8,000 ft. min.$^{-1}$ or 133 ft. sec.$^{-1}$ is about 1½ times greater than any encountered by the Thunderstorm Project and is 61 percent of the theoretical value computed above.

REFERENCES

1. H. R. Byers and R. R. Braham, *The Thunderstorm*, U.S. Weather Bureau, Washington, D.C. 1949, 282 pp. (pp. 40, 53, 130).
2. D. T. Williams, "A Surface Micro-Study of Squall-Line Thunderstorms," *Monthly Weather Review*, vol. 76, No. 11, Nov. 1948, pp. 239–246.
3. Robert G. Beebe and Ferdinand C. Bates, "A Mechanism for Assisting in the Release of Convective Instability," *Monthly Weather Review*, vol. 83, No. 1, Jan. 1955, pp. 1–10.

CORRECTION

Vol. 86, September 1958, p. 133: In the caption the time for figure 1B should read "1200 GMT, May 27, 1958."

METEOROLOGICAL CONDITIONS OVER PUERTO RICO DURING HURRICANE BETSY, 1956

JOSÉ A. COLÓN

U.S. Weather Bureau, San Juan, P.R.[1]

[Manuscript received January 26, 1959; revised November 28, 1958]

ABSTRACT

The observations of wind, pressure, rainfall, and radar bands recorded over Puerto Rico during the passage of Hurricane Betsy are presented and discussed. The track of the hurricane across the Atlantic and eastern Caribbean Sea, which shows an apparent sinusoidal oscillation around the mean path, is also included. The radar observations are used to obtain the detailed path of the hurricane across Puerto Rico and to study the changes in the structure of the precipitation bands that resulted from the passage over the mountainous section. Photographs are presented to illustrate the variations in the radar structure. Some inferences are made in regard to the changes in the intensity of the wind and pressure fields. It is shown that some weakening of the wind field and filling of the central pressure occurred with motion over the land area, and that rapid deepening followed as soon as the hurricane moved over water on the north side of the island. The rainfall observations are compared with those recorded in the great "San Felipe" hurricane of September 13, 1928.

1. INTRODUCTION

On August 12, 1956, hurricane Betsy, the second tropical storm of the season, moved across the island of Puerto Rico. It was the first hurricane to pass directly over the island since September 24, 1932—a period of 24 years. Hurricane Betsy was a fast-moving storm of relatively small size and its effects, fortunately, did not compare with the larger and more severe hurricanes of the past, like the "San Felipe" hurricane of September 13, 1928, and the "San Ciriaco" of August 8, 1899.[2]

From a meteorological point of view the occurrence of hurricane Betsy was significant in that it provided an opportunity to obtain observational data of a nature and scope never before possible in the eastern Caribbean area. The installation of storm-detection radar at San Juan was completed a few days before the arrival of hurricane Betsy and provided a first hand view of the changes taking place in the radar configuration as the hurricane moved across the mountain range of Puerto Rico. Observations by airborne radar gave valuable information on the storm during the period previous to its arrival at Puerto Rico. Considerable radar and aerological data were also obtained after the hurricane passed Puerto Rico and moved along the net of stations in the Bahamas Islands. This report is concerned only with the meteorological aspects of hurricane Betsy over Puerto Rico and the area to the east. Emphasis is placed on the changes in the structure of the hurricane caused by the motion over the mountains of Puerto Rico.

[1] Present affiliation: National Hurricane Research Project, Miami, Fla.

[2] According to the traditional method of naming hurricanes after the saint's day on which they occurred, hurricane Betsy was baptized in Puerto Rico as "Santa Clara."

2. SYNOPTIC HISTORY

Hurricane Betsy was detected on August 9, 1956, near latitude 14° N, longitude 49° W. with the aid of ship reports [1]. Reconnaissance aircraft penetrated the storm for the first time on the afternoon of August 10 and reported a small but well developed system of hurricane intensity. The maximum winds were 100 knots in the southwestern quadrant, 90 knots in the northern, and 75 knots in the eastern quadrants. The minimum pressure was 979 mb. and the eye diameter 20 n. mi. The radius of the circulation was quite small with 45-knot winds extending only 60 n. mi. to the north and 50 n. mi. to the south of the vortex.

The hurricane moved westward to west-northwestward and passed over the island of Guadeloupe, F.W.I., around 1200 GMT of August 11 (fig. 1.). Considerable damage was reported in the islands of Guadeloupe, Marie Galante, Dominica, and Les Saintes. The hurricane continued to move generally west-northwestward over the eastern Caribbean Sea and arrived on the southeastern coast of Puerto Rico around 1200 GMT (0800 LST), August 12.

3. OSCILLATORY MOTION IN THE TRACK

During its motion over the Atlantic and eastern Caribbean Sea hurricane Betsy was almost continuously tracked by reconnaissance aircraft. Center fixes based on airborne radar observations were available at 30-minute intervals during a considerable part of the period from the morning of August 11 onward (fig. 1). If all the fixes are taken at full value, a sinusoidal variation around the mean path is quite evident. Such oscillations in hurricane tracks have been the subject of discussion among

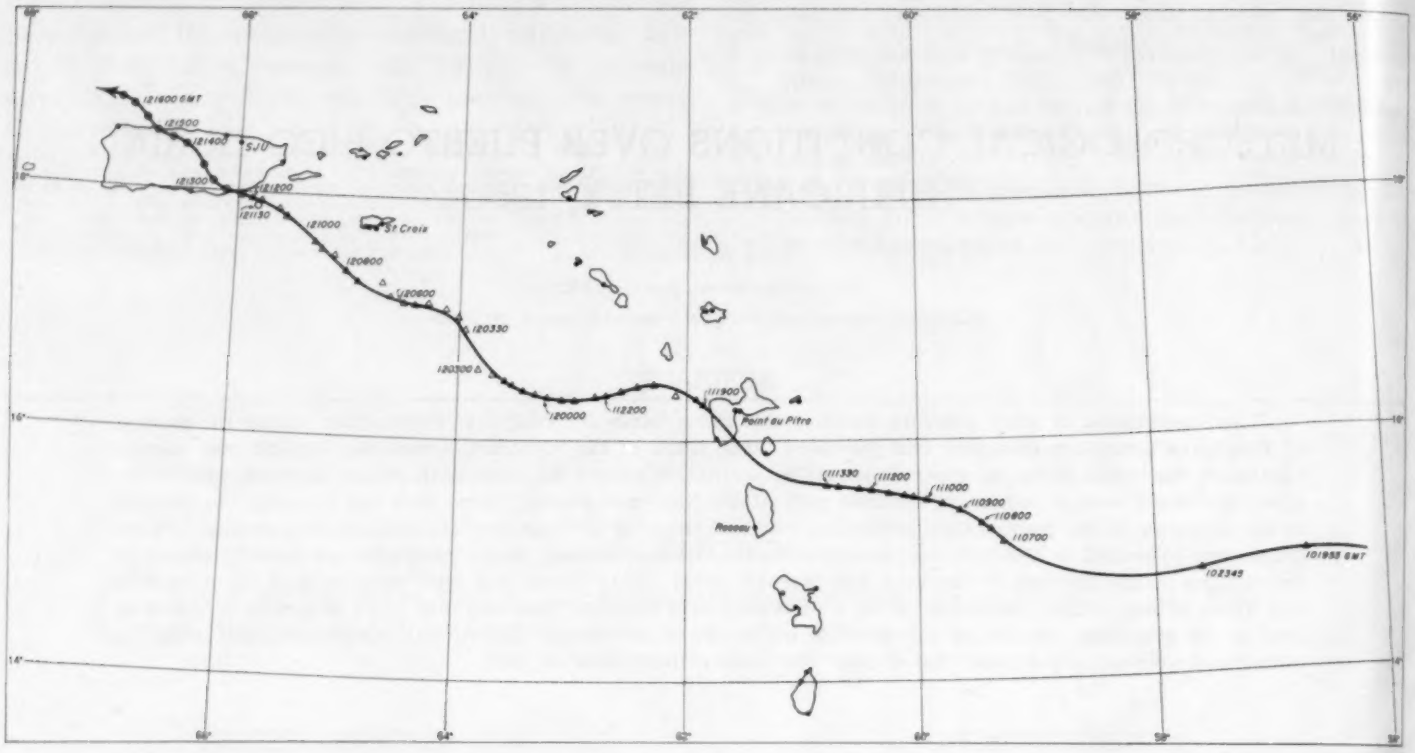

FIGURE 1.—Track of hurricane Betsy, August 10–12, 1956. Aircraft positions indicated by triangles, positions from San Juan radar by circles. Positions for which no time is directly indicated are in 30-minute intervals.

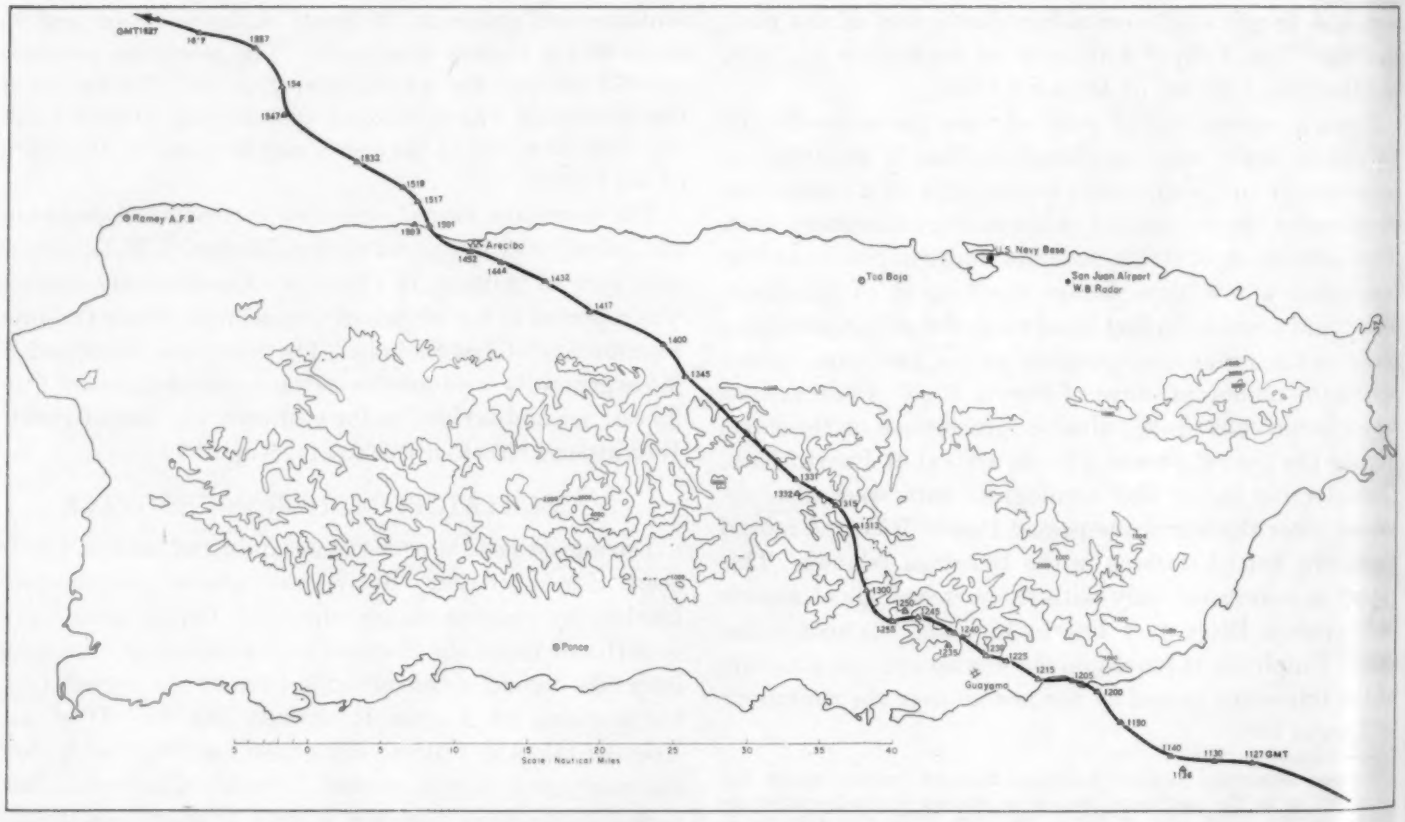

FIGURE 2.—Track of hurricane Betsy across Puerto Rico as determined from San Juan radar. Contours in 1000-ft. intervals.

tropical meteorologists during the last 10 years [3, 4, 7]. Ordinarily people are inclined to disbelieve them because the amplitude of the variations often is of about the same magnitude as the errors in determining the center fixes.

The two most important sources of error in determining center positions with airborne radar are the navigational errors in the position of the aircraft and the errors in determining the exact center of the radar bands. In the case of hurricane Betsy the reconnaissance aircraft were flying at all times over or near the neighboring islands and therefore navigational errors were probably at a minimum. The set of positions between 0700 and 1330 GMT August 11 were obtained by an airplane operating in the vicinity of the islands of Dominica and Martinique at an altitude close to 10,000 feet. According to the reports from the aerologist aboard, the storm consistently presented excellent eye targets, with a precipitation eye mostly circular, 9 to 15 n. mi. in diameter. The navigation was reported as accurate within 3 n. mi. Between 1900 GMT August 11 and 0300 GMT August 12 a different aircraft tracked the center mostly from the right or northward side of the hurricane around the islands of Antigua, St. Kitts, and St. Croix. After 0330 GMT a third aircraft operated from the vicinity of Puerto Rico and the Virgin Islands. Judging from the reports of the reconnaissance aircraft and from the appearance of the hurricane when it came within range of the San Juan radar (fig. 3), the radar eye was well-defined and generally closed so that errors in placing the center should also have been small. Throughout the period, errors in the center fixes were reported as from 3 to 5 n. mi. which is well below the estimated amplitude of the oscillation. There was only one serious discrepancy in the continuity of the center fixes and it occurred between 0300 and 0330 GMT, August 12, at the time of a change in the observing aircraft, when the first position obtained by the new observer did not make good continuity with the last position of the departing one. However, all factors considered, it appears that the accuracy of the reports shown in figure 1 is as good as can ever be expected.

The wavelength of the oscillation of the track (fig. 1) was of the order of 160 n. mi. in the eastern section of the track and decreased to around 100 n. mi. farther west. This indicates a period of about 7 to 12 hours. The amplitude was 10 to 15 n. mi., but decreased and was practically insignificant in the vicinity of Puerto Rico. These values for the period and amplitude are considerably smaller than those reported previously in the literature [3, 4, 7].

4. PATH OF THE STORM CENTER ACROSS THE ISLAND

Figure 2 shows the path of the center across the island on a base map that contains height contours at 1,000-ft. intervals. The mountain system consists essentially of an east-west oriented range with highest peaks a little over 4,000 feet. The storm moved inland in a section where the coastal lowland is very narrow and the height of the terrain rises rapidly. The highest peaks in the section along the track are close to 3,000 feet.

All the center positions in figure 2 were evaluated from the radar film obtained at San Juan, and indicate the approximate center of the radar eye. Up to 1300 GMT the eye was well defined (see figs. 3 to 7) and the accuracy of the fixes good. Between 1300 and 1400 GMT, while the center was moving over the mountains, the eye structure deteriorated and it was then more difficult to determine the exact center of the hurricane. Another cause of difficulty in the tracking was the inability to operate the radar continuously. After 1300 GMT, because of severe interference with local communications, the radar equipment was operated only for 3-minute intervals every 15 minutes. With such a gap in the observations it was more difficult to maintain continuity of the eye opening. At 1400 GMT and afterwards the center was located in the northern lowlands and reformed rapidly. The fixes after that time are more reliable. In the evaluation of the track proper consideration was given to the independent fixes obtained by the radar technician at the time of the hurricane.

The path in figure 2 has been drawn connecting most of the fixes, but no significance is claimed for all the minor variations. Some changes in the direction of motion, however, appear to have been significant. For example, between 1130 and 1300 GMT the average direction was around 290–295°; between 1300 and 1400 GMT the motion was toward 315–320°; and after 1400 GMT it was around 300–305°. It is interesting to see that these changes in direction fit rather well into the pattern of the oscillation evident previous to the arrival of the center over the island.

5. CHANGES IN THE RADAR STRUCTURE

Figures 3 to 14 present a series of photographs of the San Juan radarscope showing the structure of the hurricane at different positions over the island. The approximate position of the storm at the time of each photograph can be determined from figure 2. In this series of pictures the echoes from the southeastern side, between directions 120° and 150° bearing from the center of the scope, are partially obscured due to physical interference from the San Juan Airport Control Tower, located on the roof a short distance from the radar antenna. Because of this interference the hurricane was not completely visible on the radar screen until just a few minutes before the time of figure 3.

Figure 3, taken at 1207 GMT when the hurricane was centered over the southern coast, shows a circular and well-defined inner band. The outer diameter is around 30 n. mi. and the inner diameter 13 n. mi. so that the inner band is 8–9 n. mi. wide. There is a sector of weak echoes, almost an opening, on the west side. The outline of the bands near the center of the scope is obscured by the

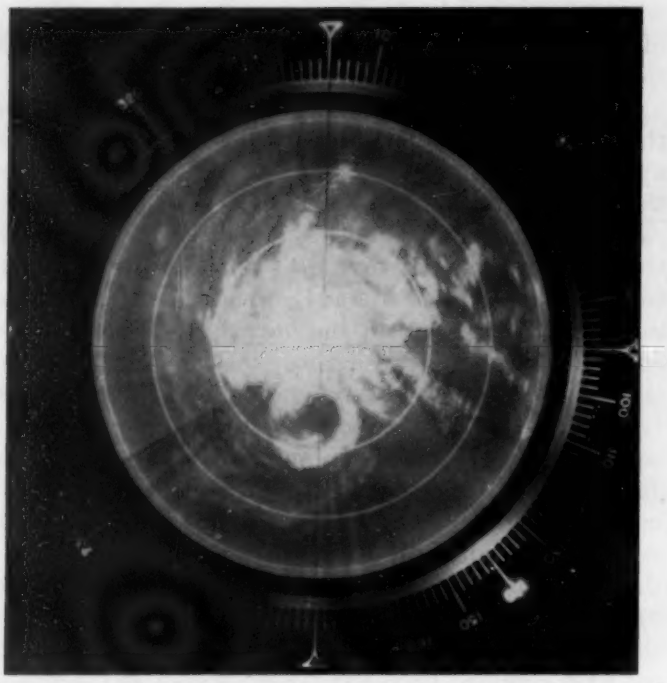

FIGURE 3.—Photograph of radarscope of San Juan radar at 1207 GMT, August 12, 1956. Range markers 20 nautical miles apart.

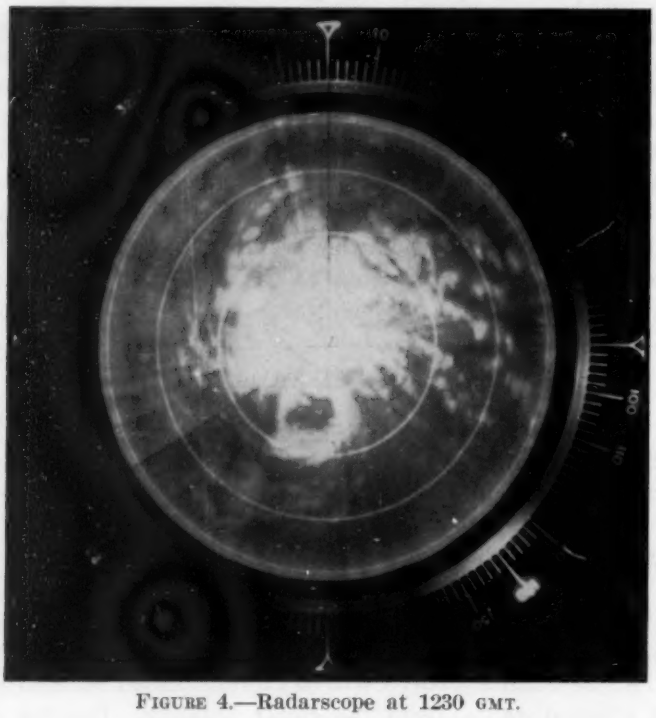

FIGURE 4.—Radarscope at 1230 GMT.

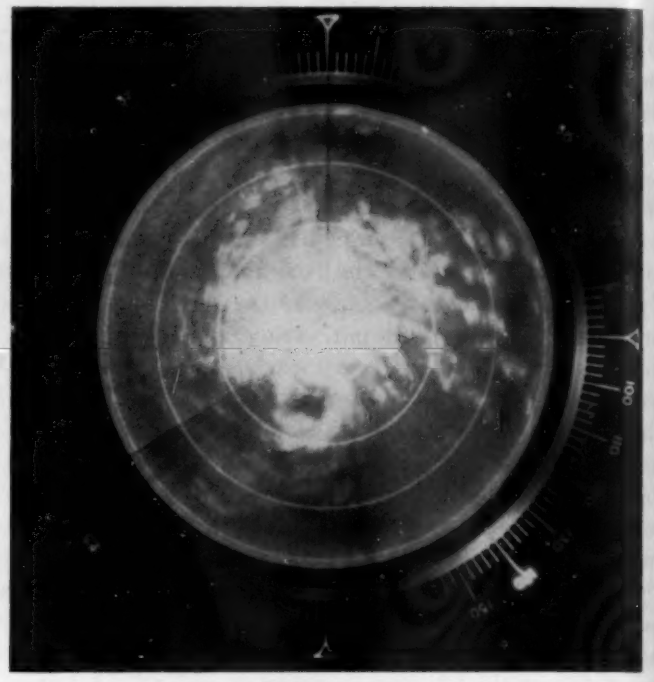

FIGURE 5.—Radarscope at 1234 GMT.

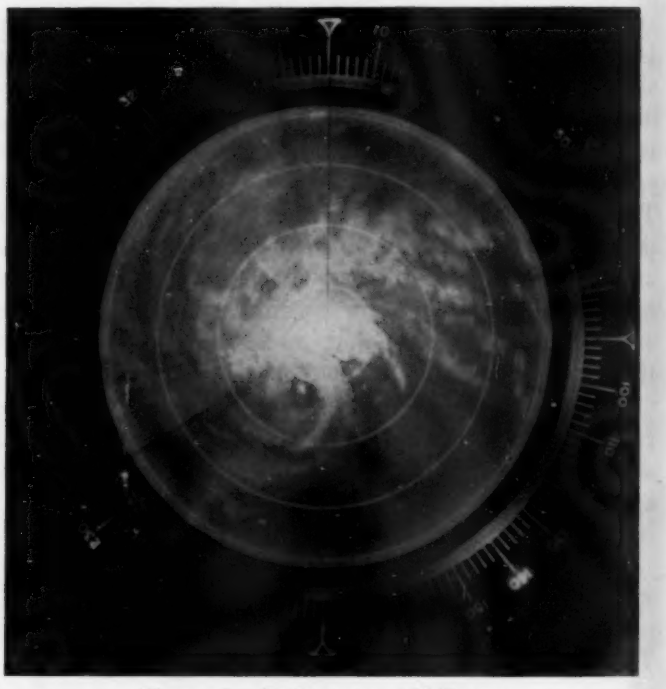

FIGURE 6.—Radarscope at 1247 GMT.

ground return, but several bands can be identified on the northeastern side of the hurricane spiraling toward the eye. On the far or southern side of the storm one band is barely discernible following closely the 60 n. mi. range marker. At the time of the photograph the storm was centered on the coast with the northern half over land and the southern half over water, but this difference in the underlying surface does not seem to have made much difference in the appearance of the radar echoes.

The outline and configuration of the radar band remained practically unchanged during the following 15 to 20 minutes, as the storm moved gradually inland. By 1230 GMT (fig. 4), with the eye center located about 4 n. mi. north of the coast, the inner boundary of the eye had taken a sort of rectangular shape. The edges of the main band were also becoming ill-defined. A few minutes later, at 1234 GMT (fig. 5), the eye showed an almost perfect rectangular form. This lasted a few minutes and then began to deteriorate. At 1247 GMT (fig. 6) the central band showed significant changes; the inner diameter was smaller, the echoes from the southern side were

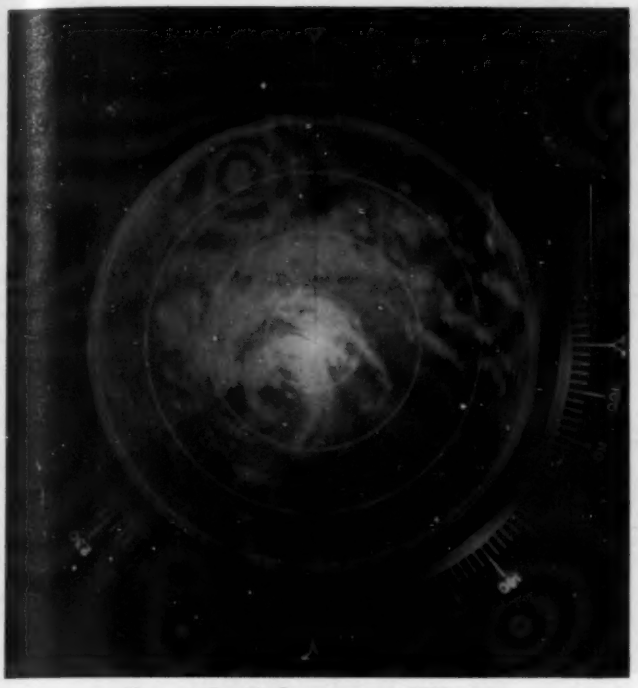

FIGURE 7.—Radarscope at 1302 GMT.

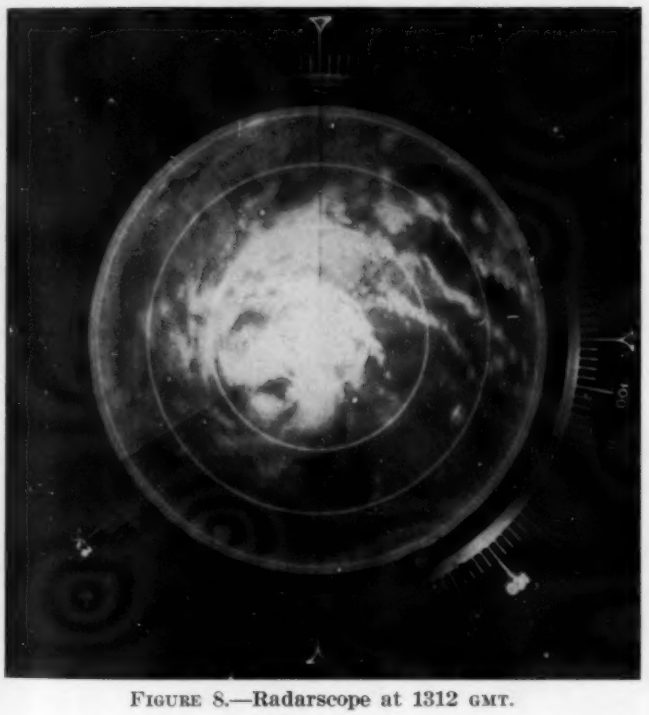

FIGURE 8.—Radarscope at 1312 GMT.

weaker, and the shape of the band look more like a spiral in contrast to the ring-like structure shown previously. At this time the center had traveled over land for about 12 n. mi. and was located in the southern slopes which have an altitude of around 1,000 feet.

At about this time the observer in charge of the radar raised the antenna and was able to notice a northwestward slope of the central band. This was explained as due to the effect of the mountains that detained the lower part of the system while the upper part continued its forward displacement [5].

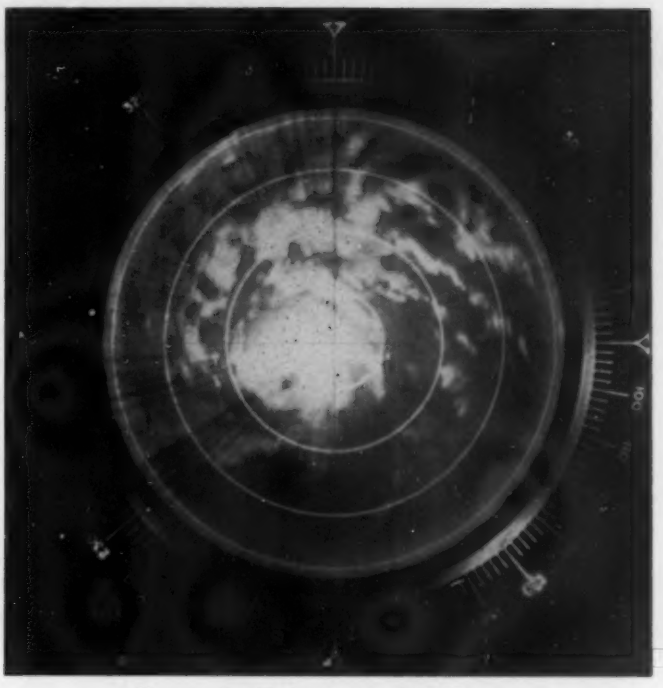

FIGURE 9.—Radarscope at 1331 GMT.

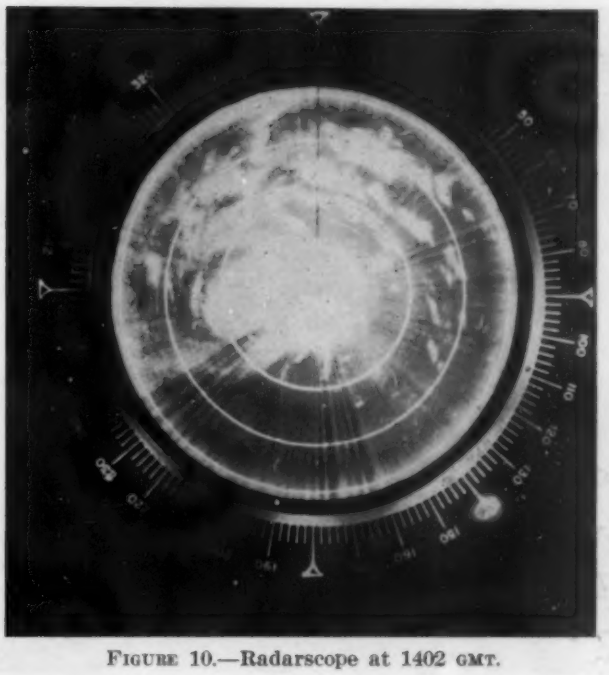

FIGURE 10.—Radarscope at 1402 GMT.

At 1302 GMT (fig. 7) the center was still south of the main mountain ridge. The inner band showed a spiral structure open to the south-southwest. Figures 8 and 9, taken at 1312 and 1331 GMT, respectively, show the storm when it was located on top of the mountains at an altitude of over 2,000 feet. The eye opening was then very small, indistinct, and irregularly shaped. The configuration of the outer bands on the northern semicircle had not changed appreciably; most of the changes occurred in the inner core of the system.

In the determination of the radar track the center of

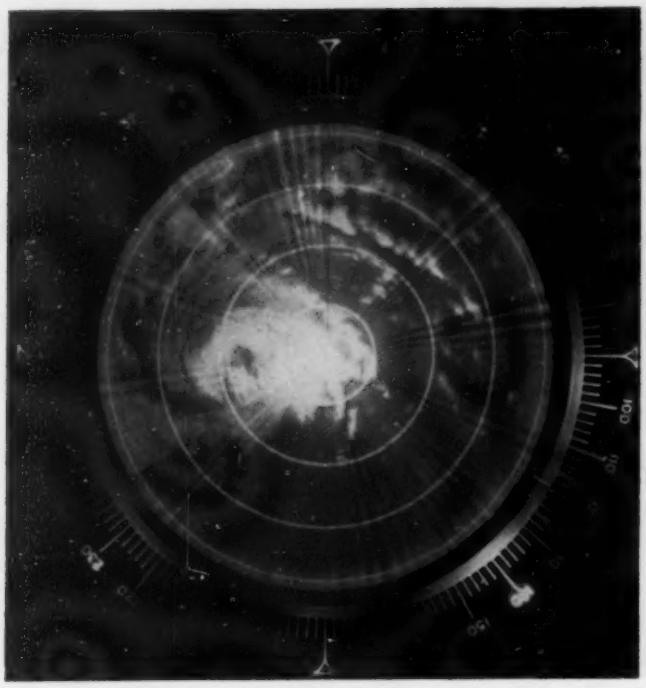

FIGURE 11.—Radarscope at 1417 GMT.

FIGURE 12.—Radarscope at 1447 GMT.

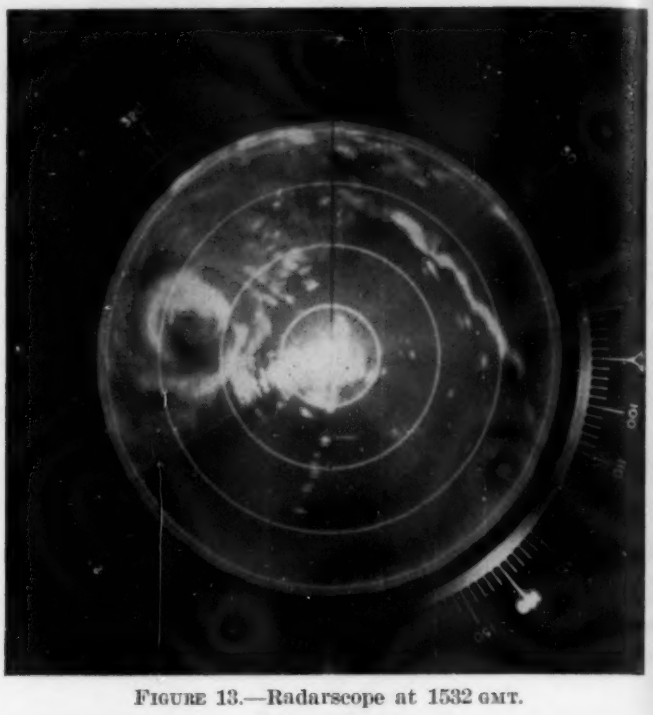

FIGURE 13.—Radarscope at 1532 GMT.

FIGURE 14.—Radarscope at 1608 GMT.

the opening was taken in each case as the center of the eye, but it is possible that that point did not exactly coincide with the center of the eye as identified in previous pictures.

The next photograph (fig. 10), which was taken at 1402 GMT when the hurricane had just moved down the mountains, shows a very small eye opening. After 1400 GMT the eye began to widen and regain its original structure as the hurricane system moved away from the mountains. At 1417 GMT (fig. 11) the eye appeared already quite wide. Some echoes from the terrain are visible in the southern section of the eye. Figure 12, taken at 1445 GMT shows the storm centered close to the northern coastline, with an eye diameter of approximately 15 n. mi. The inner band appears practically complete. In figure 13, at 1532 GMT, the hurricane center was located over water about 4 n. mi. north of the coast. The inner band shows a spiraling structure with an eye diameter of 18–20 n. mi. The last photograph, figure 14, shows the hurricane at 1608 GMT when it was located about 12 n. mi. north of the coast.

The central band was then almost completely over water. Figure 14 shows a band structure quite different from the compact ring evident in figure 3.

There are a few significant points related to the changes in the radar structure. First, the progress of the hurricane system from a water to a land surface, and similarly from a land to a water surface, by itself did not seem to have much of an effect on the structure or appearance of the precipitation bands. Practically all the changes resulted from the motion over the mountainous section. The rapidity with which the inner band reformed as soon as it moved away from the mountains was striking.

An interesting point concerning the speed of motion of the center across the island was noticed and it may be connected to the changes in the radar structure. The average speed of the hurricane center across the island was 18–19 knots (a distance of 56 n. mi. from the point of entry to the point of departure, disregarding the minor variations in the path, in a period of 3 hours). The average speed in the 12- and 24-hour periods previous to the arrival of the center on the south coast, and also after the departure from the north coast, was in both cases only 15–16 knots. There was, apparently, a faster motion while the hurricane was moving over land. The fastest motion seems to have occurred between 1300 and 1400 GMT, but that was precisely the period during which the eye was more distorted and the accuracy in the center positions was less. Since the geometric center of the central opening, which was changing shape and diameter rapidly, was taken in each case as the eye center it is easy to see how discontinuities could occur. In fact, a study of the radar film suggests that the eye formation that developed when the hurricane moved into the northern coastal area did not follow in exact continuity from the previously existent eye that had deteriorated over the mountains. This could account for the apparent acceleration. Unfortunately, due to the breaks in the radar picture, the phenomenon could not be verified unquestionably.

6. WIND OBSERVATIONS

Detailed wind observations were recorded at three stations on the island: San Juan Airport (Weather Bureau station); U.S. Naval Base, San Juan, located about 6 n. mi. west of the Airport; and Ramey Air Force Base, located on the northwestern corner of the island. At the Naval Base, in addition to the hourly, airways observations, a gust recorder giving a continuous graph of the wind speed and direction was available.

The winds in the San Juan area (fig. 15) were from the northeast with speeds of around 15 knots during the evening of August 11. No significant change in direction or speed was noticed until around 0530 to 0600 GMT August 12, when a decrease to a near calm occurred. At that time the hurricane center was approximately 120 n. mi. away. The wind recorder at the Naval Base showed that the period of calm lasted for about 45 minutes. The speeds during the interval were never more than 5 knots. A rather strong shower, with a measurement of 0.30 inch of rainfall, was observed at the San Juan Airport at that time, and was the first heavy precipitation there associated with the hurricane. After 0600 GMT there was a slight increase in the speed and gustiness of the wind. The precipitation became light, but fairly continuous for the next 4 hours.

Another significant change in the character of the winds, and also of the pressure and rainfall, was noticed around 1000 GMT, when the center was about 50 n. mi. away. There was a sharp increase in the wind speed and in the intensity of the precipitation. At the same time the pressure curve showed a more rapid downward trend. That marked the beginning of the intense inner core of the hurricane. Thereafter the wind speed increased rapidly and steadily to its maximum which was recorded from 1200 to 1245 GMT. The precipitation started increasing a little earlier than the wind speed and continued heavy until shortly after the time of the peak gusts. The visibility curve, which to a large extent is a reflection of the intensity of the rainfall, made a sharp drop to around 1–2 statute miles about 0930 GMT and continued low until 1330 GMT. The maximum wind speed of around 65 knots with gusts to 80 was recorded at 1235 GMT. Afterwards the winds decreased rapidly; at 1300 GMT the reading was 38 knots with gusts to 52. By 1400 GMT the wind had reduced to 26 knots with gusts to 43, the precipitation had practically ceased, and the visibility had increased to near its normal magnitude. At that time, however, the storm center was located only 28 n. mi. away.

The maximum winds in the San Juan area were from the northeast; the southeasterly flow on the right rear quadrant was extremely light. The minimum pressure, 1003 mb., was recorded at around 1300 GMT, a little later than the maximum winds, but before the radar center had arrived at the point of minimum distance from the station. The radar center was closest to San Juan, at a distance of about 22 n. mi., near 1315 GMT; that is, about 40 minutes after the time of the peak gusts and 15 minutes after the minimum pressure. There was evidently a great distortion in the hurricane circulation. The non-coincidence of the pressure eye with the circulation eye or the radar eye has been reported previously [6] as a more or less normal occurrence. In the present situation the motion of the hurricane over the mountainous area must have been the main factor in causing the observed irregular distribution in the meteorological parameters around the center.

The observations at the Naval Base, San Juan, agreed very well with those made at the Airport. The maximum winds, 46 knots with gusts to 67, and the minimum pressure, 1001 mb., were both recorded at the same time as at the Airport. The lower speeds at the Naval Base were probably due to the differences in exposure; the Base is located on the western side of the city and has greater obstructions to an easterly flow than the Airport Station.

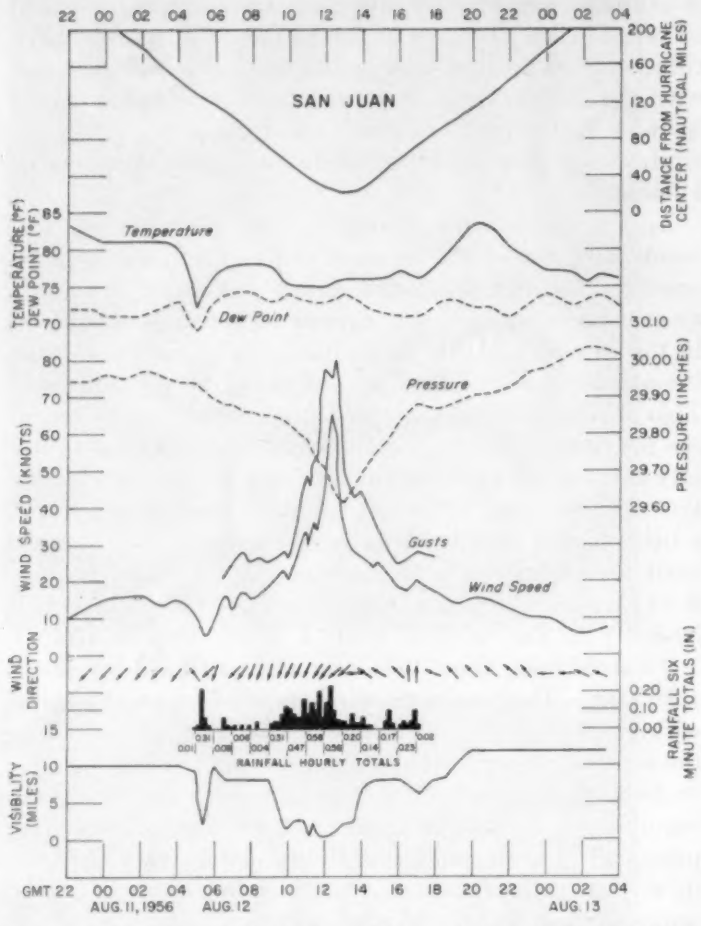

FIGURE 15.—Meteorological observations at the Airport Station, San Juan, P.R., during the passage of hurricane Betsy, August 12, 1956. Time scale in GMT.

Figures 3 to 6, which show the radar pictures during the period of strongest winds and precipitation in the San Juan area, indicate that the activity there was associated with a radar band next to the central one.

The effect of the mountains in Puerto Rico on the isotach field around the center is revealed by the difference in the character of the wind speed variations at San Juan and at St. Croix, V.I. (fig. 16). Both stations were located on the same side of the hurricane and came within approximately the same distance of the center. The station at St. Croix is located near the southern coast; the island is small and relatively flat so that distortions of the hurricane circulation due to the terrain should have been minor. The pressure and rainfall observations at the two stations showed very close agreement. St. Croix recorded a minimum sea level pressure of 1002 mb. and a total rainfall of 3.20 inches, as compared to 1003 mb. and 3.21 inches at San Juan. Both stations recorded around 2.00 inches of rain in the 6-hour period of peak activity. The minimum pressure at St. Croix was recorded at the time of minimum distance from the center; the maximum winds were recorded a little later. There was, therefore, a better coincidence of the pressure and radar centers at the time the hurricane passed abeam St. Croix.

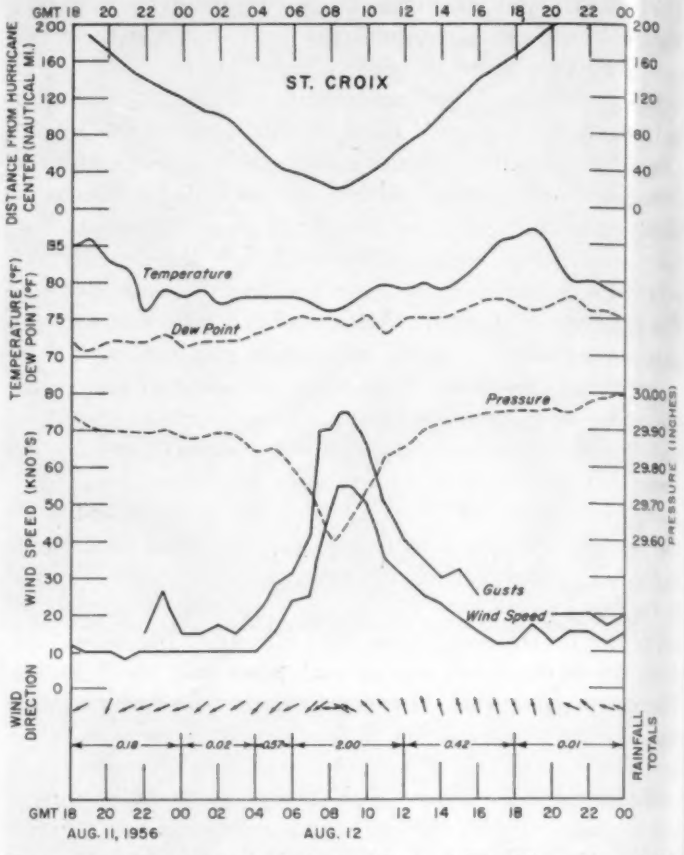

FIGURE 16.—Meteorological observations at Hamilton Airport, St. Croix, V.I., during the passage of hurricane Betsy, August 11–12, 1956. Time scale in GMT.

During the approach of the hurricane the variations in wind speed, although not the magnitudes, were about the same at the two stations; the wind profile in both cases showed changes in the rate of increase at distances of about 50 and 30 n. mi. away from the center. The maximum winds at St. Croix, 55 knots with gusts to 75, were lower than at San Juan, but the difference was small and probably due to differences in exposure. For the purpose of this discussion, however, this difference in magnitude is not important. The major difference in the observations was in the character of the wind speeds recorded in the rear or departing side of the hurricane. At St. Croix the winds continued strong after the center passed the point of minimum distance. The highest speeds were from the southeast and were evidently associated with the flow in the right rear quadrant. At San Juan, on the other hand, the observations indicate a complete breakdown of the isotach field as soon as the hurricane entered the mountainous area. As a result the wind circulation had decreased considerably by the time the center arrived at the point of minimum distance from the station, and the southeasterly flow in the right rear quadrant of the hurricane was extremely light. Presumably, except for the effect of the mountains, the San Juan area, and similarly every other section on the island, would have been under the effect of stronger winds for a considerably longer period.

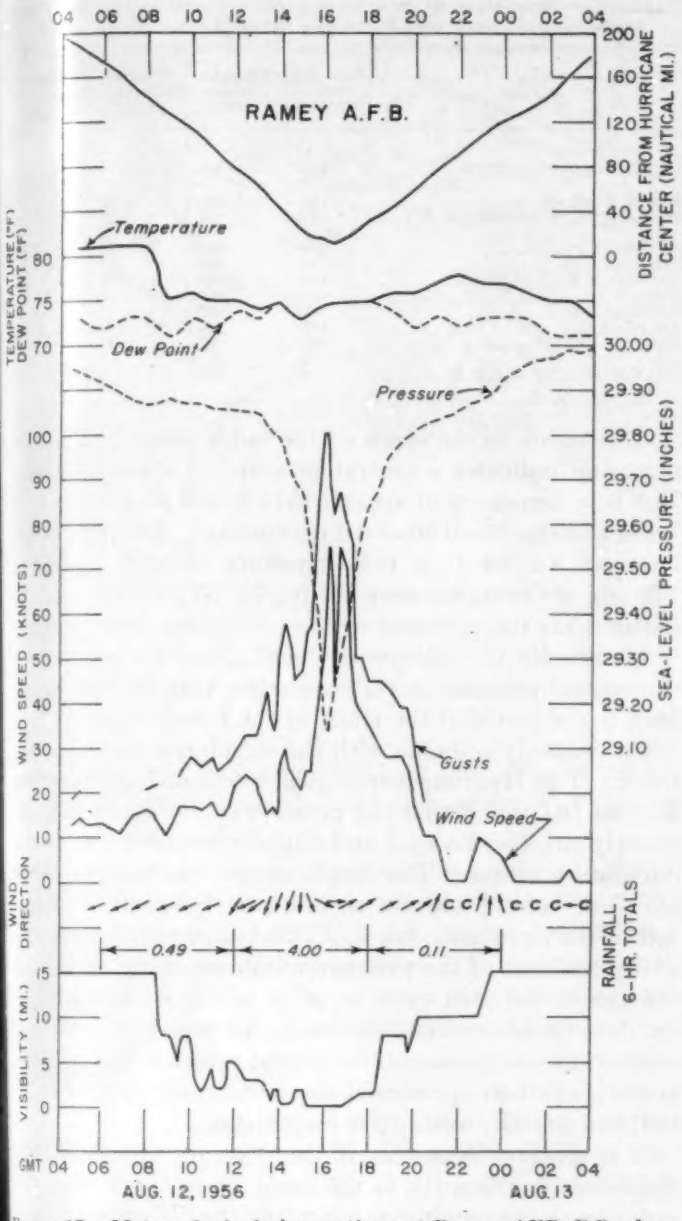

FIGURE 17.—Meteorological observations at Ramey AFB, P.R., during the passage of hurricane Betsy, August 12, 1956. Time scale in GMT.

The observations at Ramey Air Force Base (fig. 17) make possible certain deductions about the intensification of the hurricane after it moved from land to water on the north side of the island. The winds at Ramey were of the order of 20 knots with gusts of 30–40 knots up to 1400 GMT when the hurricane, after crossing the mountains, was located about 40 n. mi. east of the station. After 1400 GMT the center moved westward approaching Ramey and at 1500 GMT was located only 22 n. mi. away. The winds, however, remained relatively low; the readings around 1500 GMT were about 25 knots with gusts to 50–55; the maximum reading by that time was 30 knots with gusts to 58. These observations indicate a weaker circulation than would normally be expected in view of the intensity of the hurricane before it entered the island.

After 1500 GMT, when the hurricane center moved over water, there was a sudden and rapid increase in the wind speed; the increase was even more pronounced after 1530 GMT. The maximum intensity, 75 knots with gusts to 100, was recorded shortly after 1600 GMT at about the time of minimum distance from the center, and also at the time of the minimum pressure. The hurricane was then about 14 n. mi. away to the north of the station. There was, evidently, a better organization of the isotach and pressure fields around the eye, and a better coincidence of the pressure and circulation centers than when the hurricane passed close to San Juan. The distribution of rainfall (fig. 19) and damages show also heavier wind and rainfall activity over the northwestern corner than in any other section of the north-coastal area. The pressure observations, discussed in greater detail in the following section, similarly indicate rapid deepening after 1500 GMT. Figure 14 shows the radar picture at the time the hurricane was close to Ramey. The peak wind and rainfall activity there was evidently associated with the southern section of the inner radar band.

7. PRESSURE OBSERVATIONS

A series of pressure observations, including some barograph traces, were obtained at a few places on the island. Two sets of observations were taken practically at the center of the hurricane: One at Guayama near the southern coast, and the other at Arecibo, on the northern coast. There was in some cases uncertainty as to the altitude and calibration of the instruments. To remedy this difficulty all observations were corrected to sea level conditions by comparison with the San Juan data. In the cases in which a barogram was available a comparison of the pressure readings during the days previous to or after the passage of the hurricane provided a reliable correction factor. In other cases correspondence with the observers served to clarify the accuracy of the data. All the observations presented in the following discussion were in that form corrected to sea level.

The number of observations available was not sufficient to establish the horizontal field of pressure and to study its changes over land. Instead the central pressure was computed at different positions along the track and the variations with time were studied. The results indicate filling of the central pressure as a result of the motion over the land mass of Puerto Rico followed by rapid deepening as soon as the hurricane moved over water again.

The procedure followed to estimate the central pressure was to determine first a representative value of the pressure gradient in the core of the hurricane and then use it to measure the minimum pressure from observations in the periphery. Various estimations of the gradient were made when the hurricane was centered near the south coast of Puerto Rico and still not greatly affected by the terrain. The barograph trace recorded near the center at Guayama (fig. 18) was very useful in this respect. A

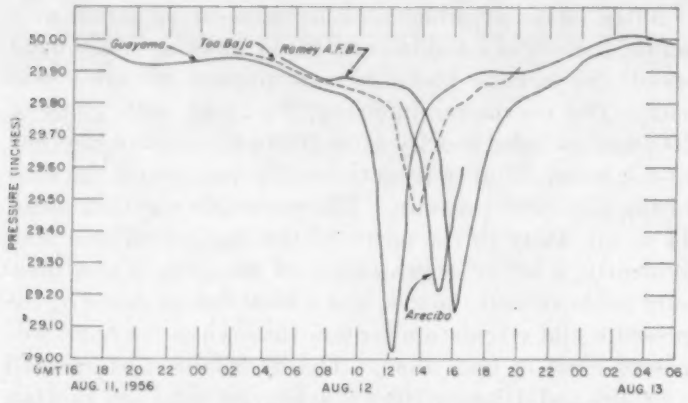

FIGURE 18.—Pressure profiles during hurricane Betsy,, August 12, 1956, as recorded in Guayama, Toa Baja, Arecibo, and Ramey AFB, P.R. Pressures reduced to sea level. See text.

value of 1.0 mb. n. mi.$^{-1}$ was accepted for stations located within 15 n. mi. of the center. For the estimations from the readings at St. Croix, San Juan, and Ponce, located 19–22 miles from the center, a gradient value of 0.9 mb. n. mi.$^{-1}$ was used; while for Roseau, Dominica, a value of 0.8 mb. n. mi.$^{-1}$ was applied. A tabulation of the pressure readings and estimated central pressures appears in table 1.

A minimum sea level pressure of 983 mb. was recorded at Guayama around 1215 GMT in a position 1 to 2 miles to the left of the radar center, and shortly after the hurricane had entered land. This observation was probably close to, but not exactly at, the center of minimum pressure, and therefore the central pressure at the time was somewhat lower, perhaps 981 mb. or even less. A minimum central pressure of 979 mb. was measured by a reconnaissance aircraft when the hurricane was located over the Atlantic on August 10. The minimum pressure observations made during the intermediate period at Roseau, Dominica; Point-au-Pitre, Guadeloupe; and St. Croix, V.I. indicate central pressures that do not differ significantly from the above. Evidently no appreciable filling or deepening of the pressure field occurred from the time the hurricane was first reconnoitered on August 10 until it arrived on the coast of Puerto Rico.

A minimum pressure of 989 mb. was read at Arecibo in a position practically at the center, around 1500 GMT, at the time that the hurricane was leaving land. Again the minimum central pressure at the time might have been slightly lower. This observation indicates a filling of about 6 to 8 mb. from the observation made on the southern coast. Other pressure observations were made at San Juan, Ponce, and Toa Baja (fig. 18) when the hurricane was moving over the mountains; all three of them are quite reliable. The estimations of central pressure from these stations are subject to greater inaccuracies, but in general they corroborate the readings at Guayama and Arecibo.

About 1 hour after the observation at Arecibo, Ramey AFB recorded a minimum pressure of 987 mb. in a position 14 n. mi. to the south of the radar center. This observation indicates a central pressure of about 973 mb.; that is, a deepening of around 15 to 16 mb. to a value even lower than had been observed previously. About 22 hours later on August 13 a reconnaissance aircraft measured 972 mb. at the center near 22° N., 72° W., which tends to substantiate the accuracy of the estimation from Ramey.

TABLE 1.—*Tabulation of minimum pressures and estimated central pressures associated with hurricane Betsy, August 10–13, 1956*

Station	Date and time (GMT)	Minimum pressure (mb.)	Distance from center (n. mi.)	Estimated central pressure (mb.)
USN Aircraft, 15° N., 57° W.	Aug. 10 1955	979	0	979
Roseau, Dominica	Aug. 11 1500	1006	29	981
Point-au-Pitre, Guadeloupe, F.W.I.	1800	991	12	979
St. Croix, V.I.	Aug. 12 0830	1002	22	982
Guayama, P.R.	1230	983	1–2	981
San Juan, P.R.	1300	1003	22	983
Ponce, P.R.	1330	1000	19	980
Toa Baja, P.R.	1350	998	13	985
Arecibo, P.R.	1500	989	0–1	989
Ramey, AFB, P.R.	1600	987	14	973
USAF Aircraft, 22° N., 72° W.	Aug. 13 1400	972	0	972

Admittedly the method outlined above for estimating the central pressure is rather crude. One serious drawback is the fact that the track of the pressure center does not necessarily coincide with the circulation or the radar track. The Hydrometeorological Section, U.S. Weather Bureau [6] found that the pressure center was most frequently displaced ahead and slightly to the right of the circulation center. The displacement was mostly either ahead or behind and not so much to the right or to the left of the circulation track. This is encouraging because a displacement of the pressure minimum ahead or behind the track, but still close to it, would not seriously invalidate the above computations. Nevertheless, although quantitative estimates of the central pressure and its variations have been presented the main conclusions can be well sustained by qualitative reasonings.

It is quite evident that if the pressure minimum was displaced significantly to the right or to the left of the radar track the conclusion regarding the filling of the central pressure over land would still be valid on the basis of the observations at Guayama and Arecibo. Furthermore, if it is assumed that the pressure minimum was displaced to the right of the radar track, then the estimate of the central pressure at Toa Baja should be higher than indicated in table 1, thus corroborating the amount of filling over land. At the same time a displacement of the pressure minimum to the right of the track would not alter the magnitude of the deepening between the observations at Arecibo and Ramey. The only possibility that might affect the results is that the pressure minimum was displaced to the left of the track between 1500 and 1600 GMT. In that case the conclusion concerning the amount of deepening between Arecibo and Ramey would be altered. Such a possibility, however, is not very likely; and it is not supported by the observations in the rest of the island. A detailed scrutiny of the available data suggests that at the time the hurricane was moving over the moun-

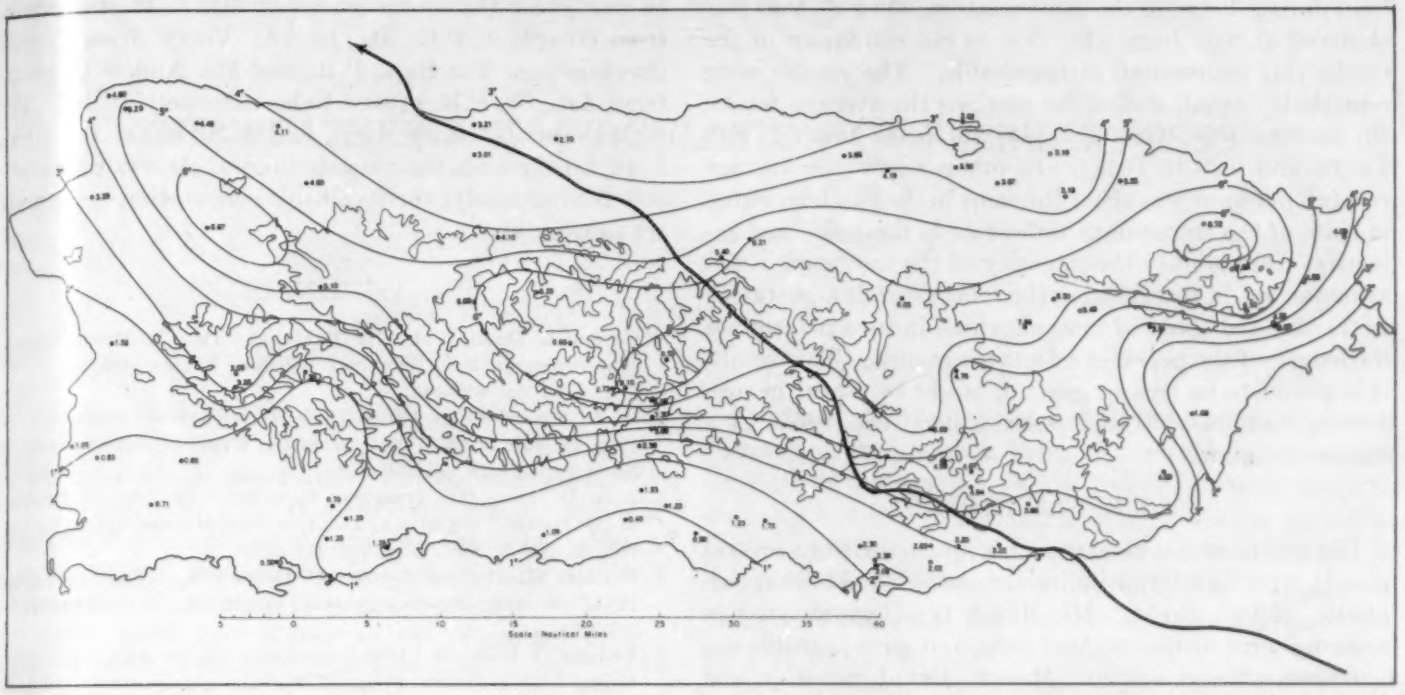

FIGURE 19.—Distribution of total rainfall recorded over Puerto Rico during the passage of hurricane Betsy. Track of the center is heavy line.

tains between 1200 and 1400 GMT the pressure minimum was probably displaced ahead and somewhat to the right of the radar track.

There are, of course, other sources of error in the pressure evaluations, aside from the relationship between the pressure and radar tracks. All factors considered, the pressure estimates listed in table 1 are quite reasonable and not unexpected. They exactly verify what one would normally anticipate in such a situation. One thing that is striking is the rapidity and magnitude of the deepening that took place when the hurricane moved again over water on the north side of the island. This result attests to the tremendous influence of water surface on the organization and maintenance of the hurricane circulation.

8. RAINFALL OBSERVATIONS

Figure 19 shows the distribution of rainfall over Puerto Rico during hurricane Betsy. The amounts range from values of about half an inch in the southern coastal areas to over 8 inches in the northeastern and central mountainous sections. The rainfall was greater on the right side of the track south of the mountain range and on the left side of the track north of the range. Evidently this distribution was mostly the result of orographic effects. The southern coastal areas to the left of the track were shielded by the mountains and thus the rainfall and wind effects were reduced. On the other hand the sections exposed to the action of the wind were affected more. The zone of heavier rainfall extending southeast-northwest over the northwestern section of the island was probably associated with the regeneration of the hurricane circulation after the center moved over water. There was probably another band of heavy rainfall over the oceanic area on the right side of the track.

A comparative study was made of the rainfall totals associated with hurricane Betsy and those of the great San Felipe hurricane of September 13, 1928 [2]. The path of the San Felipe hurricane across Puerto Rico was fairly close to that of Betsy; it entered land in about the same location as Betsy, passed about 25 n. mi. to the southwest of San Juan, and left the island through the northwestern corner. On that occasion San Juan recorded a minimum pressure of 973 mb. and a maximum wind of 160 m.p.h., which still rates as one of the highest hurricane winds ever measured. There were 11 consecutive hours of winds greater than 60 m.p.h. and about 6 hours of winds over 100 m.p.h. During hurricane Betsy San Juan recorded only 1 hour of winds greater than 60 m.p.h. On the basis of the observations at San Juan the radius of the intense inner core of the San Felipe hurricane was estimated as about 180 n. mi., as compared to only 50 n. mi. for hurricane Betsy. Hurricane Betsy was, therefore, relatively small.

The rainy period at San Juan during hurricane Betsy lasted 13 hours and 3.19 inches of rain were measured. During hurricane San Felipe 9.37 inches were measured in a period of 33 hours. Dividing the total rainfall by the length of the period gives a value representing average rainfall per hurricane-hour. This came out as 0.28 inch per hour for hurricane San Felipe and 0.25 for hurricane Betsy. Similar computations were tried for 36 stations over the island that had rainfall records in both hurricanes. It was assumed that the length of the rainy period at each station during San Felipe was greater

than during Betsy in the same relation, 33 to 13, that was observed at San Juan. In view of the similarity in the tracks this assumption is reasonable. The results were remarkably equal, station for station; the average for all 36 stations was 0.28 inch per hurricane-hour in San Felipe and 0.26 in Betsy. In other words the average rainfall per hour was about the same in the two hurricanes in spite of the tremendous difference in their size and intensity. Apparently the intensity of the hurricane is not as important in determining the total rainfall at a station as the size and speed of motion, which in turn determines the length of the period it affects the station. This result, if it proves to be true in general, might be useful in predicting total rainfall and ensuing flood conditions in a similar situation.

ACKNOWLEDGMENTS

The writer wishes to express his appreciation to several people, who, directly or indirectly, contributed to the completion of this report. Mr. Ralph L. Higgs assisted in securing some of the original data, and gave valuable encouragement and advice. Messrs. David Smedley and Americo Maldonado also contributed in assembling data. Messrs. Harry M. Hoose and D. C. McDowell read the manuscript and gave valuable suggestions. The interest and spirit of cooperation of amateur weather observers over the island who recorded observations and made them available to the Weather Bureau is deeply appreciated. In particular the contributions of Mr. J. M. de Andino, from Guayama, P.R., Mr. Luis G. Veray, from Central Constancia in Toa Baja, P.R., and Mr. Andres Gelabert, from Arecibo, P.R. proved to be extremely useful. The authorities at Ramey AFB, and U.S. Naval Base, San Juan, kindly made their meteorological observations available for this study; their valuable cooperation is sincerely acknowledged.

REFERENCES

1. Gordon E. Dunn, Walter R. Davis, and Paul L. Moore, "Hurricane Season of 1956," *Monthly Weather Review*, vol. 84, No. 12, Dec. 1956, pp. 436–443.
2. O. L. Fassig, "San Felipe—The Hurricane of September 13, 1928 at San Juan, P.R.," *Monthly Weather Review*, vol. 56, No. 9, Sept., 1928, pp. 350–352.
3. John D. Horn, "On Irregular Movements of Tropical Cyclones in the Pacific," *Bulletin of the American Meteorological Society*, vol. 32, No. 9, Nov. 1951, pp. 344–346.
4. William Malkin and George C. Holzworth, "Hurricane Edna, 1954," *Monthly Weather Review*, vol. 82, No. 9, Sept. 1954, pp. 267–279.
5. Vaughn D. Rockney, "Hurricane Detection by Radar and Other Means," *Proceedings Tropical Cyclone Symposium, Brisbane, Australia, Dec. 10–14, 1956*, Melbourne, 1956, pp. 179–197.
6. U.S. Weather Bureau, "Characteristics of United States Hurricanes Pertinent to Levee Design for Lake Okeechobee, Florida," *Hydrometeorological Report* No. 32, March 1954, 106 pp.
7. T. -C. Yeh, "The Motion of Tropical Storms under the Influence of a Superimposed Southerly Current," *Journal of Meteorology*, vol. 7, No. 2, April 1950, pp. 108–113.

THE WEATHER AND CIRCULATION OF FEBRUARY 1959

J. F. O'CONNOR

Extended Forecast Section, U.S. Weather Bureau, Washington, D.C.

1. HIGHLIGHTS

February 1959 was a month of marked variability in weather across the United States, as manifested partly by weekly alternations of above and below normal temperatures and of record maximum and minimum temperatures (for the date) at some stations in the East (table 1). This month was featured by the highest daily sea level pressures (up to 1053 mb.) on record at some stations in the upper Mississippi Valley at the beginning of the month. It was also highlighted by a disastrous storm on the 9th and 10th, accompanied by tornadoes, one of which took the lives of 21 persons in St. Louis, Mo., early on the morning of the 10th, with hundreds injured and millions of dollars in property damage. In addition to tornadoes, this storm included a wide variety of severe weather, such as blowing dust, glaze, high winds, floods, snow, and thunderstorms. It brought a repeat of flood conditions requiring evacuation to sections of Indiana and Ohio, where only 20 days before similar disaster struck on January 21 [1].

On a monthly basis few records were broken, although near-record snowfall occurred at some stations, such as Missoula, Mont., Rochester, Minn., Green Bay and La Crosse, Wis., and also at the higher elevations in the West, such as Blue Canyon and Mt. Shasta, Calif., Sexton Summit, Oreg., and Ely, Nev. The month was cold and snowy in parts of the Northeast such as Rochester, N.Y., and Burlington, Vt., but, by way of contrast, Binghamton, N.Y. had its lightest snowfall in 40 years. This was the coldest February in over 20 years in many parts of the northern border States from Montana to Michigan (and the coldest winter season as well). It was a very cloudy and rainy month in the Gulf States with Brownsville, Tex., reporting rain on 22 days and Lake Charles, La., reporting only one clear day during the month.

TABLE 1.—*Some reversals of daily record temperatures (°F.) during February 1959*

	Maximum	Date	Minimum	Date
Newark, N.J.	49	5th	8	2d
Schenectady, N.Y.	46	5th	−4	12th
Birmingham, Ala.	78	14th	18	21st
Richmond, Va.	73	10th	13	21st

2. CONTRAST WITH PREVIOUS MONTHS

February 1959 contrasted sharply with its predecessor, January, as well as with February of 1958. In the eastern half of the country, except New England, a general warming, relative to normal, occurred from the cold that had prevailed during January, and marked cooling in the West ended the extreme warmth that had existed there in January. Few extremes of temperature developed, however.

This month was also a welcome contrast in the eastern United States, particularly in Florida, to February of the preceding year, which had been the coldest February on record in the southeastern quarter of the country [2]. As might be expected, the axis of maximum westerly winds at 700 mb. was considerably farther north over the Western Hemisphere this February than a year ago, when the great index cycle of 1958 was in its most depressed state with the westerlies at 32° N. or 6° south of normal [2]. This February the westerly wind axis remained persistently near 43° N., or about 5° north of

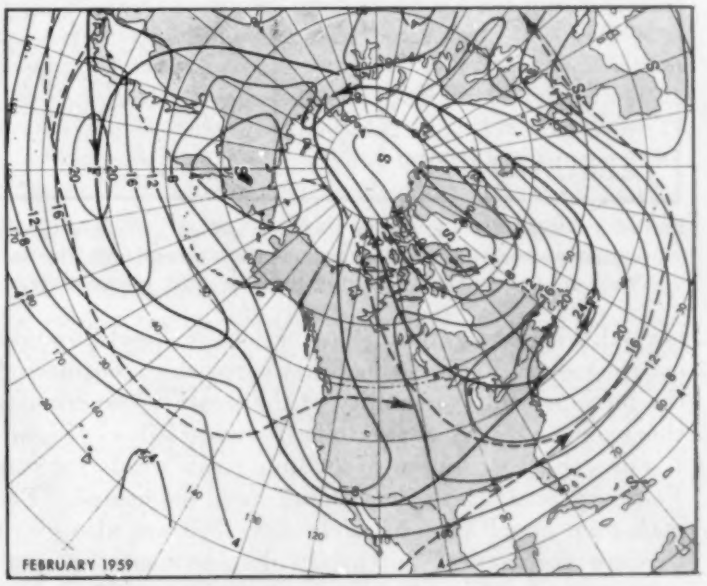

FIGURE 1.—Mean 700-mb. isotachs for February 1959 in meters per second. Solid arrows are axes of maximum speed (jets). Dashed lines are jet axes in February 1958. Important feature is confluence of jets in the Northeast.

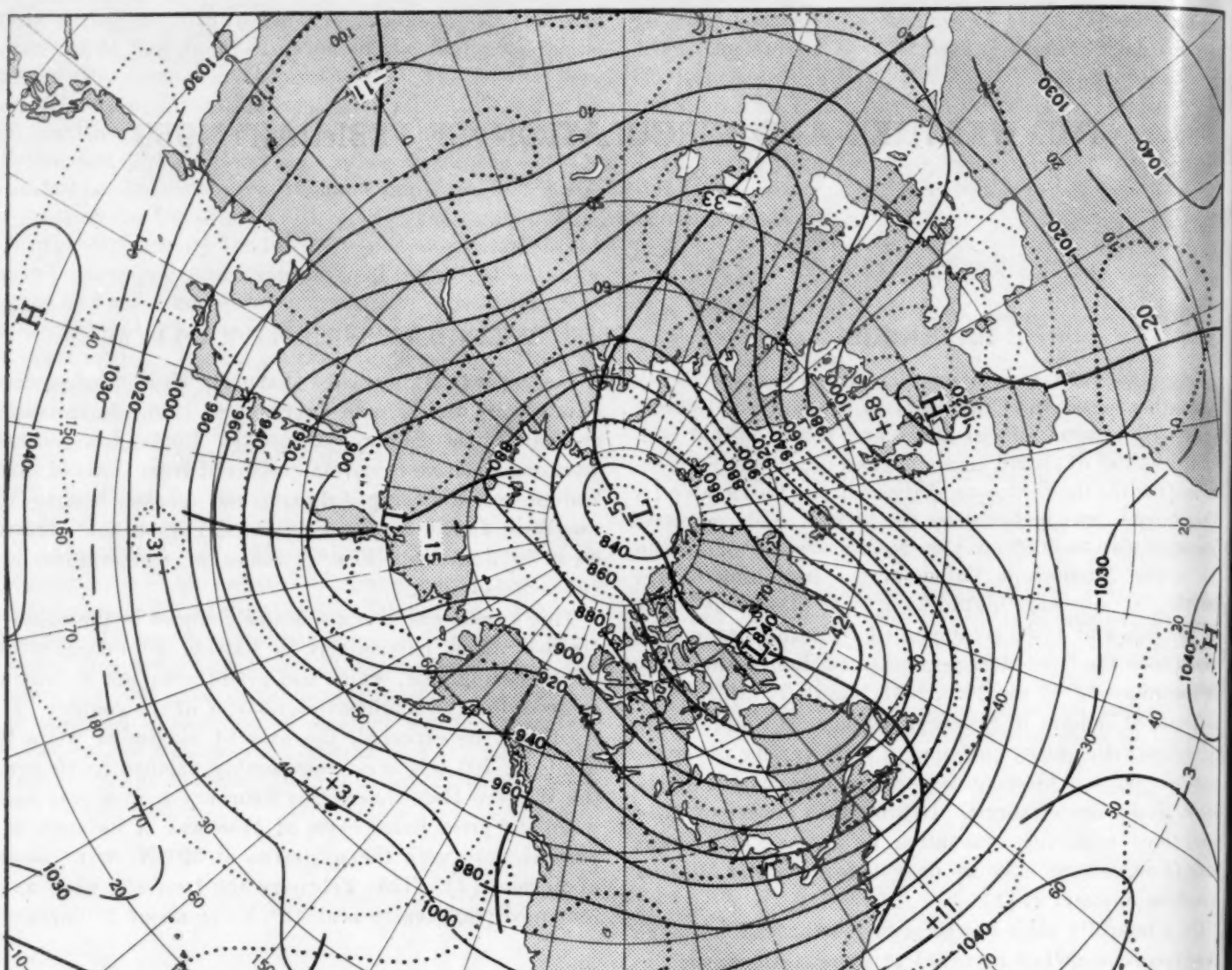

FIGURE 2.—Mean 700-mb. height contours (solid) and departures from normal (dotted) (both in tens of feet) for February 1959. Large negative anomalies in polar regions were accompanied by an almost circumpolar ring of positive anomalies at middle latitudes in the Western Hemisphere, resulting in contracted circumpolar westerlies—an almost complete reversal from February 1958.

normal, with no significant fluctuations in speed throughout the month. This is somewhat surprising, considering the intra-monthly variability of the weather and circulation over the United States to be discussed below. Figure 1 shows the distribution of 700-mb. mean winds for this February, with axes of maximum speed delineated. The maximum speed axes for February 1958 are also given to show the marked northward displacement this year over most of the hemisphere in comparison with a year ago. In the western States the axis was farther south this year, reflecting cooler conditions in this area in contrast to the extreme warmth of February a year ago.

3. MONTHLY MEAN CIRCULATION AND WEATHER

Figure 2 shows the characteristics of this month's mean circulation. The large-scale waves were generally close to their normal positions, with the Asiatic coastal trough much weaker than normal and the Kamchatka center of action about normal in intensity. The gradient of height departures from normal in the northern part of the North Pacific shows that the westerlies in this area were stronger than normal. This may have contributed to the fact that the trough in the Maritime Provinces of Canada was slightly east of its normal position. Above normal northwesterly flow over Canada was associated with a deeper

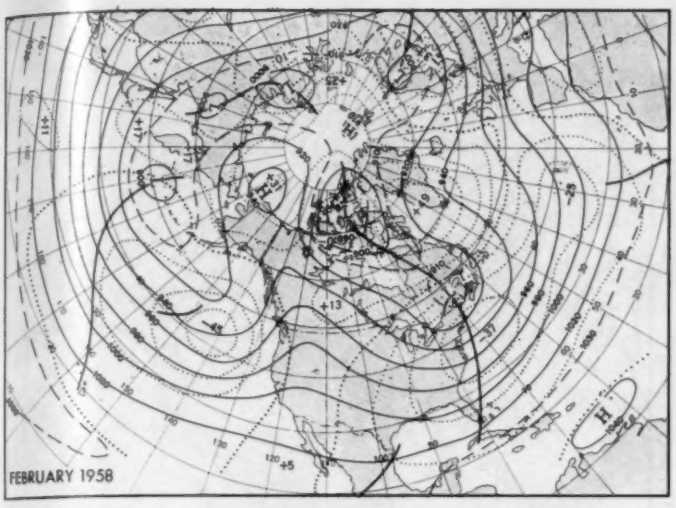

FIGURE 3.—700-mb. height contours (solid) and departures from normal (dotted) for February 1958. Note expanded circumpolar westerlies due to positive anomalies in polar regions with negative anomalies to south.

than normal center of action near Baffin Island. The most prominent abnormalities of the monthly circulation were the extremely deep polar vortex, 550 feet below normal, and the intense and persistent blocking High over western Europe, averaging 580 feet above normal for the month. Between the European block and the polar Low an anomalous southwesterly gradient of almost 1,000 feet existed, on the average, between the eastern coast of Greenland and the British Isles. This was expressed as a remarkably strong southwesterly jet in the North Atlantic across Iceland (fig. 1).

The subtropical westerlies at 700 mb. were weaker than normal during the month throughout the Western Hemisphere, especially in the Pacific where they were 6 to 8 meters per second below normal. At sea level the subtropical easterlies were stronger than normal, bringing heavy precipitation to windward locations in Hawaii. Hilo, a windward station which normally has a prevailing southwest wind due to local peculiarities, this month reported a prevailing wind direction of east-northeast, averaging about 3 miles per hour above normal, with a resulting rainfall of 3.61 inches more than normal.

In contrast to the marked persistence of the large-scale circulation from December 1958 to January 1959 [1], the circulation this month showed a dramatic reversal from the earlier state, particularly as portrayed by the monthly mean 700-mb. height anomalies. The extensive band of positive anomaly from the Bering Sea to the Denmark Strait in January gave way to equally large negative values this month, with height anomalies decreasing almost 1,100 feet over southern Greenland. Negative height departures of January were also reversed this month in the eastern Pacific, eastern United States, and in Scandinavia where a strong block became entrenched early in the month. To complete the reversal, above normal heights in the southwestern United States gave way to negative departures this month.

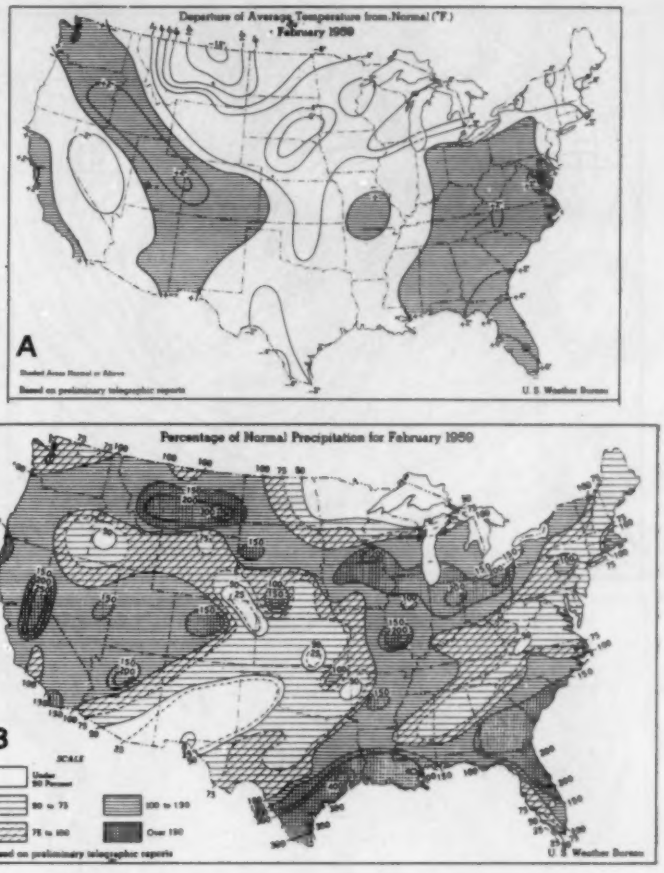

FIGURE 4.—(A) Departure of average surface temperature (°F.) from normal for February 1959. (B) Percentage of normal precipitation for February 1959. (From *Weekly Weather and Crop Bulletin, National Summary*, vol. XLVI, No. 9, March 2, 1959. and No. 10, March 9, 1959).

The similar contrast of this month with its counterpart in 1958 may be seen by comparing figures 2 and 3, and, in particular, the height departures from normal. It is of interest, in this connection, that February of 1958 was quite similar throughout the hemisphere to January 1959, except that the below normal heights and temperatures in the East and Southeast were less intense in January 1959.

Figure 4 summarizes the monthly departures of temperature and precipitation from normal. The northwesterly flow along the northern border States, together with snow cover, kept this area well below normal. Montana was the coldest region, relative to normal, over the whole of North America, with some sections of Quebec Province running a close second. Nitchequon and Seven Islands, Quebec, averaged 10° below normal due to strong northerly flow associated with the much deeper than normal trough in Davis Strait. The warmest section of the continent, relative to normal, was Aklavik, N.W.T. which averaged 12° above normal under the influence of faster than normal southwesterly flow.

A weak ridge kept the eastern sections of the United States, from the Ohio Valley southward, relatively warm for this time of year, with Florida the warmest section of the country on both a relative and absolute basis. Fort

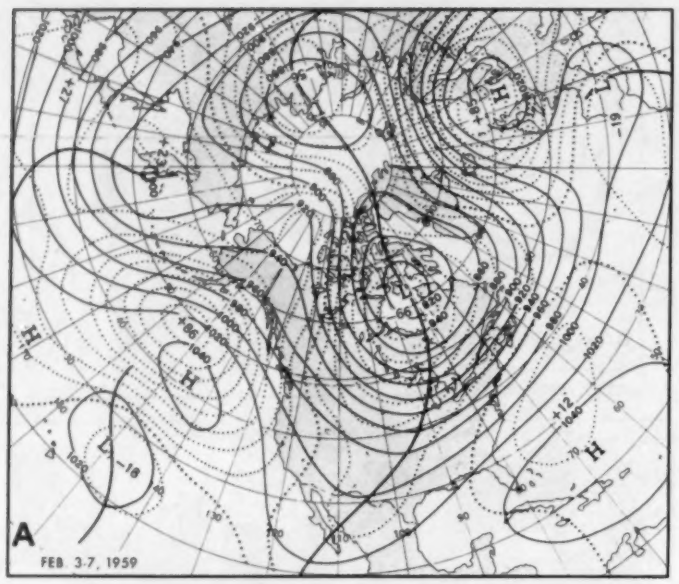

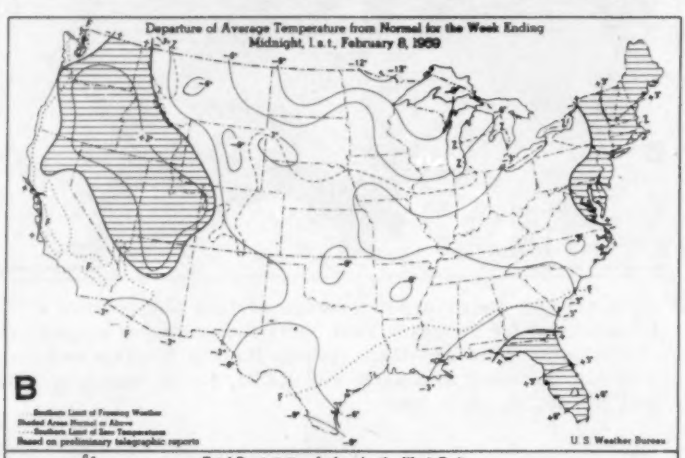

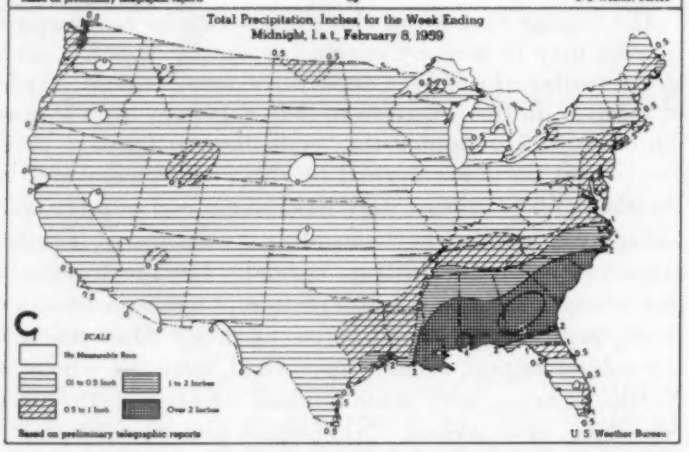

FIGURE 5.—(A) 5-day mean 700-mb. contours (solid) and height departures from normal (dotted) (both in tens of feet) for February 3–7, 1959. (B) Departure of average surface temperature from normal (°F.), and (C) total precipitation (inches) for the week ending February 8, 1959. (From *Weekly Weather and Crop Bulletin, National Summary*, vol. XLVI, No. 6, Feb. 9, 1959.)

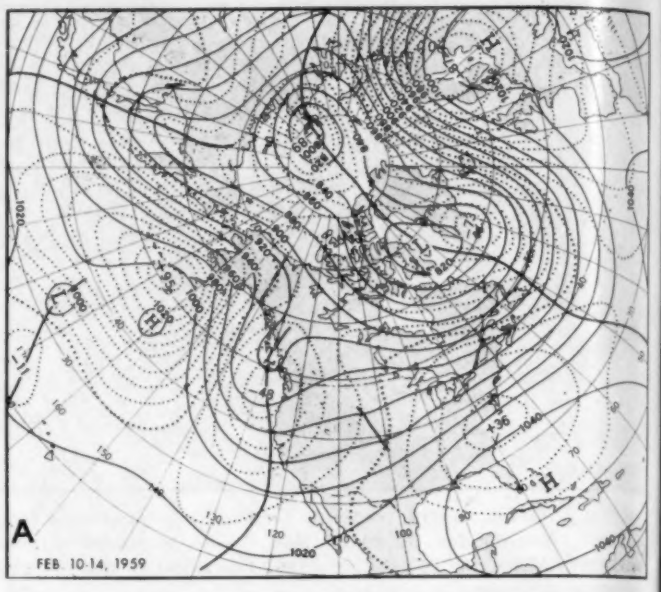

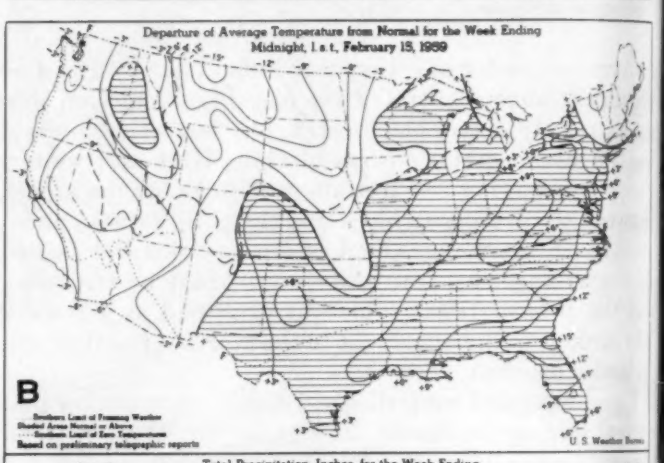

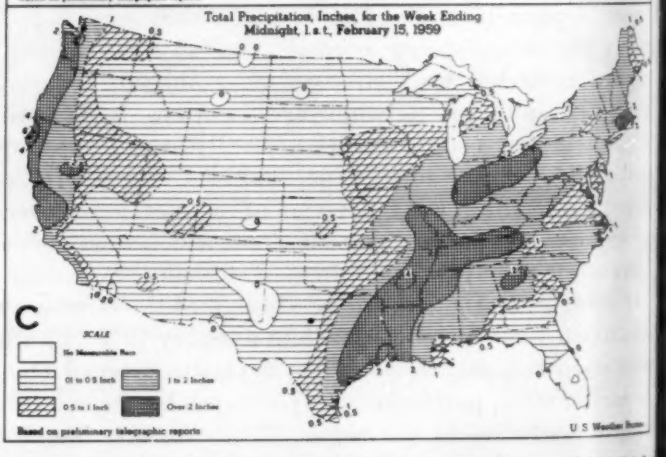

FIGURE 6.—(A) 5-day mean 700-mb. contours (solid) and height departures from normal (dotted) (both in tens of feet) for February 10–14, 1959. (B) Departure of average surface temperature from normal (°F.), and (C) total precipitation (inches) for the week ending February 15, 1959. (From *Weekly Weather and Crop Bulletin, National Summary*, vol. XLVI, No. 7, Feb. 16, 1959.)

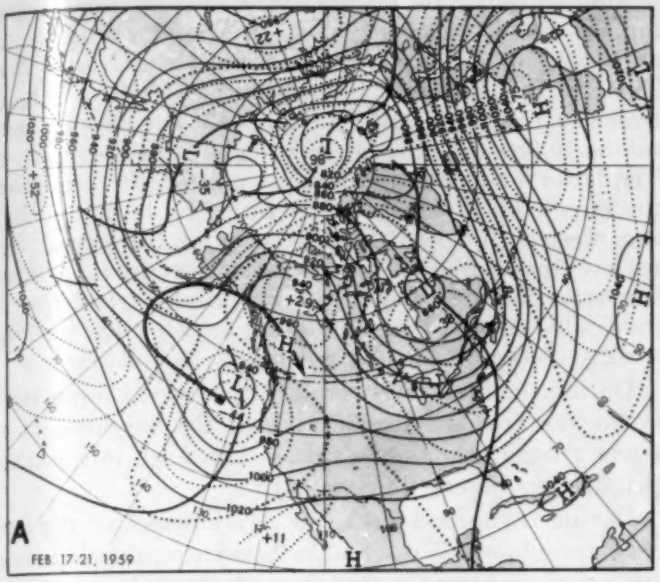

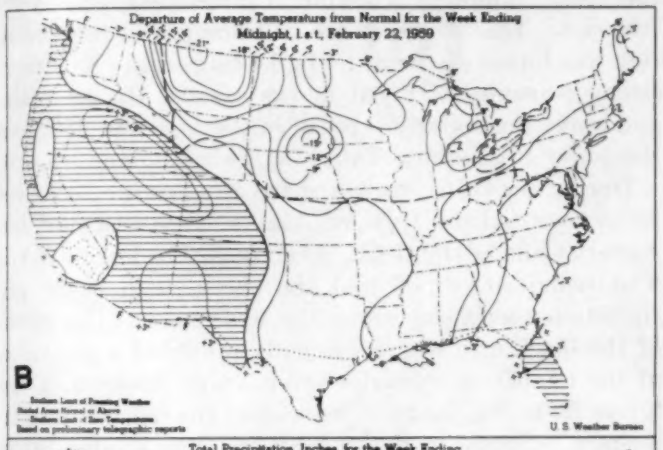

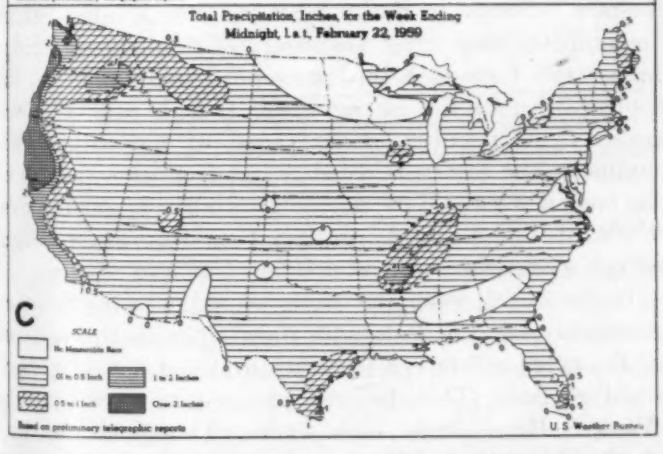

FIGURE 7.—(A) 5-day mean 700-mb. contours (solid) and height departures from normal (dotted) (both in tens of feet) for February 17–21, 1959. Heavy solid arrow is the track of the eastern Pacific anticyclone from the beginning of the month. (B) Departure of average surface temperature from normal (°F.), and (C) total precipitation (inches) for the week ending February 22, 1959. (From *Weekly Weather and Crop Bulletin, National Summary*, vol. XLVI, No. 8, Feb. 23, 1959.)

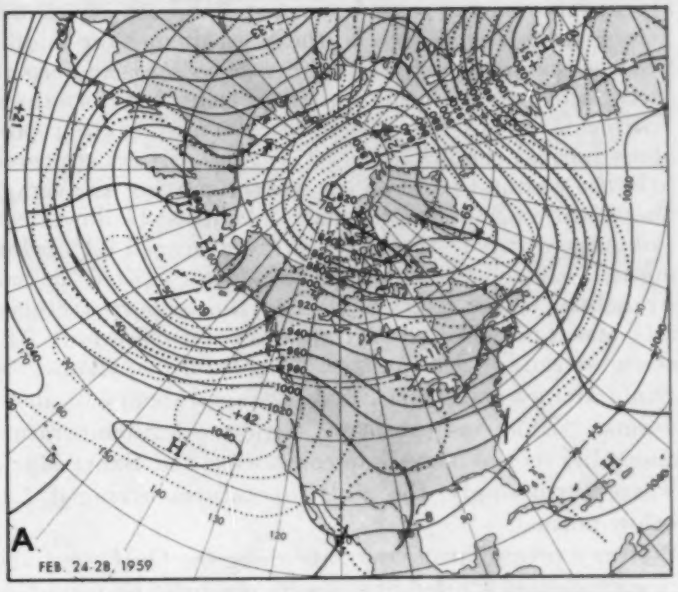

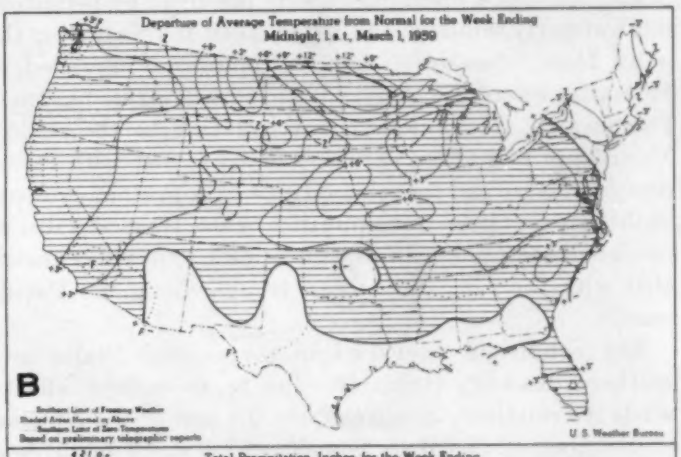

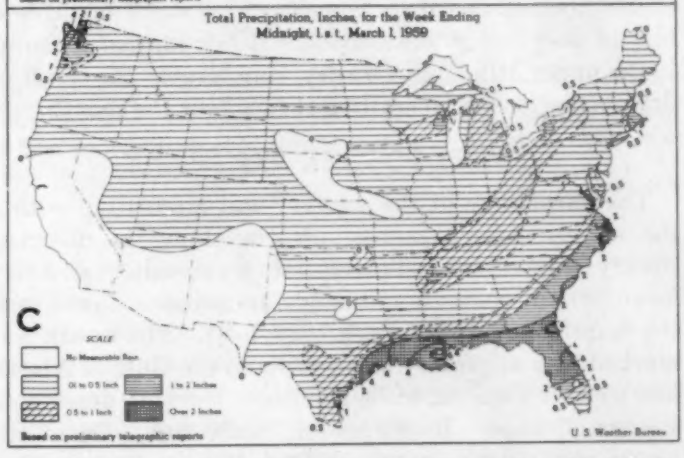

FIGURE 8.—(A) 5-day mean 700-mb. contours (solid) and height departures from normal (dotted) (both in tens of feet) for February 24–28, 1959. (B) Departure of average surface temperature from normal (°F.), and (C) total precipitation (inches) for the week ending March 1, 1959. (From *Weekly Weather and Crop Bulletin, National Summary*, vol. XLVI, No. 9, March 2, 1959.)

Myers reported the second warmest February on record. Strong trough conditions in the West during the middle two weeks kept the extreme Southwest cooler than normal, except along the immediate coast of central and southern California where the major cities continued to report above normal conditions. Los Angeles airport appeared to be the warmest point on the coast, reporting an average temperature 3.2° above normal, in contrast to downtown Los Angeles where the temperature averaged 0.1° below normal. A somewhat similar condition existed at San Francisco, where temperatures at the airport averaged 2.4° above normal and at the downtown office only 0.5° above normal. Sea surface temperature anomalies at Santa Monica and Avila Beach averaged about 3.0° above normal. This was consistent with the air temperature anomalies on the immediate coast, except at Santa Maria where surprisingly, the air temperatures averaged 1.2° below normal.

Heavy precipitation amounts along the Gulf coast and in southeastern United States were produced by persistent southwesterly winds which lifted moist Gulf air over the polar front. Somewhat similar conditions prevailed in Montana, where the Arctic front was overrun by moist Pacific air. Above-normal precipitation in the middle Mississippi and Ohio Valleys was associated with recurrent confluence and the related track of migratory cyclones in this area. Heavy precipitation in the West was due to persistent storminess during the middle two weeks associated with the very deep mean trough along the Pacific coast.

Dry conditions prevailed in the central Plains and southern Rockies, primarily due to downslope effects, while the relatively dry area from the foot of the Appalachians northeastward to New England was a manifestation of post-trough desiccation. Below normal amounts in the upper Mississippi Valley were largely the result of dry northerly flow prevailing throughout the month.

4. WEEK-TO-WEEK VARIABILITY

The variability of the weather and circulation within the month is perhaps best illustrated by the observed weekly temperature and precipitation anomalies and 5-day mean 700-mb. contours and height anomalies centered near the middle day of each week (figs. 5–8). The month was marked by a migratory anticyclone in the Gulf of Alaska and western Canada, while persistent blocking dominated western Europe. Retrogression in the first part of the month resulted in new trough formation, and progression was the rule toward the end of the month when the westerlies speeded up to their maximum of 13 m.p.s., averaged over the Western Hemisphere at temperate latitudes.

An important aspect of the mean circulation in the first part of the month was retrogression of the eastern Pacific anticyclone, which subsequently recurved eastward along the southern coast of Alaska, thence southeastward into British Columbia by the 3d week, as shown by the trajectory in figure 7A.

Another important feature of the mean circulation during the month was the gradual migration of the center of action in northern Siberia toward the North Pole. This was brought about in part by the persistent ridging tendency over the Lake Baikal area due to persistent southerly flow out of the deep trough in the Caspian Sea. The latter was maintained in great strength throughout the month by flow emanating from the blocking High over western Europe. The tendency toward a polar vortex eventually resulted in fast westerlies around the entire hemisphere with spring-like weather over almost all the United States at the end of the month. The week-to-week evolution is summarized briefly as follows:

During the first week, retrogression of the mean High in the northeastern Pacific favored the development of a new trough near the west coast (fig. 5A), in a manner that has been observed previously [3].

During the second week, the development of the west coast trough, which resulted in heavy precipitation along the coast, produced a major readjustment over North America. The trough which had dominated the midsection was forced eastward to the Davis Strait. As a result strong warming occurred in the eastern United States, and heavy precipitation spread in the confluent flow from the lower Mississippi Valley to New England (fig. 6).

During the third week, a sharp recurvature in its trajectory carried the Gulf of Alaska High eastward into western Canada (fig. 7A). The Low in the Pacific Northwest remained cut off and stationary, with heavy precipitation continuing along the west coast. The advent of the block into western Canada produced a relaxation of the temperate westerlies over North America, a condition favorable for retrogression of the trough from the western Atlantic to the east coast of the United States. In addition, flow from the stronger than normal ridge in western Canada helped transport cold Canadian air southward into the retrograding trough near the east coast. This resulted in a reversal of the temperature regime in the eastern United States from the warmth of the second week. With northerly wind components over much of the country, precipitation was mostly light except along the west coast (fig. 7 B and C).

In the fourth week, the center of action in the Siberian Arctic crossed the Pole and, together with the collapse of the ridge in western Canada, produced a strong zonal wind regime. This favored progressive waves in the Western Hemisphere, with warm and dry air flooding much of the United States, except near the Gulf coast which was wet and cool (fig. 8).

5. CYCLONE AND ANTICYCLONE TRACKS

This month there were two preferred tracks of anticyclones from northwestern Canada, in close agreement with the normal tracks [4], one just north of the Great Lakes and across New England, and the other south of the Lakes and across the Virginia Capes. In all, 10 Highs crossed the east coast during the month, evenly divided

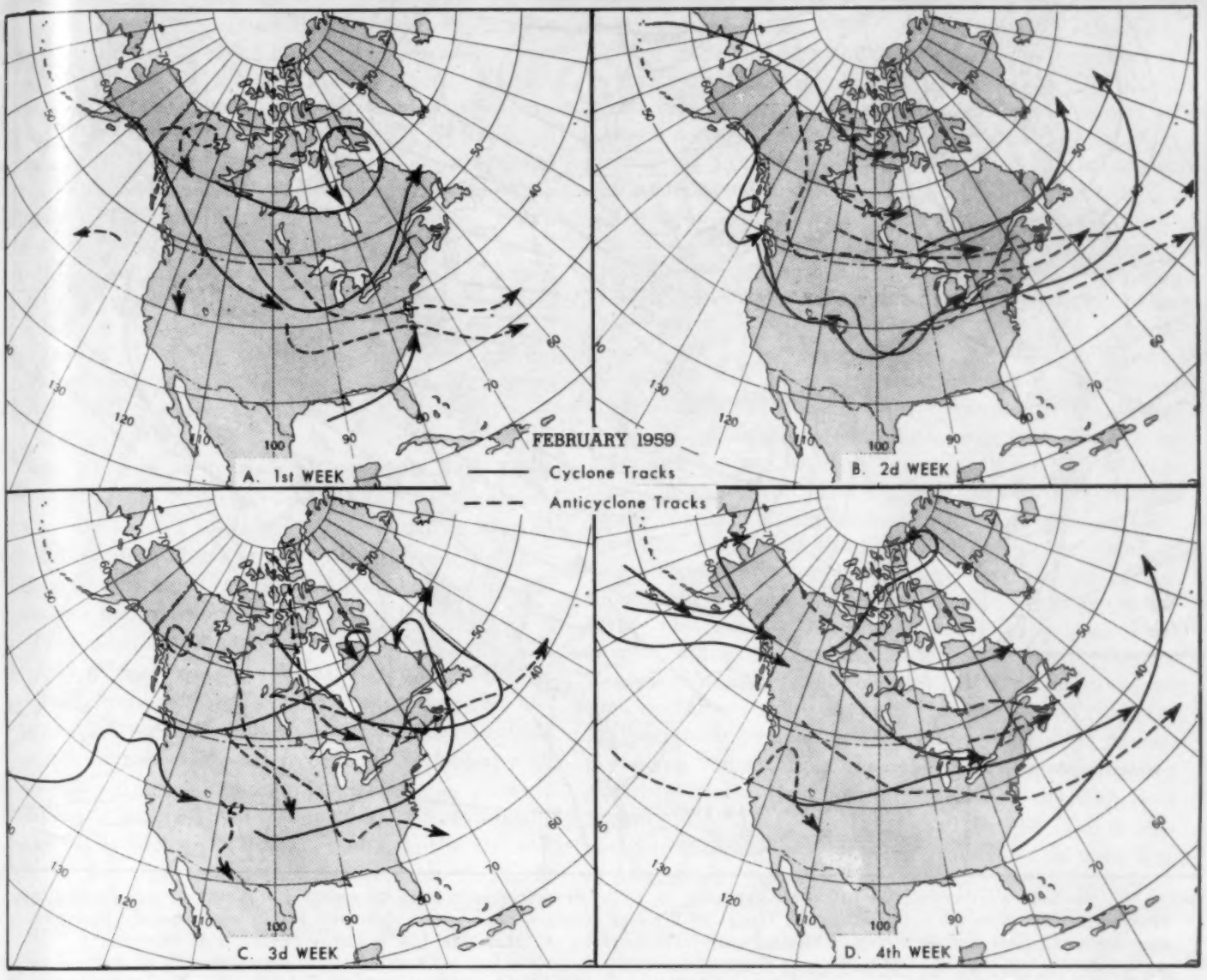

FIGURE 9.—Daily tracks of migratory cyclones (solid) and anticyclones (dashed) at sea level by weeks. Each track begins at approximate location of center at beginning of week, or at location of formation, and ends at approximate position at end of week, or at location of disappearance. Tracks may be compared with mean flow in figures 5A–8A.

between the two tracks. The most frequent interval between Highs crossing the coast was 2 days but with intervals in the second half of the month quite variable; e.g., a 6-day interval in the 3d week. This was the coldest period of the month in the eastern and central United States as a cold High from the Yukon, moving steadily southward, took about a week to arrive at the North Carolina coast, producing some record minimum temperatures en route, such as −30° at Huron, S. Dak. on the 19th and 13° at Richmond, Va., on the 21st.

Cyclonic systems originated over a wide range of latitudes in the western part of North America, with the majority converging toward the Great Lakes region and thence moving across southern New England, in general agreement with the prevailing confluent flow of the monthly circulation (fig. 2). The principal track crossed the east coast near 40° N., well to the south of the normal February track.

A comparison of weekly tracks in figure 9 with the corresponding week's mean circulation in figures 5A—8A shows that generally the cyclones followed the mean flow northward on the east side of the mean troughs toward the centers of action, while the Highs glanced off toward the subtropical Highs.

A brief inspection of the weekly tracks shows that in the first week, with a strong Low over Hudson Bay and depressed westerlies along the east coast, the Highs followed the southern track. In the second week, with trough development along the west coast accompanied by ridging over the Southeast and strong confluence over most of North America (fig. 6A), the Canadian Highs glanced off eastward north of the Great Lakes, with the principal

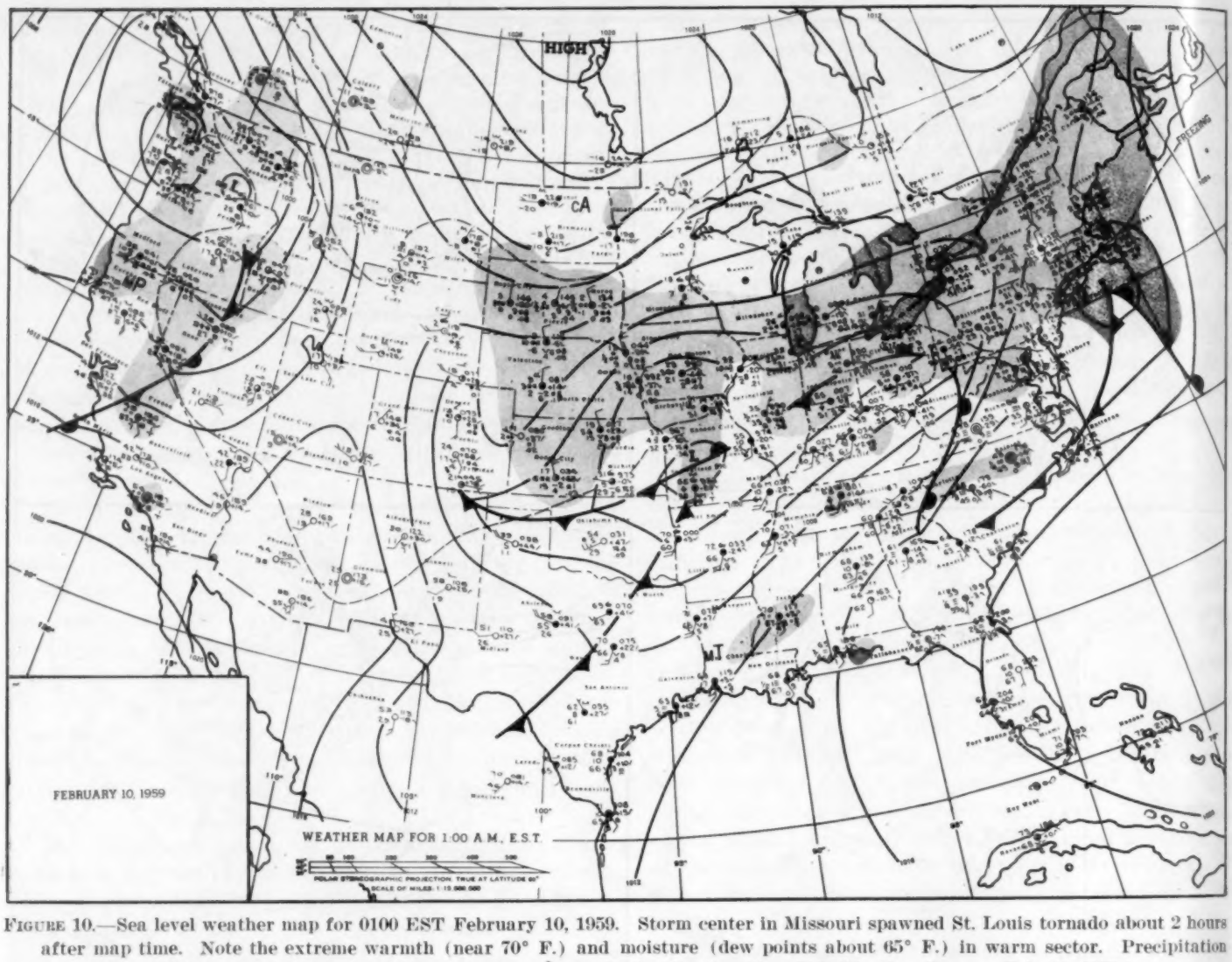

FIGURE 10.—Sea level weather map for 0100 EST February 10, 1959. Storm center in Missouri spawned St. Louis tornado about 2 hours after map time. Note the extreme warmth (near 70° F.) and moisture (dew points about 65° F.) in warm sector. Precipitation area north of front consisted largely of freezing rain. (From *Daily Weather Map*, U.S. Weather Bureau, Feb. 10, 1959.)

storm track from out of the Great Basin. In the third week, due to new trough development near the east coast, the tracks exhibited the influence of both east and west coast troughs, with some additional transitory influences in evidence. The fourth week's tracks were more zonal.

6. DAILY WEATHER SYSTEMS

Early in the first week a Canadian anticyclone developed to a record intensity of about 1053 mb. as it moved southeastward across the upper Mississippi Valley, producing record minimum temperatures at some stations such as Flint, Mich. (−18° F. and −22° F. on Feb. 1 and 2) and Nantucket, Mass. (8° F. minimum on the 2d). During midweek, cyclonic activity swept southeastward from Alberta toward the lower Great Lakes, then northeastward in the mean flow (fig. 5A), producing mostly moderate precipitation in the East. However heavy amounts fell in the Southeast due to wave activity on the polar front. Late in the week another anticyclone developed in the central part of the United States and crossed the Carolina coast at the weekend.

By the beginning of the second week there were abundant signs of an impending change in the large-scale regime. For example, the west coast ridge aloft and the eastern Pacific High cell had retrograded about 15° of longitude from their positions a week earlier to about 150° W., permitting cyclonic vorticity maxima to plunge southward along the west coast. This was manifested by a surface disturbance of the "A" type [5] in the western Great Basin. With 700-mb. heights increasing and temperatures warming to well above normal in the East as a result of trough development in the West, an Arctic anticyclone in Alberta glanced off eastward along the track north of the Great Lakes as did its successors in the same week (fig. 9). By the 9th the Great Basin disturbance had deepened to a storm in southwestern Colorado. With another deepening "A"-type system approaching the Oregon coast, the Colorado storm accelerated eastward across

the midsection of the country toward the Ohio Valley. This storm and its associated fronts produced the most severe weather of the month. Hourly wind speeds in many places along its path were well over 50 knots. For example, Roswell, N. Mex. on the 9th reported 68 knots, St. Louis, Mo., 66 knots, and Dayton, Ohio, 54 knots, on the 10th. In the dry, unstable, maritime polar air behind the first cold front dust storms developed in parts of the southern Plains such as Amarillo and Dallas, Tex. North of the sharp stationary front along which the storm raced toward Ohio, a widespread area of freezing rain occurred as extremely warm and moist tropical air in the warm sector overran the Arctic air north of the front. Moderate to heavy glazing on the 9th and 10th was reported at such stations as Topeka, Kans., St. Joseph, Mo., Rockford, Ill., Williamsport, Pa., Albany, N.Y., and Providence, R.I.

Figure 10, a reproduction of the published *Daily Weather Map*, for 0100 EST February 10, shows conditions at the surface about 2 hours before a devastating tornado hit St. Louis, Mo. This map shows the storm center just northwest of Springfield, Mo., where a tornado was also reported one hour earlier about 25 miles northwest of the city. The conditions depicted on this map closely resemble those for typical tornado cases [6] which show a confluence of extremely moist tropical air, dry maritime polar air, and continental polar air into a deep storm center (about 992 mb. minimum pressure was recorded at St. Louis) with a cyclonic speed maximum at upper levels (not shown).

Flood conditions revisited Indiana and Ohio as a result of heavy rains falling on frozen ground on the 9th and 10th, after less than a month's respite from floods in January. Some places experienced the worst flood conditions since 1913. Hard hit areas were the Wabash and Maumee Rivers in Indiana and the Sandusky in Ohio. Such cities as Fort Wayne, Ind., and Toledo, Sandusky, Fremont, Dayton, Akron, Cleveland, and Youngstown, Ohio, reported various degrees of flooding with evacuation and heavy damage in some areas.

This storm passed rapidly off the middle Atlantic coast on the 10th, setting maximum temperature records at Washington, D.C., Augusta, Ga., Norfolk, and Richmond, Va. The anticyclone which followed in its wake brought a record minimum of −4° F. to Schenectady, N.Y. on the 12th.

During this period another disturbance was traversing the Great Basin from the 10th to the 13th. This storm produced heavy snows in the West, over a foot at Olympia, Wash., almost 3 feet at Blue Canyon, Calif., 22 inches at Reno, Nev., and a record 7.7 inches at Ely, Nev. This system, in contrast to its predecessor, remained weak while crossing the middle of the United States, but deepened markedly on the 14th as it passed off the New England coast. Late in this week a third deep storm plunged southeastward from Alaska, lashing the Pacific Northwest, and producing heavy snows at higher elevations. Record 24-hr. amounts of 22.6 inches were reported at Sexton Summit, Oreg. on the 13th and 14th, and 28 inches at Mt. Shasta, Calif. This system was forced inland on a track across Canada toward Hudson Bay on the 15th, in contrast to the prevailing storm track of the second week across the midsection of the United States.

On the 16th and 17th a secondary disturbance was forming over the southern Plains, accompanied by a record maximum temperature for the date of 87° F. at Dallas, Tex. At the same time the coldest anticyclone of the month developed in western Canada due to the recurvature of the upper anticyclone in the Gulf of Alaska, and started to inch southward toward the northern Rockies and Great Plains. Over-running of the Arctic front by Pacific air produced about a foot of snow in parts of Montana such as Great Falls and Helena on the 16th and 17th. The disturbance which originated in the southern Plains started to develop strongly near the Carolina coast on the 18th, and became the center of action near Labrador in the mean circulation of the third week, thus effecting retrogression of the mean trough to the east coast. This development was in part a response to the strong buildup of pressure in western Canada that followed development of a major storm off the Oregon coast three days earlier. The Yukon ridge deployed Arctic air southeastward over the United States, producing record minimum temperatures at such places as North Platte, Nebr., with −19° F. on the 20th, and Birmingham, Ala., with 18° F. on the 21st, and it also permitted shorter wave spacing from coast to coast due to reduction of the westerlies. The storm that dominated the eastern Pacific off the Oregon coast during the 3d week deepened to about 960 mb. on the 16th after migrating northeastward from the Hawaiian area on the previous three days. It remained stationary off the coast for the remainder of the week and filled slowly as the blocking High recurving eastward farther north kept it cut off. This storm produced the mean Low off the Pacific Northwest coast in figure 7A.

During the last week a ridge replaced the Pacific coastal trough, ending the abundant precipitation regime of the middle two weeks of the month in the West. At the same time the polar vortex became entrenched near the Canadian archipelago, strengthening the westerlies across North America and favoring progression of the large-scale upper waves. Early in the week the last Great Basin disturbance emerged on the 22d, deepening and crossing the Great Lakes region as it headed for the New England coast. This storm produced about ½ to 1 inch of rain with some flooding reported in Rockford, Ill., and heavy snow in the Northeast. It was followed by a Pacific anticyclone and little weather of any significance during the remainder of the month.

REFERENCES

1. L. P. Stark, "The Weather and Circulation of January 1959—A Month of Exceptional Persistence from the Preceding December," *Monthly Weather Review*, vol. 87, No. 1, Jan. 1958, pp. 33–39.
2. W. H. Klein, "The Weather and Circulation of February 1958—A Month with an Expanded Circumpolar Vortex of Record Intensity," *Monthly Weather Review*, vol. 86, No. 2, Feb. 1958, pp. 60–70.
3. C. M. Woffinden, "The Weather and Circulation of February 1957—Another February with a Pronounced Index Cycle and Temperature Reversal over the United States," *Monthly Weather Review*, vol. 85, No. 2, Feb. 1957, pp. 53–61.
4. W. H. Klein, "Principal Tracks and Mean Frequencies of Cyclones and Anticyclones in the Northern Hemisphere," U.S. Weather Bureau, *Research Paper* No. 40, Washington, D.C., 1957.
5. R. D. Elliot, "Weather Types of North America," *Weatherwise*, vol. 2, Nos. 1–6, Feb.–Dec. 1949.
6. Staff Members, Severe Local Storms Forecast Center, Kansas City, Mo., "Forecasting Tornadoes and Severe Thunderstorms," U.S. Weather Bureau, *Forecasting Guide* No. 1, Washington, D.C., Sept. 1956. (See pp. 22–24.)

U.S. GOVERNMENT PRINTING OFFICE: 1959